

physLight

physical units in light transport

Copyright © the Contributors of the PhysLight Project

Full source available at <https://github.com/wetadigital/physlight>

v 1.3 - AUGUST 5, 2023

Contents

I	Models & Specification	6
1	Introduction	7
1.1	Why physical units?	7
1.2	Quantities in light transport	9
1.3	Measuring light and brightness	14
2	Imaging and lighting models	19
2.1	Describing imaging	19
2.1.1	The film response function	21
2.2	Luminance and sensor response	24
2.3	Describing light sources	28
2.3.1	Area Lights	29
2.3.2	Image-Based Lighting	30
2.3.3	Sun light	32
3	Calculation sheets	34
3.1	Imaging	34
3.2	Emission constant	35
3.2.1	Area Light	35
3.3	Surface interaction	37
3.4	Light to sensor interaction	38
II	Reference	39
4	Illuminants	40
4.1	Spectral Distribution Functions	40
4.1.1	Black body radiator	40
4.1.2	CIE Standard Illuminants	42
4.2	Standard Illuminants	45
4.2.1	Illuminant D	45
4.3	Angular distributions	46
4.3.1	Powered cosine	46
4.3.2	IES profiles	46
4.4	Tint functions	46
4.4.1	Texture maps	46
4.4.2	Tabulated spectral data	46

5	Sensors	48
5.0.1	ISO Sensitivity	48
5.0.2	Counting photons	48
5.0.3	Digital sensors	48
5.1	Color matching functions	49
5.2	Camera sensitivity data	49
5.2.1	Red Mysterium X	51
5.2.2	Canon 1D Mark III	52
5.2.3	Canon 5D Mark II	53
III	Appendices	54
A	Handling color	55
A.1	Spectral basis representation	55
B	Reference implementation	57
B.1	Pipeline integration	57
B.2	Tristimulus rendering	58
B.2.1	Area lights	58
B.2.2	Image Based Lighting sources	61
B.2.3	Sun lights	61
B.2.4	Materials	61
B.2.5	Imaging	61
B.3	Spectral setting	65
B.3.1	Lights	65
B.4	Color space conversion code	65
B.5	Texture maps	67
B.5.1	RGB to spectrum conversions	67
C	Radiance	69
C.1	Introduction	69
C.2	Analysis	71
C.3	Practical applications	76
C.4	Discussion of introductory examples	76
C.5	Summary	77
C.6	Acknowledgement	78
C.7	Bibliography	78
D	Notation and symbols	80
E	Index and glossary	82
	Bibliography	88
F	References	88
G	Standards and technical reports	91
H	Motion pictures	92

List of Figures

1.1	A visualization of various measures of radiant energy incident onto a surface incident radiant power (top left), incident radiant intensity (top right), irradiance (bottom left), and incident radiance (bottom right). Incident radiant power Φ_e is the total energy per unit time incident everywhere on the area R from all directions Ω . Incident radiant intensity $I_e(\omega)$ is the energy incident from a specific direction ω everywhere on R , while irradiance $E_e(x)$ is the energy incident at a given point x from all direction Ω and radiance $L_e^\downarrow(x, \omega)$ at a given location x from a given direction ω . Intensity can be obtained by integrating radiance $L_e^\downarrow(x, \omega)$ over R , while irradiance can be obtained by integrating radiance over the set of all directions Ω . Integrating L_e^\downarrow over both the surface and all directions yields incident power.	13
1.2	Two views of the same scene: the left hand side shows intensity of a relatively narrow infrared band around 850 nm, while the right hand side shows ultraviolet light, in the 345–380 nm band. Both bands are moderately beyond what is visible by humans	16
1.3	Reproduction of an old advertisement image, illustrating the difference between orthochromatic film, most sensitive to greens and blues, and panchromatic film, having a somewhat more even response across the visible spectrum. Note that neither sensitivity curve is all that close to the luminous efficiency function $V(\lambda)$	17
2.1	Setup for our proof about the exposure equation. The Lambertian reflector with albedo ρ is parallel to the image plane, and the incident illumination is E_v	24
2.2	Relating image and object size in a camera where the aperture is small compared to the distance $o - a$ between the aperture and the object. . . .	25
3.1	Integration over area light.	38
4.1	Spectral distributions of black body radiator at various temperatures . .	41
4.2	Comparison of CCTs for black body and Illuminant D	41
4.3	Spectral distributions of common Standard Illuminants	42
4.4	Spectral distributions of CIE Standard Fluorescent Illuminants	44
4.5	Spectral distributions of CIE Broadband Fluorescent Illuminants	44
4.6	Spectral distributions of CIE Narrowband Fluorescent Illuminants	44
4.7	Spectral transmittance of <i>RoscoLux</i> gel series	47
5.1	Comparison of color matching functions from Wyman vs. CIE data . . .	49

LIST OF FIGURES

C.1	An elementary pencil of radiation	72
C.2	An elementary beam of radiation between two surface elements dA_1 and dA_2	73
C.3	Refraction at a smooth boundary between media of different refractive indices (n and n')	75

List of Tables

1.1	Correspondence between radiometric and photometric units	15
5.1	Data for the CIE Color matching functions $\bar{x}(\lambda), \bar{y}(\lambda), \bar{z}(\lambda)$	50

Part I

Models & Specification

Chapter 1

Introduction

1.1 Why physical units?

One of the reasons physically-based image synthesis has become such an indispensable ingredient for pushing realism and consistency in very complex scenarios is predictability. Material modelling is based on physical properties and thus allows to reproduce increasingly complex natural phenomena. In traditional rendering systems, control of the look was often owned by the shading system, often allowing artistic control knobs for artificial emission or non-physical behavior to compensate for lighting, for example missing indirect illumination.

The physically-based rendering paradigm dictates that **material models**, lighting and camera response are independent entities and must hence always be controlled with this separation in mind. This makes **virtual** assets more reusable, and allows to achieve better consistency when integrating digitally produced content with live action **footage**.

Naturally, since a wide range of different effects interplay with each other in complex and subtle ways, it is absolutely crucial that all components are accurately represented by their virtual analogues to be able to reproduce real-world footage realistically. Furthermore, the description of the **virtual scene** being based on real-world quantities enables easier control and verification.

In this document we focus on the specification of **virtual illuminants** and **sensors** and make the case for using the same conventions and physical units as used by lighters and photographers on a motion picture set or in a photographic studio. For example, it is preferable in terms of predictability to think about brightness of a light source in terms of **photometric** units, i.e., units which represent brightness as perceived by a **human observer**, rather than **radiometric** ones (commonly called **wattage**) for two reasons: firstly there is convention: the normally used wattage reported on a light fixture or bulb is a measure of the power absorbed by the object, not the power of the radiation it emits *in the visible range*¹ onto the **scene**. Secondly, the perceived **brightness** of a source has a fairly marked dependence on its color, making lights emitting the same amount of radiative power (even when measured limited to the visible spectrum only) appear to have different brightnesses.

¹This is effectively the concept of **luminous efficacy**, being the ratio of power absorbed by the emitter to the luminous power emitted. What used to be the common household lightbulb, containing incandescent tungsten and rated for 100W, had a luminous efficacy of roughly 15lm/W, a contemporary **LED** lightbulb would be somewhere between 100lm/W and 200lm/W, a Xenon arc-lamp somewhere between 30lm/W and 90lm/W. Note that conservation of energy dictates that when considering all the radiation emitted by the bulb, the total radiated power *must* be equal to the absorbed “electrical” power

We want instead to specify a system of units and models, in such a manner that given a real-world scene and a virtual model of it, specifying the same illuminants via our chosen units, using the same camera settings and feeding the scene to a compliant renderer will replicate the same pixel values as would come from a real-world camera places in the real-world version. Naturally, for reproducing color, we will not only need to develop an accurate understanding of brightness, but also be aware of how **spectral** data flows through the **pipeline**.

The resulting system has been in use in the production pipeline at Wētā FX since about 2015. Because of the origin of this system in the motion picture industry, several terms of the trade have made it into this document.

The prevalent way of reasoning about image synthesis through rendering is built on the notion of the *light ray*, which is the fundamental element of geometrical optics. Light rays are the path segments² through space that light follows when traveling across the **virtual scene**.

This document is divided in parts: Part **I** contains an introduction on basic quantities that are relevant in light transport simulation and review the relation of photometric and radiometric units and describes the modelling aspects. In Chapter **2** we describe imaging and light models and propose the relevant sets of parameters to specify them accurately. Chapter **3** provides some examples on how to derive some of the described quantities from real world examples.

Part **II** provides a reference covering measurements of various illuminants (Chapter **4**) and cameras (Chapter **5**).

Part **III** contains the appendices: Appendix **A** discusses various considerations on color, in particular covering the relation between the tristimulus versus spectral settings, Appendix **B** describes an implementation of a color manipulation library and Appendix **C** is an extensive excerpt from Frederic Nicodemus’s excellent 1963 paper [Nicodemus, 1963] in which the concept of **radiance** is introduced: unsurprisingly we found his explanation far clearer than what we had been able to come up with, so we decided to retype his words, with the only change being we have changed the equations to use current conventions for quantity names and symbols, and adopted **SI** units throughout.

Because this document is the result of work started from the movie industry, we are aware several concepts may not be as well known to our readers from different backgrounds. For this reasons we have compiled a reference of notation and symbols used in Appendix **D** as well as a glossary in Appendix **E** with the hope these might help clarify potential issues arising from our use of movie-making jargon.

²In the vast majority of renderers in use today, rays are implemented as straight line segments, which enormously simplifies the implementation of the code that finds their endpoints. This ignores two effects: the first is that gravity bends light rays and the second it that variations in the index of refraction will alter the direction of a light ray. Usually bending resulting from gravity won’t be an important effect except for scenes that are particularly large and include body with very high mass concentrations like black holes. Scenes like this are occasionally rendered, though: for example the movie *Interstellar* (2014) did need to capture the bending effect of gravity onto light paths accurately, and a specialized rendering system was developed for use on the show. The task was complex enough that the Nobel laureate and CalTech professor Kip Thorne was included as consultant to support the team developing this technology. The second effect ignored by the straight-line approximation is that variations in the index of refraction will also bend the light paths. This is a substantially more common effect at human scale, for example it’s the origin of the *mirage* phenomenon. While there are several research projects that have built renderers able to capture this effect, the computational costs associated with this capability are high enough to make it impractical for everyday use

1.2 Quantities in light transport

It has been my experience that most people find it peculiarly difficult to master the fundamental concepts and relations of radiometry (or photometry) as they apply to extended sources. And I have come to believe that the key to this difficulty lies in the interrelated concepts of an elementary beam of radiation and its radiance (or luminance)

FRED NICODEMUS, 1963

We discussed how **rendering** is concerned with simulating how light travels around in a **virtual scene**, so this section introduces names for the quantities transported along these paths during the simulation and outlines the theory behind them. The naming we adopt was originally introduced by Fred Nicodemus in [Nicodemus et al., 1977] and is in line with several current international standards, among which we mention **International Organization for Standardization (ISO)/International Electrotechnical Commission (IEC)** Standard 80000, *Quantities and units, part 7: Light and radiation* [ISO 80000-7:2020], the *International lighting vocabulary* published³ by the **International Commission on Illumination (CIE)** [CIE S 017.2020], and the lighting section of the so-called “Electropedia” from the **IEC** [IEC 60050-845:2020]. Work in recent years has gone into harmonizing these bodies of knowledge so that the resulting vocabularies and symbols are in alignment. All the units in use descend directly from the **International System of Units (SI)**, described in [BIPM SI.2019].

Thinking about light flowing through a scene, rendering is concerned with the so-called *particle theory* of light: these particles are called *photons*, and *light rays* represent paths along which these photons flow. The particle theory of light describes a photon as a very small “object” (a *particle*) having no mass and no electrical charge, instead being made entirely of energy⁴. Max Planck talked about energy *quanta*: because of what photons are (namely, little “drops” of energy), energy can only come to be in certain specific amounts as can be captured by integral amounts of photons. There is no such thing as 1.736 photons: because photons are integer and indivisible, they are viewed in this theory as *elementary particles*, so one can only have 1 photon, or 2 photons or 3 and so on, and this limits the possible amounts of energy one can have.

As each photon effectively *is* a (small) quantity of energy, there comes about the natural question of how much energy a given photon actually is. It turns out that this depends on the photon’s *wavelength* λ and is equal to $Q_p = hc/\lambda$, where h is a universal constant named after Planck himself and c is the speed of light in vacuum⁵. The subscript \square_p indicates we are discussing photon quantities: we will need to introduce more of these subscripts as we go along to differentiate under what perspective we are considering

³Can also be consulted online at <https://cie.co.at/e-ilv>

⁴All readers troubled by this description are in good company. In fact there are certainly substantial theoretical and experimental problems in describing precisely aspects of a photon-as-particle such as its position. This is an instance of *Heisenberg uncertainty* and it only begins to scratch the surface of the problems in this area

⁵This concept of *wavelength* hints at the other way of thinking about light, the so-called *wave theory* of light. The wave theory says that light exists in a *field* that is present everywhere along our “light ray” and is called *wave* because the strength of this field oscillates over time at a given frequency $\nu = c/\lambda$, measured in [Hz]. In fact, the energy of a photon is technically defined as $Q_p = h\nu$. Because we’re mainly concerned with a geometric-optics/particle-theory view of light, in this work we have chosen to work with wavelengths, so we won’t see much discussion, if any, of frequency and ν ’s

the quantities in play. For what concerns graphics and rendering, light rays are *thin* objects, by which we mean if we imagined a ray like a tube, or a pipe, it would have a cross section, or width, of 0. However it is occasionally useful to think about the “size” of a photon, and it turns out a good model for a photon’s size is to use its wavelength as a measure of its cross-section diameter. This is far from an abstract concern: photons will only travel through openings that are bigger than their own size (which is relatively natural to expect, thinking about photons as particles). They will also be relatively undisturbed by things that are substantially smaller than their size (which instead is natural to expect from a view where photons are waves: it’s similar to how you would observe waves in a lake behave).

As much as photons are the elemental ingredients of light transport, they obviously must come from somewhere, which we call *light sources*. Given a light source that has been shining for a period of time, it will have emitted a certain number N_p of photons, delivering a corresponding amount of energy Q_e , measured in joule [J]. Note how the subscript here is $_e$, for *energetic*, indicating we are looking at a quantity coming from *radiometry*. If all of these photons had the same wavelength λ , maybe because they were coming from a laser source, we would have $Q_e = N_p Q_p = N_p hc / \lambda$. In the general case of light sources emitting in several different frequencies, we’d have to tally them separately and sum patiently, or integrate their distribution if we had access to it.

One way or the other, this brings us to discuss the notion of *power* of our source, being its ability to emit light over time. Given that light is energy, and as we said we measure energy in [J], the emission rate of light (which *is* energy) over time Q_e/t will be measured in watts [W], being joules per second [W] = [J/s]. This under the assumption that our source emits light at a constant rate, and indeed one might as well think of it as N_p photons per second, as long as one also tallies accurately the various wavelengths of these emitted photons exiting the source. We will come back to this point later in this work, because it’s the key ingredient to be able to discuss the light’s *color*, which is of course a matter of central importance in our discussion.

What we are going to do over the rest of this section is to continue to break down this aggregate notion of “energy from a light source” into simpler components, aiming to understand what quantity flows through one “ray of light” in more of a “bulk” way, and we’ll eventually double back and reason about the color of this light. For this reason, we were saying we had received from a light source S , a certain amount of energy Q_e [J]. If we got this energy over a certain period of time t [s] (measured in seconds) at a constant rate, we can determine the light’s power as $\Phi_e = Q_e/t$ [W]. Due to the fact that it is said that such a source *radiates* energy, this quantity Φ_e is called the *radiant power* of the source. Further, because it’s a measure of how much energy *flows* out of it, it is also equivalently called the source’s *radiant flux*, which is why the symbol is Φ , the greek letter for sound ‘f’.

This idea of flow makes it relatively natural to think about light flowing *through* something like a window, a door, more technically called an *aperture*. Obviously light can flow into an aperture just as well as it can flow out of it: when light leaves an aperture we will say that the quantity is *exitant*, for example we could talk of “exitant radiant power” to indicate light leaving from an aperture flowing out of it, whereas when light arrives at an aperture flowing into it we will say it is *incident* to it. Lastly, as much as it’s valuable to discuss light through a specific given aperture, sometime we will want to talk about all the light that leaves a source without much of an interest as to where exactly this flow happens: in this case the mental model is to think about all light flowing through an imaginary sphere surrounding the whole source. When there is a need to underline that

we're talking about all the light in this sense, we will use the adjective *total*, so for a light source we will say in short "radiant power" in most cases meaning "total exitant radiant power".

This sphere idea is the key to understand the so-called *inverse square law* for light intensity: we will see in a moment that our everyday sense of a light's brightness is how much energy we receive at a location of interest in terms of its density over area. In the simple case where the light emits photons uniformly in all directions, the area density of their flow at a distance r [m] from their origin will be $\Phi_e/(4\pi r^2)$ (being total power for the source divided by the surface area of the sphere). You can see that if you grow the area of the sphere this area density will go down like the square of the radius, being the distance from the source, while conservation of energy will keep the light's power Φ_e unchanged.

It is natural to think of radiant power as originating from a location x on our source, or more formally we should say a small region δS around x on the source: for instance a source like a stained glass window would transmit different amounts of energy across its surface, as a consequence of the different absorptions of the various pieces of colored glass that it's made of. This leads to an intuitive notion of radiant power from a specific point x on the surface of the source $M_e(x)$, and we would like this to be defined so that total power from the source S would be computed directly by integration over all of its surface S :

$$\Phi_e = \int_S M_e(x) dx \quad [\text{W}]$$

this quantity M_e is called *radiant exitance* and represents the area density of radiant power emitted by a source, formally

$$M_e = \frac{d\Phi_e}{dS} \quad \left[\frac{\text{W}}{\text{m}^2} \right]$$

In the simple case where we have a uniformly emissive source the radiant exitance is simply the ratio of emissive power to its area $M_e = \Phi_e/S$.

Note that this concept of exitance only covers the direct *emission* from a surface, typical case being its emission as a *black body* according to Planck's model. Of course not all photons leaving a surface do so because of emission, some of them will simply be bouncing off in various kinds of *reflection* events (think of an object illuminated by a lamp: you see the object because what you really see are photons originating at the lamp, and bouncing off the object's surface), while others photons might just travel through the surface in *transmission* events (as we've discussed before in the case of a stained glass window).

The sum of these three components is called *radiosity*, and it's the only quantity in this document that is not covered by standardized lighting vocabulary. Rather it's a name and quantity borrowed from the heat transfer vocabulary (see for example [ISO 9288:2022]). So in general we would have radiosity defined as

$$J_e = M_e + J_{e,r} + J_{e,tr} \quad \left[\frac{\text{W}}{\text{m}^2} \right]$$

where $J_{e,r}$ is the component due to reflection and $J_{e,tr}$ is the component due to transmission.

In a similar way, instead of considering power coming from a specific location, when dealing with sources that are small when compared to other dimensions in play, one could consider a notion of power leaving the source S in a given direction ω . This is what

is done in architectural modeling to capture the lighting patterns formed by specific physical light fixtures, for example: the source *per se* is considered to have negligible spatial extents, but the shape of the light it gives off is of interest to study how a given room would receive light. As before we would like this quantity defined so that the power comprised within a range of directions, all coming from this small source which has no lateral extents, could be directly computed by integration over a solid angle Ω :

$$\Phi_e = \int_{\Omega} I_e(\omega) d\omega \quad [\text{W}]$$

the integrand $I_e(\omega)$ is called *radiant intensity* and represent the density of power with respect to directions from the source, formally

$$I_e = \frac{d\Phi_e}{d\Omega} \quad \left[\frac{\text{W}}{\text{sr}} \right]$$

Once again, it is important to note that radiant intensity should be considered a “far-field” quantity, that is to say, a quantity that is only valid when the source is extremely small in comparison to the other dimensions at play.

Now that we have a notion of power *from a location* (radiosity or exitance) and power *in a given direction* (intensity), we can combine the two to get power *from a region in a given direction*, which as before is a quantity that lets us compute radiant power by integration in area and direction:

$$\Phi_e = \int_S \int_{\Omega} L_e^{\uparrow}(x, \omega) \cos \theta dx d\omega \quad [\text{W}]$$

the integrand $L_e^{\uparrow}(x, \omega)$ is called (exitant) *radiance* and represents the power density with respect to area and directions from the source, formally

$$L_e^{\uparrow} = \frac{d\Phi_e}{\cos \theta dS d\Omega} \quad \left[\frac{\text{W}}{\text{m}^2 \cdot \text{sr}} \right]$$

in most of what follows it will be useful to explicitly distinguish the direction of flow for our rays, for this reason we’ll annotate *exitant* radiance and *incident* radiance with a little arrow in the exponent: exitant radiance pointing up L_e^{\uparrow} and incident radiance pointing down L_e^{\downarrow} . Here, θ denotes the angle between the direction ω and the normal. The so called *projected solid angle* $d\omega^{\perp} := \cos \theta d\omega$ accounts for the change of flux received per infinitesimal area by a beam of light according to its orientation towards the surface.

We invite our readers to consult [Nicodemus, 1963] for a deeper dive into the meaning and origin of *radiance*, a relevant extract of which is included in Appendix C of this document.

As we said, one can think of radiance as photons per second along a ray, leaving or reaching a given location along a given direction. As much as energy can leave a region or location, it can also arrive there, and as before this also can vary across our region (imagine the light cast by our stained glass window from before onto a floor, or the dappling of light and shadow you’d have when standing under a tree) so it is natural to formulate a notion of *incident* power density across an area of a receiver. The total incident radiant power over a region R on the receiver can then be computed by integration across its surface:

$$\Phi_e = \int_R E_e(x) dx \quad [\text{W}]$$

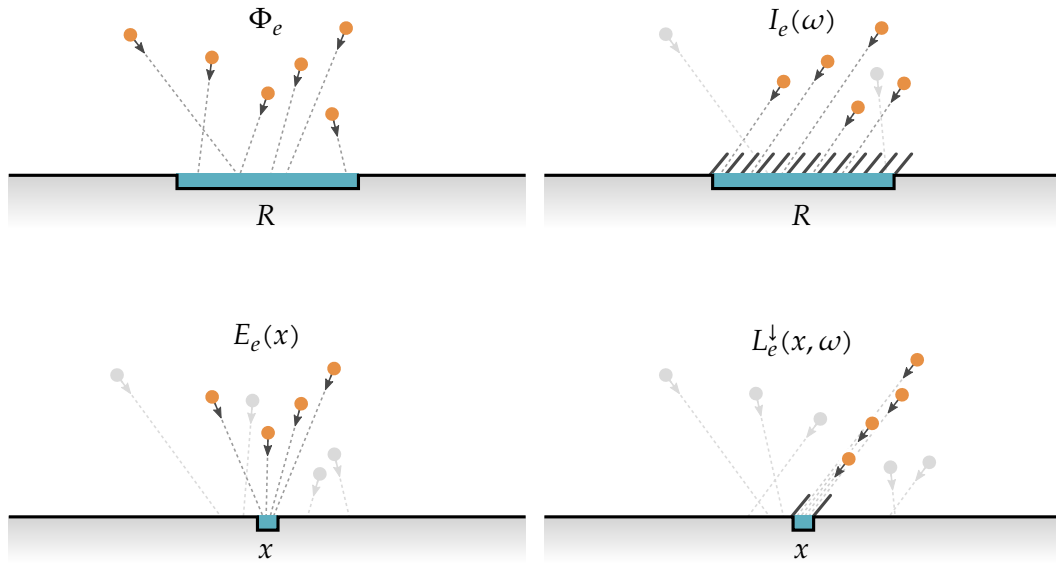


Figure 1.1: A visualization of various measures of radiant energy incident onto a surface: incident radiant power (top left), incident radiant intensity (top right), irradiance (bottom left), and incident radiance (bottom right). Incident radiant power Φ_e is the total energy per unit time incident everywhere on the area R from all directions Ω . Incident radiant intensity $I_e(\omega)$ is the energy incident from a specific direction ω everywhere on R , while irradiance $E_e(x)$ is the energy incident at a given point x from all direction Ω and radiance $L_e^\downarrow(x, \omega)$ at a given location x from a given direction ω . Intensity can be obtained by integrating radiance $L_e^\downarrow(x, \omega)$ over R , while irradiance can be obtained by integrating radiance over the set of all directions Ω . Integrating L_e^\downarrow over both the surface and all directions yields incident power.

the value $E_e(x)$ is the receiver's area density of incident radiant power and is called *irradiance*, and it's in a way some kind of opposite of radiant exitance in that one describes incident flow while the other described exitant flow. And indeed, exactly like radiant exitance, irradiance as well has a differential formulation:

$$E_e = \frac{d\Phi_e}{dR} \quad \left[\frac{\text{W}}{\text{m}^2} \right]$$

Comparing all the relations above, we can express radiant exitance and irradiance in terms of radiance as a solid angle integral:

$$M_e(x) = \int_{\Omega} L_e^\uparrow(x, \omega) \cos \theta d\omega \quad E_e(x) = \int_{\Omega} L_e^\downarrow(x, \omega) \cos \theta d\omega$$

and a similar relation holds radiant intensity in terms of an area integral

$$I_e(\omega) = \int_A L_e(x, \omega) dx$$

The last quantity that is of interest to us is *radiant exposure*, in fact, in terms of making images, one could say this is the *most* important quantity of them all. Exposure is a measure of the area density of the photons that landed in a region, and it's precisely what a camera measures: film cameras contain photosensitive film, where more arriving photons transfer more energy onto the sensitive media and give a stronger effect⁶,

⁶Although counterintuitive this implies that the sensitivity grading of physical film stock depends on the size of image being formed. And in fact this is the case in practice: in order to take photographs with the same exposure settings using media of different formats, the larger stock needs to be chemically more sensitive to light to compensate for the lower *exposure* resulting from the larger area. Manufacturers do take this into account when film is graded

whereas digital cameras (be them **CMOS**-based or **CCD**-based) directly count photons. The definition of **exposure** is similar to the definition of **irradiance**

$$H_e(x) = \frac{dQ_e}{dR} \quad \left[\frac{\text{J}}{\text{m}^2} \right]$$

where the source radiant power Φ_e was replaced with the source *energy* Q_e . Thinking about it, you can convince yourself that exposure is quite clearly what a camera sensor does: it receives photons for a certain period of time at a position from all directions admitted by the lens aperture. This can be seen mathematically too:

$$H_e(x) = \int_{\Delta t} E_e(x) dt = \int_{\Delta t} \frac{d\Phi_e}{dR} dt = \frac{d}{dR} \int_{\Delta t} \Phi_e dt = \frac{dQ_e}{dR}$$

Somewhat orthogonally to all the above, we can consider spectral distributions of all these quantities, which are the spectral densities of the quantities above. First we define *spectral radiant power* as the density of radiant power with respect to wavelength:

$$\Phi_{e,\lambda} = \frac{d\Phi_e}{d\lambda}$$

and then we obtain the *spectral* version of all the quantities discussed so far either by differentiation along λ or by substitution from above

$$\begin{aligned} M_{e,\lambda} &= \frac{dM_e}{d\lambda} = \frac{d\Phi_{e,\lambda}}{dS} & E_{e,\lambda} &= \frac{dE_e}{d\lambda} = \frac{d\Phi_{e,\lambda}}{dR} & H_{e,\lambda} &= \frac{dH_e}{d\lambda} = \frac{dQ_{e,\lambda}}{dR} \\ I_{e,\lambda} &= \frac{dI_e}{d\lambda} = \frac{d\Phi_{e,\lambda}}{d\Omega} \\ L_{e,\lambda} &= \frac{dL_e}{d\lambda} = \frac{d\Phi_{e,\lambda}}{dS d\Omega} \end{aligned}$$

1.3 Measuring light and brightness

We must remember that a photograph can hold just as much as we put into it, and no one has ever approached the full possibilities of the medium.

ANSEL ADAMS

One of the central points of this document is to put units to the pixel values in a raster image. For the scope of this introductory section, we will ignore the chromatic issue, and focus on the generation of grayscale images, where each pixel records the *brightness* of a scene at its respective location. In particular, and throughout this whole document, we will use the term *brightness* to indicate a non-specific, informal, plain-English, everyday meaning that a quantity may feel more or less “dim” to a human observer, this will be our generic, non-specific word to speak about the “strength” of our visual stimulus, when a more specific term would evoke too narrow a meaning. Our discussion will then proceed to specify the exact meaning in question more precisely and give it an appropriate name.

As we have just seen, radiometric quantities can be used to measure brightness in terms of *radiant power* and its derived quantities. However, if our image was generated

Radiometric		Radiometric spectral		Photometric	
name symbol	unit	name symbol	unit	name symbol	unit
Radiant Energy	Q_e	Spectral Radiant Energy	$Q_{e,\lambda}$	Luminous Energy	Q_v
Radiant Power	Φ_e	Spectral Radiant Power	$\Phi_{e,\lambda}$	Luminous Power	Φ_v
Radiant Exitance	M_e	Spectral Radiant Exitance	$M_{e,\lambda}$	Luminous Exitance	M_v
Radiosity	I_e	Spectral Radiosity	$I_{e,\lambda}$	Luminosity	I_v
Irradiance	E_e	Spectral Irradiance	$E_{e,\lambda}$	Illuminance	E_v
Exposure	H_e	Spectral Exposure	$H_{e,\lambda}$	Luminous Exposure	H_v
Radiant Intensity	I_e	Spectral Radiant Intensity	$I_{e,\lambda}$	Luminous Intensity	I_v
Radiance	L_e	Spectral Radiance	$L_{e,\lambda}$	Luminance	L_v

Throughput

étendue

area-solid-angle-product

$A\Omega$ product

Absorptance

Reflectance

Transmittance

G

$\text{m}^2 \cdot \text{sr}$

α

ρ

τ

Table 1.1: Correspondence between radiometric and photometric units

We abbreviate the unit for luminous energy talbot as Tb instead of the also common T to avoid confusion with the unit for magnetic flux tesla. We also use the convention of subscripting photometric quantities with v (for visual), radiometric quantities with e (for energetic) and spectral radiometric quantities with e, λ ; this follows the recommendations in [ISO 80000-7:2020]; [CIE S 017:2020]; [IEC 60050-845:2020].



Figure 1.2: Two views of the same scene: the left hand side shows intensity of a relatively narrow infrared band around 850 nm, while the right hand side shows ultraviolet light, in the 345–380 nm band. Both bands are moderately beyond what is visible by humans

Photograph by Tomas <https://www.nofocus.blog/>

using values proportional to this quantity, we would obtain an image that will not correspond well to the subjective sense of brightness in the scene as experienced by a person looking at it. And it wouldn't look much like a black-and-white photograph either, not one made with film stock a photographer would commonly use, or the black-and-white mode of a digital camera anyways. There are two broad classes of reasons why this is the case: on the one side radiant power includes *all* radiation bands, and so this radiant power “image” would have information about all sorts of wavelengths that have little to do with vision. Let's imagine for a moment a semi-realistic scenario where we'd build a device capable of capturing energy of wavelengths in the millimeters (say radar waves or far infrared waves) all the way to maybe single nanometers⁷ (which would be X-rays): it might be fun to try and imagine what pictures it would make. This brings up many questions, for example: photons in longer wavelengths don't carry all that much energy (one by one), so if we imagine that the number of photons arriving is roughly even across wavelengths (say maybe in a range of 100 : 1) we'd still need to make up for the fact that one nanometer photon will be a million times brighter than one millimeter photon, so it seems difficult to make useful pictures from such an incredibly wide dynamic range. In fact, without going to these extremes, even bands quite near to the visible range look substantially different than they do in the visible, as you can see in Figure 1.2. The other class of reasons is that, even restricting ourselves to the visible range, our sensitivity to brightness exhibits a marked dependency on the wavelength (as you can see in a plot of the luminous efficiency function $V(\lambda)$, for example in Figure 4.3). When black and white film was originally developed this was a very carefully considered affair, as you can see from Figure 1.3.

Because of how the human visual system is not equally sensitive to all wavelengths of light, our eyes may well perceive light emanating or reflecting off two objects with different radiant intensity as having the same brightness, as a consequence of differences in the

⁷And for short wavelengths all sorts of problems appear, for example many materials such as flesh cease being opaque, or scattering photons that much, a key capability for medical imaging



Figure 1.3: *Reproduction of an old advertisement image, illustrating the difference between orthochromatic film, most sensitive to greens and blues, and panchromatic film, having a somewhat more even response across the visible spectrum. Note that neither sensitivity curve is all that close to the luminous efficiency function $V(\lambda)$*

Photograph from <https://thedarkroom.com/orthochromatic-vs-panchromatic-film-a-photo-comparison/>

spectral distributions compensating away the difference in intensity. Conversely, **spectral distributions** carrying the same amount of radiant power are likely to be perceived as having different brightness levels when they appear to have different colors.

It is therefore useful, and in a way *necessary*, to reason about the power of light in two different ways, one dealing with energy levels as you would have in physics, called *radiometric*, and the other tuned or rebalanced, to account for the workings of human perception, called *photometric*⁸. As discussed before, in this document we will use **SI** units and the harmonized vocabulary resulting from [ISO 80000-7:2020]; [CIE S 017:2020]; [IEC 60050-845:2020].

From the point of view of *radiometry*, we saw how the *radiant power* of a source S is measured in *watts* [W] and is the total amount of energy per unit time emitted by S . From the point of view of *photometry*, there is a corresponding definition of *luminous power* for our source S (also called *luminous flux* as for the radiometry nomenclature) measured in *lumens* [lm], and being the amount of energy per unit time weighted by the *photopic spectral luminous efficiency function* $V(\lambda)$. This function was designed to model the response of the human visual system as a function of wavelength λ ⁹.

⁸The two approaches have historically used a great many units, until the *candela* [cd] was adopted as a base unit as part of Resolution 6 of the Tenth Conference on Weights and Measures held in 1954 [BIPM SI.2019], p. 163, and then supplemented by derived units for quantities *luminous flux* [lm], *luminance* [cd/m²] and *illuminance* [lx] at the Eleventh Conference on Weights and Measures held in 1960. At this Eleventh conference the base units (which were six at the time) were first given the name “Système International d’Unités” and its abbreviation **SI**. Many more details around various historical and **SI** units are described in [Meyer-Arendt, 1968]

⁹The photopic spectral luminous efficiency function $V(\lambda)$ is the result of a series of experiments and tabulations first published by the **CIE** in 1924 and then included as $\bar{y}(\lambda)$ in the color matching functions for

This means that two different light sources emitting the same luminous power will appear as having about the same brightness even when having different spectral distributions¹⁰.

Much like we’ve been using the subscript \square_e to indicate radiant quantities such as radiant power Φ_e or radiant intensity I_e , and the subscript $\square_{e,\lambda}$ to indicate their spectral counterparts $\Phi_{e,\lambda}$ and $I_{e,\lambda}$, we will indicate *photometric* quantities with the subscript \square_v for “visual”. Their definition follows one-to-one the corresponding radiometric quantity: for a given radiometric spectral quantity $X_{e,\lambda}$ we can construct its corresponding photometric quantity X_v integrating like this

$$X_v(\dots) = K_{cd} \int X_{e,\lambda}(\dots, \lambda) V(\lambda) d\lambda. \quad (1.1)$$

the corresponding names will also change, replacing “(spectral) radiant” with “luminous”. For example, given spectral radiant power $\Phi_{e,\lambda}(\lambda)$, the corresponding luminous power Φ_v is

$$\Phi_v = K_{cd} \int \Phi_{e,\lambda}(\lambda) V(\lambda) d\lambda \text{ [lm]}$$

The scaling constant $K_{cd} = 683 \text{ lm/W}$, formally called *luminous efficacy of monochromatic radiation*, scales these “reweighted watts” to lumens and is currently one of the seven defining constants for the **SI**. As such it defines¹¹ the base **SI** unit *candela* [cd], as the amount of luminous intensity of a source of monochromatic radiation of frequency 540 [THz] having a radiant intensity of 1/683 [W/sr].

Table 1.1 lists summarized names, units and symbols of the radiometric quantities we’ve discussed, as well as their spectral and photometric counterparts.

the *standard 2 degree colorimetric observer* [Smith and Guild, 1931].

¹⁰This statement can only be true approximately, as the specific spectral response of different humans exhibits a certain amount of variation, even among normal subjects. Also there are subjects having various different kinds of anomalies in their visual systems (called color vision deficiencies or color blindness), for whom this statement ends up being even less accurate

¹¹The details of the current definition are in [BIPM SI.2019], p. 135. The frequency of 540 [THz] corresponds to a wavelength of about 555.016 [nm] in *standard air*, a wavelength in the greens to which the eye of the standard observer is most sensitive. The radiant intensity of 1/683 [W/sr] was chosen to make the amount of 1 [cd] about equal to the older unit *standard candle*, which it superseded. This definition has been updated several times from the original definition, which had been established in 1933, based on the emission of a black body radiator at the freezing point of platinum (about 2042 [K]). This outdated definition is sometimes also found in literature [Meyer-Arendt, 1968].

Chapter 2

Imaging and lighting models

2.1 Describing imaging

Imaging is the process of capturing the **radiant power** resulting from a specific **scene** configuration and turning it into pixel values. This is done by creating a camera and sensor or film model and computing their response to the energy flowing through the scene. The imaging parameters describe how specifically this conversion should happen are collected here together with their symbols and dimensions:

focal length	f	[mm]
aperture number	N	[f – number]
focus distance	o	[m]
exposure time	Δt	[s]
film speed	S	[ISO]
CCT of the white point	T_{cp}	[K]
filmback dimensions		[m ²]
image resolution		[pxl]

In our imaging model, the pixels in the image are triples of floating point numbers, known as **tristimulus values**, their magnitudes being linear in the spectral radiant **exposure** of the various pixels. The **imaging equation**¹, relating the final color C_{col} of a pixel p^{img} to the incoming **spectral radiance** may appear daunting at first

$$C_{col}(p^{img}) = \frac{1}{A_p^{img}} \int_{\Delta t} \int_{\lambda} \int_{\Omega_a^{img}} \int_{A_p^{img}} W(x, \lambda) L_{e, \lambda}^{img}(x, \omega, \lambda, t) \cos \theta dx d\omega d\lambda dt \quad (2.1)$$

In order to understand what's happening, we'll start making a simplifying assumption: we will ignore for the time being the dependency of $W(x, \lambda)$ on x , and pretend it was simply $W(\lambda)$. Once we have a clearer vision of how the imaging equation would work in this simpler case, it'll be clear what to do in the more general case. We will also explain what's the meaning and purpose of $W(x, \lambda)$ in Section 2.1.1, for the moment we just know we need to do *something* to **spectral radiance** $L_{e, \lambda}^l$ to make pictures out of it.

We've seen in Section 1.3 what's the reasoning behind a need for the values of our pixels to be proportional to the **luminous exposure** there. In practice two realities will

¹This equation is present in [Kolb et al., 1995], Eq. 1 in an effectively equivalent form, there it's called the *measurement equation*. However several other authors don't include in their definition of the *measurement equation* the aspect of integration in the time domain, which is of key importance for our work [Dutr   et al., 2003], p. 45, Eq 2.33; [Pharr et al., 2023], so to minimize confusion we chose to use a different name

manifest: one is that the pixel has a certain, non-0 area: we used the symbol A_p^{img} for this little region². The other is that over this area the incoming **spectral radiance** won't necessarily be uniform (at least not in the general case: there might be a shadow boundary across the pixel, or more likely some kind of gradient across it). The innermost integral

$$\bar{L}_{e,\lambda}^{img}(p^{img}, \omega, \lambda, t) = \frac{1}{A_p^{img}} \int_{A_p^{img}} L_{e,\lambda}^{img}(x, \omega, \lambda, t) dx$$

is how we replace the incident **spectral radiance** L^\downarrow with its own average \bar{L}^\downarrow over A_p^{img} , which is our pixel region located at p^{img} . There is no need for $W(\lambda)$ here: it doesn't depend on x so we can factor it out of this integration step.

The next integral is then

$$E_{e,\lambda}(p^{img}, \lambda, t) = \int_{\Omega_a^{img}} \bar{L}_{e,\lambda}^{img}(p^{img}, \omega, \lambda, t) \cos \theta d\omega$$

which is an expression to compute **spectral irradiance** over this given solid angle Ω_a^{img} : much like p^{img} is our location on the image, a is the opening that makes up our aperture, so that Ω_a^{img} is the solid angle with apex at our image location p^{img} (ie. on the filmback) that spans the aperture³. And there is no $W(\lambda)$ here either: like before it doesn't depend on ω so we can factor it out of this integration step too.

The next layer of the integral is where we take care of the **spectral** side of things:

$$E_{col}(p^{img}, t) = \int_{\lambda} W(\lambda) E_{e,\lambda}(p^{img}, \lambda, t) d\lambda$$

and here we have to include $W(\lambda)$, obtaining something *similar* to **irradiance** or **illuminance**, but not quite. Rather, it's some kind of weighted average of the spectral irradiance, where $W(\lambda)$ provides the (spectral) weighting. There is light at the end of the tunnel, after all (if you pardon the pun).

The subscript \square_{col} reminds us there is some weighting that has happened here, and of course it suggests there will have to be some relation to *color* in a way or the other. We can now finish turning our **irradiance/illuminance**-like quantity into a corresponding **exposure**-like quantity integrating over time:

$$H_{col}(p^{img}) = \int_t E_{col}(p^{img}, t) dt$$

and this concludes our analysis of the *imaging equation*. We've reduced it to a rather innocent looking expression

$$C_{col}(p^{img}) = H_{col}(p^{img})$$

or in words: "to make a picture, set the color of each pixel to the exposure there", but we'll want to pay attention to just what exactly we mean by "exposure".

²We'll be using the \square^{img} superscript to indicate *image* space locations, positions on the plane where the image is formed (we call this the **filmback**). And we're using a \square_p subscript to signify we're interested in the specific location p , which will normally be an argument of a function being defined. To reduce clutter we won't repeat the \square^{img} superscript in more than one place in a single symbol

³Our eagle-eyed readers will have observed that Ω_a^{img} will have a dependency on p^{img} as well: we've omitted it from the symbol to avoid making the notation even more complex. Note that $\cos \theta$ does take the dependency into account correctly

2.1.1 The film response function

With the mathematical meaning of the *imaging equation* under our belt, we still need to double back and understand what is the story with that original $W(p^{img}, \lambda)$ term. We call this function *film response function* and we use it to capture how the film or sensor responds to incident *spectral radiance* (being a whole bunch of photons landing on it). Because in certain situations the sensitivity is not spatially uniform across the *filmback*, we need to keep this weighting factor right in the heart of our integral.

It will probably help gain some intuition for the purpose and meaning of W if we go and see what happens in a few practical cases. In the case in which $W(p^{img}, \lambda)$ is the identity function, the result of the integral would be measured in $[J/m^2]$, and we would have $H_{col} = H_e$. As discussed in Section 1.3, images constructed this way, even if they were possible⁴ just won't look natural, and are quite unlikely to have much practical use at all.

That same discussion might inspire us to use $W(p^{img}, \lambda) = K_{cd}V(\lambda)$, which would result in $H_{col} = H_v$: doing this would give us images where the pixel values are a direct readout of the scene's luminous *exposure*. These would be images that track fairly well a human's sense of brightness of a scene, and provide a passable, but not very accurate, approximation of an orthochromatic film stock with reduced blue sensitivity⁵, the difference from the look of what we'd normally consider to be a black-and-white photo is illustrated in Figure 1.3.

All this being said, the reality is that in practice the film response functions that one finds in common use are typically modeled as a product of components, each dependent either on wavelength or on position, and so we decompose it as follows

$$W(p^{img}, \lambda) = k_i S W_{pos}(p^{img}) W_{col}(\lambda) \quad (2.2)$$

where k_i is the *imaging constant* (defined in Equation (2.6)), S is the *film speed*, $W_{pos}(p^{img})$ describes the *local response* of the filmback and $W_{col}(\lambda)$ describes its *spectral response*.

Spectral response

We've already seen a couple examples of candidates for the spectral component of the *film response function*. These however had mostly theoretical value, to illustrate the purpose of the film response function as a whole. In order for us to make ordinary color images, we need to produce data suitable to convert into a color space of our liking.

Color spaces are in turn normally defined using a 3×3 matrix, which transforms data from *CIE XYZ* coordinates to the space of interest. For example to obtain data appropriate for the *sRGB* primaries, starting from a color C_{XYZ} in *CIE XYZ* coordinates stored in a column vector, we would use

$$C_{sRGB_t} = M_{sRGB_t} C_{XYZ} = \begin{bmatrix} 3.2404542 & -1.5371385 & -0.4985314 \\ -0.9692660 & 1.8760108 & 0.0415560 \\ 0.0556434 & -0.2040259 & 1.0572252 \end{bmatrix} C_{XYZ}$$

⁴As discussed before, film stock or a digital device that behaves like this across a wide region of the electromagnetic spectrum simply cannot be built: if nothing else because photons larger than a pixel on the sensor will just "bounce" right off, and photons much smaller than the sensor's components will simply traverse it and continue mostly undisturbed. This makes it impossible to have values even roughly representative of H_e .

⁵Silver halides are very sensitive to short-wavelength light, so film stock with reduced sensitivity in the blues is exceptionally difficult to produce

The reason for this is that the **CIE XYZ** color space, described in [CIE 015.2018], is a space that was built⁶ to capture the response to color of the human visual system. This makes it effectively a *lingua franca* of color, that people can use to objectively capture and reproduce a color sensation.

To state in our notation what's commonly done in digital image synthesis we would construct a film response function $W_{XYZ}(\lambda)$ defined like this:

$$W_{XYZ}(\lambda) = \begin{pmatrix} \bar{x}(\lambda) \\ \bar{y}(\lambda) \\ \bar{z}(\lambda) \end{pmatrix} \quad (2.3)$$

this is a function that given a wavelength λ returns a column vector made from the values of the three defining functions of **CIE XYZ** space, namely $\bar{x}(\lambda), \bar{y}(\lambda), \bar{z}(\lambda)$.

This is a notational convenience that saves us the work to write down the imaging equation three times: with $W_{XYZ}(\lambda)$ defined this way, we obtain a result C_{XYZ} in **CIE XYZ** space. We can then construct our **sRGB** image multiplying this result by the M_{sRGB_t} matrix as above and applying a gamma function as needed according to the definition of **sRGB** space (details on this and other color space transformations are available in Appendix B).

Equivalently, we can simply transform the **CIE XYZ** function samples for each wavelength λ of interest, thus obtaining a new response function that construct for us directly linear **sRGB** values:

$$W_{sRGB_t}(\lambda) = M_{sRGB_t} W_{XYZ}(\lambda)$$

Although using **CIE XYZ** spectral response is common practice in digital image synthesis (see for example [Pharr et al., 2023]; [Jakob et al., 2022]; [Ward, 1994]), we actually have in front of us a different, intriguing opportunity to explore. In fact it's quite evident that this is not how a camera actually works, be that digital or film-based. Rather, the sensing media in the device will have its own spectral response, defining a camera-specific **RGB** space which we'll call cameraRGB_t . For analogy with how **CIE XYZ** space is defined, we'll call these response curves $\bar{r}(\lambda), \bar{g}(\lambda), \bar{b}(\lambda)$, where the r, g, b function names indicate these correspond to our red, green and blue photosites, and the overbar indicates some normalization had been applied. With this in hand, our spectral film response function would be

$$W_{\text{cameraRGB}_t}(\lambda) = \begin{pmatrix} \bar{r}_{\text{cameraRGB}_t}(\lambda) \\ \bar{g}_{\text{cameraRGB}_t}(\lambda) \\ \bar{b}_{\text{cameraRGB}_t}(\lambda) \end{pmatrix} \quad (2.4)$$

giving us a framework which will make our rendered images match our “camera raw” data.

This is a valuable thing to do in the interest of matching the metamerism of the camera and in general its specific ability to perceive color. In turn this will eliminate one source of discrepancies in the appearance of photographed objects when compared to renders of their virtual counterparts.

At this point, the same image processing pipeline used for the real camera that is being modeled will apply unchanged to the rendered data, further details are outlined in Appendix B.

⁶The **CIE XYZ** color space was very carefully derived from measurements done in the late 1920's by W. David Wright and John Guild to capture as accurately as possible how humans see color. The color space was introduced in [Smith and Guild, 1931] and a fascinating account of the process was collected in [Fairman et al., 1997]

Local response

As spectral radiance $L_{\lambda}^{img}(x, \omega, \lambda, t)$ lands on a pixel away from the center of the image, its effect on the image decreases by a factor $\cos \theta$ due to its angle of incidence on the filmback, a phenomenon that dominates the appearance of vignetting. In digital image synthesis this is often compensated away using a position dependent component of the sensor response function

$$W_{pos}(x) = \frac{1}{\cos \theta_x} \quad (2.5)$$

where θ_x is the angle between the incident ray and the normal to the filmback at x .

Note that we're using x here and not p^{img} : this function is used within our innermost integral, the one we used to compute $\bar{L}_{\lambda}^{img}(p^{img}, \omega, \lambda, t)$ where x varies over A_p^{img} to compute the average of incoming spectral **radiance** across our filmback pixel area.

The real implementation will actually have a wider integration support, and $W_{pos}(x)$ will normally also include a band-limiting function⁷, used to reduce or eliminate the emergence of *moiré patterns* in the image. Introducing band-limiting in the image limits sharpness attainable in pictures, which is undesirable in certain application domains. The evolution of digital camera products has been interesting in this respect: the early digital cameras simply had a **CCD** or **CMOS** sensor at the filmback and then users started complaining from the appearance of moiré patterns in their pictures. To alleviate this, several of the manufacturers introduced cameras where a blurring filter was mounted in front of the sensing element, so that moiré was reduced or eliminated. However, as camera resolutions became higher and higher some users became unhappy again with these blurring filters, lamenting excessive blur in certain conditions, and models without this filter were reintroduced as premium niche products, for example NIKON's D800E model from 2014.

Imaging constant The remaining factor in the sensor response function $W(x, \lambda)$ is the imaging constant k_i , which is defined as

$$k_i = \frac{4K_{cd}}{C} \simeq \frac{4 \cdot 683}{312.5} = 8.7424. \quad (2.6)$$

The constant C (valued at $312.5 = 100 \frac{25}{8}$ in this document) is sometimes called the *incident light meter calibration constant* and effectively defines the units for the **film speed** S . Note that as we use exact integration, our value for C is close to what would be used on a meter fitted with a hemispherical receptor and somewhat lower, because our exact implementation doesn't suffer from losses at near-grazing angles as a physical device would.



This section is under construction

Discussion covering the use of C versus K calibration constants and the use of flat-receiver (cosine response) versus hemispherical receiver (cardioid response).

⁷In rendering this is sometimes called a **pixel filter**, and it's been a very active area of research. See [Pharr et al., 2023] for a detailed introduction to the subject

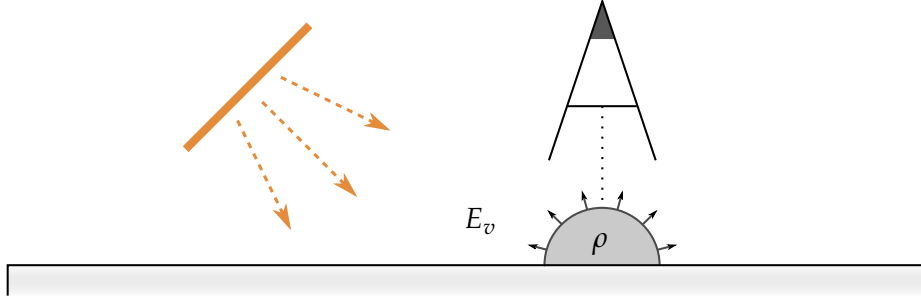


Figure 2.1: Setup for our proof about the exposure equation. The Lambertian reflector with albedo ρ is parallel to the image plane, and the incident illumination is E_v .

2.2 Luminance and sensor response

We initially posed the question of how a given pixel value concretely relates to the measurement. As we will derive below, Equation (2.1) can be simplified to the following compact form.

$$Y(p^{img}) \approx \frac{\pi \Delta t S}{C N^2} L_v^{\uparrow obj}, \quad (2.7)$$

which directly relates the luminance emitted towards the camera pupil with the luminance of the corresponding sensor response value. This approximation is valid for distant to mid-field objects for which angular variation is insignificant. For simplicity we confine ourselves here to luminance, although in reality the sensor response is carried out in *camera RGB*. However, the analysis can be carried out analogously by applying the camera response curves instead of \bar{y} . Furthermore, due to physical constraints and limited storage precision, physical camera sensors obey the linearity of (2.7) only within certain ranges of incoming light: while most of them are very close to being linear for the majority of their range, they will of course stop responding at the upper limit of brightness (they “clip”) and often exhibit a mild over-sensitivity in the darkest side of the range. This behavior is very specific to each device, for example cameras meant for use in astrophotography contain provisions to better linearize the sensitivity to dim light.

From this it directly becomes obvious that if the aperture number N , exposure time Δt , and film speed S are set to satisfy the so-called *exposure equation*

$$E_v = C \frac{N^2}{\Delta t S} = \frac{C 2^{EV}}{S} \quad (2.8)$$

the image of a Lambertian reflector with albedo ρ (i.e., $L_v^{\uparrow obj} = E_v \frac{\rho}{\pi}$) at the center of the sensor will have luminance $Y(p^{img}) = \rho$ if the illuminance incident on the reflector is E_v . Or in other words, given a measured scene illuminance, camera exposure values chosen to satisfy the exposure equation thus yields pixel values in a reasonable range.

To see why Equation (2.7) is true, first consider that in the center of the sensor, $W_{pos}(x) = 1$. The sensitivity then reduces to $W(x, \lambda) = k_i S \bar{y}(\lambda)$, and we can rewrite Equation (2.1) in terms of luminance $L_v^{\downarrow img}$ passing through the aperture:

$$Y(p^{img}) = \frac{k_i \Delta t S}{K_{cd} A_p^{img}} \int_{A_p^{img}} \int_{\Omega_a^{img}} L_v^{\downarrow img}(x, \omega) \cos \theta dx d\omega. \quad (2.9)$$

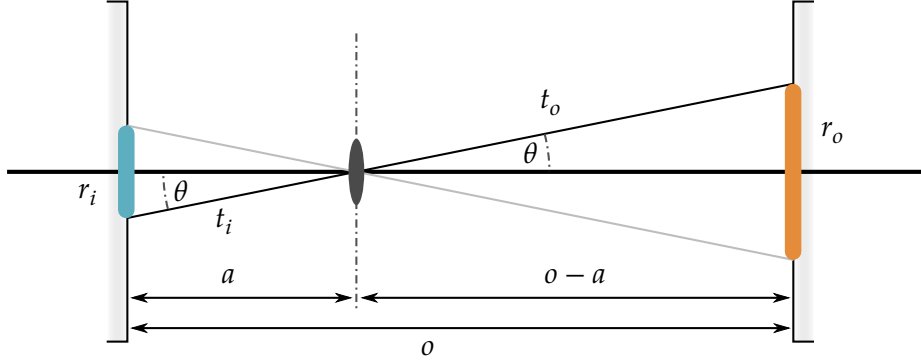


Figure 2.2: Relating image and object size in a camera where the aperture is small compared to the distance $o - a$ between the aperture and the object.

The integration along the time dimension t reduces to a multiplication by Δt due to the illumination field being constant in time.

Each point p^{img} on the filmback corresponds to a point p^{obj} on the focus plane in object space. Energy conservation demands that the luminous flux Φ_{av} through the aperture must have the same value when computed from the sensor side or the object side. Assuming the aperture is a disk parallel to the filmback plane, and using the luminance $L_v^{\uparrow obj}$ reflected off the Lambertian surface into the imaging system,

$$\begin{aligned}\Phi_{av} &= \int_{A_p^{img}} \int_{\Omega_a^{img}} L_v^{img}(x, \omega) \cos \theta d\omega dx \\ &= \int_{A_p^{obj}} \int_{\Omega_a^{obj}} L_v^{\uparrow obj}(x, \omega) \cos \theta d\omega dx \\ &= A_p^{obj} \Omega_a^{obj} L_v^{\uparrow obj}\end{aligned}\quad (2.10)$$

The last equality assumed that $L_v^{\uparrow obj}(x, \omega)$ has negligible variation over $(x, \omega) \in A_p^{obj} \times \Omega_a^{obj}$ and $\cos \theta \simeq 1$ for all $\omega \in \Omega_a^{obj}$. In other words, the aperture is small as seen from p^{obj} and p^{obj} is very near the optical axis of the system. Consequently,

$$\int_{A_p^{img}} \int_{\Omega_a^{img}} L_v^{img}(x, \omega) \cos \theta d\omega dx = A_p^{obj} \Omega_a^{obj} L_v^{\uparrow obj}. \quad (2.11)$$

Substituting into Equation (2.9), we obtain

$$Y(p^{img}) = \frac{k_i \Delta t S}{K_{cd} A_p^{img}} A_p^{obj} \Omega_a^{obj} L_v^{\uparrow obj}. \quad (2.12)$$

At this point, in order to compute $Y(p^{img})$ we need to compute the ratio of areas A_p^{obj}/A_p^{img} , and the solid angle Ω_a^{obj} . Let a be the distance between the filmback and the aperture on the optical axis and o the distance between filmback and focus plane. From Figure 2.2, we can see that

$$\frac{A_p^{obj}}{A_p^{img}} = \frac{r_o^2}{r_i^2} = \frac{t_o^2 \sin^2 \theta}{t_i^2 \sin^2 \theta} = \frac{t_o^2}{t_i^2} \cdot 1 = \frac{t_o^2 \cos^2 \theta}{t_i^2 \cos^2 \theta} = \frac{(o - a)^2}{a^2}.$$

The solid angle Ω_p^{obj} can be computed assuming that the radius of the aperture

$$r = \frac{f}{2N} \quad (2.13)$$

is much smaller than the distance $o - a$ between the object and the center of the aperture. In this configuration we have simply

$$\Omega_p^{obj} \simeq \frac{\pi r^2}{(o - a)^2} \quad r \ll o - a. \quad (2.14)$$

Substituting both results into Equation (2.12), we obtain

$$Y(p^{img}) = \frac{k_i \Delta t S}{K_{cd}} \frac{(o - a)^2}{a^2} \frac{\pi r^2}{(o - a)^2} L_v^{\uparrow obj}. \quad (2.15)$$

If the object distance o is far greater than the focal length f we have

$$f \ll o \Rightarrow f \simeq a \quad (2.16)$$

and thus

$$Y(p^{img}) = \frac{k_i \Delta t S}{K_{cd}} \frac{\pi r^2}{a^2} L_v^{\uparrow obj} \stackrel{(2.13)}{=} \frac{\pi k_i \Delta t S}{4 N^2 K_{cd}} L_v^{\uparrow obj} \quad (2.17)$$

which using Equation (2.6) concludes our proof. \square

Applying white balance White balance is a color correction step intended to give a certain spectral distribution neutral gray coordinates in the target color space. The whitepoint is often specified using the **Correlated Color Temperature (cct)** of the given color, sometimes augmented by a second value called *tint* that is intended to represent a color shift in some other direction in the chromaticity plane.

Conceptually, the idea is that color temperature correction gives an adjustment along the orange-blue axis, and tint provides a mean to correct along the remaining dimension of the chromaticity space, which is a green-magenta shift.

Unfortunately there is little agreement in the implementations as to how exactly this should be performed: the color correction temperature seems to be mostly understood as the color of a black body emitter for temperatures below 4000K and of **CIE Illuminant D** above that.

The case of the tint correction is somewhat more complicated with various interpretations of how such an axis should be oriented: in some descriptions the axis is orthogonal to the spectral locus of the black body emitter, so that the orientation depends on the specific **cct** chosen. In others, it has a constant orientation.

Further, the amount of color shift along the tint axis has various ranges such as $[0, 1]$, $[-100, 100]$ and various interpretation as to whether the amount of apparent adjustment should be uniform along the range or not.

On the other hand, there seems to be consensus that white balance be implemented as a component-wise division performed in camera **RGB** coordinates, meant to divide out the coloration of the target whitepoint from the image. In order to not introduce excessive brightness alterations to the image, the correction color is adjusted to have either unit luminance Y in **CIE XYZ** coordinates or unit camera **RGB** green component, an approximation of unit brightness, useful for compute-constrained devices such as digital cameras.

This means that the image would be computed in camera **RGB** coordinates, divided by the color of the whitepoint in camera **RGB** coordinates, and then multiplied by the camera **RGB** values obtained by inverse transforming $(1, 1, 1)$ from the target **RGB** space to the camera **RGB** space.

2.3 Describing light sources

Light sources are modeled as emitters characterized by spectral distribution and angular profile, and further modified by a “filter” or “gel” (called *tint function* in this document). We want to derive a formulation for spectral exitant radiance $L_\lambda^\uparrow(x, \omega, \lambda)$ given specific light properties. We will do that by means of an *intrinsic emission function* $\bar{L}_\lambda^\uparrow(x, \omega, \lambda)$ describing the directional and spectral properties of the light source (inclusive of the tint) and scale this function as needed to obtain exitant radiance:

$$L_\lambda^\uparrow(x, \omega, \lambda) = k_e \cdot \bar{L}_\lambda^\uparrow(x, \omega, \lambda) \quad (2.18)$$

where k_e is a scaling factor called the *emission constant*.

The value of the emission constant is derived *a posteriori* from the source’s power once the emission profile, the angular distribution and the tint function are fixed, as opposed to a more traditional specification in which it would be the emission constant to be specified directly as a light parameter and the power computed from the other quantities.

We propose using luminous power for finite sources (such as area lights) and illuminance for non-finite sources (such as **Image based lighting (IBL)** sources) to specify source brightness and to consider these to be quantities inclusive of the effects of the tint function.

The rationale behind this choice is that it is desirable to setup lighting on a scene in terms of perceived brightness of the final rendered image, abstracting away concerns with such matters as specific spectral or angular profiles of emitters, in an effort to try and focus attention towards the broad brightness ratios of a scene. For example, this arrangement minimizes changes in perceived scene brightness (and more so brightness ratios) in the event of substitution of a tint function with another.

Texture maps It is common to use texture maps to define some of the emission distribution functions. A texture map can be seen as a function $M(x, \lambda)$ that specifies a spatial distribution of color values, the function is dependent on pixel position x and wavelength λ . For later calculations it is useful to separate the spectral dependency from the spatial dependency. For example, in the case of an **RGB** map, a possibility could be to use a three-primary decomposition to separate pixel position from color values:

$$M(x, \lambda) = M_r(x)r(\lambda) + M_g(x)g(\lambda) + M_b(x)b(\lambda) \quad (2.19)$$

where $r(\lambda)$, $g(\lambda)$ and $b(\lambda)$ are the hypothetical spectral distributions of the map’s primaries for red, green and blue and $M_r(p)$, $M_g(p)$ and $M_b(p)$ are the corresponding values stored in the map for a given pixel position x .

It will be convenient in the upcoming sections to make use of a different notation: we call $M_{col}(x) : X \rightarrow \mathbb{R}^n$ the function that maps the position x to its coordinates in a specified n dimensional color space col . For example for the **RGB** color space we would have $n = 3$:

$$M_{rgb}(p) = (M_r(p), M_g(p), M_b(p)) \in \mathbb{R}^3 \quad (2.20)$$

but see Appendix B for an $n = 7$ example. A similar thing can be done for the primaries, joining them into a single function $col(\lambda) : \mathbb{R}^+ \rightarrow \mathbb{R}^n$ which maps a wavelength to the response of the n primaries at once. For **RGB** we would have $n = 3$ and $rgb(\lambda)$ would be:

$$rgb(\lambda) = (r(\lambda), b(\lambda), g(\lambda)) \in \mathbb{R}^3 \quad (2.21)$$

This notation lets us write an equivalent, more compact definition for $M(x, \lambda)$ in terms of the scalar product operation in \mathbb{R}^n

$$M(x, \lambda) = \langle M_{col}(x), col(\lambda) \rangle \quad (2.22)$$

or for **RGB** in \mathbb{R}^3

$$M(x, \lambda) = \langle M_{rgb}(x), rgb(\lambda) \rangle \quad (2.23)$$

Appendix B contains some further details on possible ways to construct these spectral distributions for the primaries. The following subsections will describe the functions needed to specify the different types of lights and show how to calculate the emission constant from the specifications.

2.3.1 Area Lights

The emission for an area light source is specified by:

- Φ_v – luminous power [lm]
- A – area [m²]
- $\hat{L}(\lambda)$ – spectral distribution
 - Black body of given temperature T : $\hat{L}(\lambda) = B_T(\lambda)$
 - Standard Illuminant D of given CCT T : eg. $\hat{L}(\lambda) = D_{65}(\lambda)$
 - Standard Illuminant E : $\hat{L}(\lambda) = 1$
 - Standard Illuminant F_1 – F_{12} : eg. $\hat{L}(\lambda) = F_1(\lambda)$
 - Tabulated spectral data from file
- $D(\omega)$ – angular distribution
 - Lambertian: $D(\omega) = 1$
 - Powered cosine: $D(\omega) = \cos^n \theta = \langle \hat{n}, \omega \rangle^n$
 - IES profile from file
- $T(x, \lambda)$ – tint function
 - Color: $T(x, \lambda) = \langle T_{col}, col(\lambda) \rangle$
 - Pick from list of known gel sets (LEE, Rosco, Wratten, ...): $T(x, \lambda) = LEE_{013}(\lambda)$
 - texture map: $T(x, \lambda) = \langle T_{col}(x), col(\lambda) \rangle$

The exitant radiance of an area light source will be specified by a spectral distribution $\hat{L}(\lambda)$, an angular distribution $D(\omega)$ that describes the dependence of exitant radiance on outgoing direction and a tint function $T(x, \lambda)$ that is used to scale exitant radiance depending on position on the source and wavelength. This leads us to the following formulation for the intrinsic emission function

$$\bar{L}_\lambda^\dagger(x, \omega, \lambda) = T(x, \lambda) \hat{L}(\lambda) D(\omega) \left[\frac{W}{m^2 \cdot sr \cdot m} \right] \quad (2.24)$$

The luminous power of the source is obtained integrating over the area of the light source A , the angular domain Ω (typically the front hemisphere for planar, forward only sources, or an entire sphere for most other sources) and the wavelength domain

$$\Phi_v = k_e K_{cd} \int_\lambda \int_\Omega \int_A \bar{L}_\lambda^\dagger(x, \omega, \lambda) \bar{y}(\lambda) \cos \theta \, dx \, d\omega \, d\lambda \quad [lm] \quad (2.25)$$

In our case Φ_v is given as a parameter of the light, and k_e can be determined by inversion:

$$k_e = \frac{\Phi_v}{K_{cd} \int_\lambda \int_\Omega \int_A T(x, \lambda) \cdot \hat{L}(\lambda) \cdot D(\omega) \cdot \bar{y}(\lambda) \cos \theta \, dx \, d\omega \, d\lambda} \quad (2.26)$$

Depending on the tint function and emission profile the triple integral for Φ_v turns out to be separable, and it factorizes into a product of integrals that can be precomputed easily. Specifically in the common case in which the tint function is based on a texture map, the triple integral for Φ_v separates into a product of integrals as follows:

- a tint vector $\|T_{col}\|$

$$\|T_{col}\| = \frac{1}{A} \int_A T_{col}(x) dx \in \mathbb{R}^n \quad (2.27)$$

- a reduced luminance vector $\|col \cdot \hat{L}\|_{\bar{y}}$

$$\|col \cdot \hat{L}\|_{\bar{y}} = \int_{\lambda} col(\lambda) \hat{L}(\lambda) \bar{y}(\lambda) d\lambda \in \mathbb{R}^n \quad (2.28)$$

- an angular norm $\|D\|$

$$\|D\| = \int_{\Omega} D(\omega) \cos \theta d\omega \in \mathbb{R} \quad (2.29)$$

with these relations we can rewrite luminous power as

$$\Phi_v = k_e K_{cd} A \|D\| \langle \|T_{col}\|, \|col \cdot \hat{L}\|_{\bar{y}} \rangle \quad (2.30)$$

so that the expression for the emission constant is simply

$$k_e = \frac{\Phi_v}{K_{cd} A \|D\| \langle \|T_{col}\|, \|col \cdot \hat{L}\|_{\bar{y}} \rangle} \quad (2.31)$$

We observe that the tinting vector can be precomputed once for texture maps, the angular norm has simple closed form solutions for the common cases (and can be precomputed and stored for tabulated profiles), and the reduced luminous power vector can be precomputed for each combination of texture map primaries and spectral emission profiles. This reduces the computation of k_e to a scalar product and a few multiplications, once the given inputs of a light are given. Appendix B contains tables for various common combinations.

Once the emission constant has been computed, exitant radiance from the source is simply

$$L_{\lambda}^{\uparrow}(x, \omega, \lambda) = k_e T(x, \lambda) \hat{L}(\lambda) D(\omega) \left[\frac{W}{m^2 \cdot sr \cdot m} \right] \quad (2.32)$$

2.3.2 Image-Based Lighting

The emission for an **IBL** source is specified by (sublists contain possible examples):

- E_v^+ – illuminance from top hemisphere [lx]
- $\hat{L}(\omega, \lambda)$ – spherical map of an image (spectral and angular distribution)
- $T(\lambda)$ – tint function
 - Color: $T(\lambda) = \langle T_{col}, col(\lambda) \rangle$
 - Pick from list of known gel sets (LEE, Rosco, Wratten, ...): $T(\lambda) = LEE_{013}(\lambda)$

IBL sources model light coming from great distance away from the scene. As such they illuminate the scene geometry in a manner that is dependent on local orientation, but not position. For this reason it is only possible to specify their brightness in terms of illuminance (area density of luminous power at the receiver) rather than luminous

power⁸. This means that for **IBL** sources the formulation is in terms of incident radiance at an unspecified position in the scene:

$$L_{\lambda}^{\downarrow}(\omega, \lambda) = k_e T(\lambda) \hat{L}(\omega, \lambda) \quad (2.33)$$

the missing dependence on the position x in the scene outlines how incident radiance from an **IBL** source is not dependent on the receiver's location but only on its orientation. The emission constant is the estimated in terms of illuminance E_v^+ from the top hemisphere

$$\begin{aligned} E_v^+ &= K_{cd} \int_{\Omega^+} \int_{\lambda} L_{\lambda}^{\downarrow}(\omega, \lambda) \cdot \bar{y}(\lambda) \cos \theta \, d\omega \, d\lambda \\ &= k_e K_{cd} \int_{\Omega^+} \int_{\lambda} T(\lambda) \cdot \hat{L}(\omega, \lambda) \cdot \bar{y}(\lambda) \cos \theta \, d\omega \, d\lambda \quad [\text{lx}] \end{aligned}$$

where Ω^+ indicates integration over the top hemisphere, intuitively modeling the idea of a receiver (such as a grey card or a hemispherical light meter) set horizontally and facing upwards. This gives us:

$$k_e = \frac{E_v^+}{K_{cd} \int_{\Omega^+} \int_{\lambda} T(\lambda) \cdot \hat{L}(\omega, \lambda) \cdot \bar{y}(\lambda) \cos \theta \, d\omega \, d\lambda} \quad (2.34)$$

The double integral in the denominator can again be factorized into simpler computations when using an **IBL** texture map in a color space $col(\lambda)$. This time the spatial component is the directional component of \hat{L} :

$$\hat{L}(\omega, \lambda) = \langle \hat{L}_{col}(\omega), col(\lambda) \rangle \quad (2.35)$$

This gives us the possibility to break down the integral into

- an irradiance coloration vector $\|\hat{L}_{col}\|$

$$\|\hat{L}_{col}\| = \int_{\Omega^+} \hat{L}_{col}(\omega) \cos \theta \, d\omega \in \mathbb{R}^n \quad (2.36)$$

- a tint vector $\|T \cdot col\|_{\bar{y}}$

$$\|T \cdot col\|_{\bar{y}} = \int_{\lambda} T(\lambda) \cdot col(\lambda) \bar{y}(\lambda) \, d\lambda \in \mathbb{R}^n \quad (2.37)$$

where the tint function itself can be specified as a vector in some color space as outlined above:

$$T(\lambda) = \langle T_{col}, col(\lambda) \rangle \quad (2.38)$$

Note that if the map and the tint are specified in color spaces col_1 and col_2 , the full expression for the tint vector is

$$\|T \cdot col\|_{\bar{y}} = \int_{\lambda} T_{col_2} col_2(\lambda)^t col_1(\lambda) \bar{y}(\lambda) \, d\lambda = T_{col_2} \|col_2 \otimes col_1\|_{\bar{y}} \in \mathbb{R}^n \quad (2.39)$$

where $\|col_2 \otimes col_1\|_{\bar{y}}$ is the \bar{y} -norm of the outer product of the color spaces col_1 and col_2 .

⁸Luminous power would be ill-defined in this case: it's easily seen that an **IBL** source emits in such a way to have the same finite illuminance at all points in a scene. This means that its luminous power, that is its illuminance integrated over the scene area, depends on the amount of geometry in the scene, implying that doubling the amount of geometry in a scene would double the power of the source, making such a definition inconsistent

This decomposition lets us compute the emission constant for **IBL** sources as follows

$$k_e = \frac{E_v^+}{K_{cd} \langle \|\hat{L}_{col}\|, \|T \cdot col\|_{\vec{y}} \rangle} \quad (2.40)$$

Once the emission constant has been computed, exitant radiance from the source is simply

$$L_\lambda^\downarrow(x, \omega, \lambda) = k_e T(\lambda) \hat{L}(\omega, \lambda) \left[\frac{\text{W}}{\text{m}^2 \cdot \text{sr} \cdot \text{m}} \right] \quad (2.41)$$

2.3.3 Sun light

The emission for a Sun light is specified by (sublists contain possible examples):

- E_v^+ – illuminance of the sun [lx]
- $D_{\omega_c}(\omega)$ – angular dependent function describing the sun with the center at ω_c
 - Disk of angular size α
 - Gaussian falloff function around ω_c
- $\hat{L}(\lambda)$ – emitter (spectral distribution)
 - Black body of given temperature T : $\hat{L}(\lambda) = B_T(\lambda)$
 - Standard Illuminant D of nominal temperature T : eg. $\hat{L}(\lambda) = D_{65}(\lambda)$
 - Standard Illuminant E: $\hat{L}(\lambda) = 1$
 - Standard Illuminant F_1 – F_{12} : eg. $\hat{L}(\lambda) = F_1(\lambda)$
 - Tabulated spectral data from file
- $T(\lambda)$ – tint function
 - Color: $T(\lambda) = \langle T_{col}, col(\lambda) \rangle$
 - Pick from list of known gel sets (LEE, Rosco, Wratten, ...): $T(\lambda) = LEE_{013}(\lambda)$

Sun lights, like **IBLS**, model a light source located at a great distance from a scene. Again the irradiance is dependent on the incident angle, but not the position in the scene.

$$L_\lambda^\downarrow(\omega, \lambda) = k_e \cdot T(\lambda) \cdot D_{\omega_c}(\omega) \cdot \hat{L}(\lambda) \quad (2.42)$$

This time no function is dependent on more than one variable, so a factorization is easily done. To compute the emission constant we again use the definition of illuminance E_v^+

$$E_v^+ = K_{cd} \int_\lambda \int_{\Omega^+} L_\lambda^\downarrow(\omega, \lambda) \cdot \vec{y}(\lambda) \cos \theta \, d\omega \, d\lambda \quad (2.43)$$

which gives us:

$$k_e = \frac{E_v^+}{K_{cd} \int_{\Omega^+} \int_\lambda T(\lambda) \cdot D_{\omega_c}(\omega) \cdot \hat{L}(\lambda) \cdot \vec{y}(\lambda) \cos \theta \, d\omega \, d\lambda} \quad (2.44)$$

If $T(\lambda)$ is defined in some color space col , we can break the down the double integral into:

- an angular norm $\|D_{\omega_c}\|$

$$\|D_{\omega_c}\| = \int_\Omega D_{\omega_c}(\omega) \cos \theta \, d\omega \quad (2.45)$$

- a reduced illuminance vector $\|col \cdot \hat{L}\|_{\bar{y}}$

$$\|col \cdot \hat{L}\|_{\bar{y}} = \int_{\lambda} col(\lambda) \cdot \hat{L}(\lambda) \cdot \bar{y}(\lambda) d\lambda \quad (2.46)$$

This gives us the emission constant k_e as

$$k_e = \frac{E_v^+}{K_{cd} \cdot \|D_{\omega_c}\| \cdot \langle T_{col}, \|col \cdot \hat{L}\|_{\bar{y}} \rangle} \quad (2.47)$$

Once the emission constant has been computed, exitant radiance from the source is simply

$$L_{\lambda}^{\uparrow}(x, \omega, \lambda) = k_e T(\lambda) D_{\omega_c}(\omega) \hat{L}(\lambda) \quad \left[\frac{\text{W}}{\text{m}^2 \cdot \text{sr} \cdot \text{m}} \right] \quad (2.48)$$

Chapter 3

Calculation sheets

This section will list examples for the required calculations when implementing support for *physLight* in a rendering pipeline.

3.1 Imaging

We will use the following camera Inputs for our calibration scenario described in Section 2.1:

- Film speed $S = 100\text{ISO}$
- Focal length $f = 24\text{mm}$
- Focus distance $o = 1\text{m}$
- Iris aperture $N = 8f$ – number
- Exposure time $t = 1/60\text{s}$
- Sensor width/height $27.7 \times 14.6\text{mm}$
- Image resolution $5120 \times 2700\text{pxl}$
- Pixel area $A_{\text{pxl}} \simeq 29.25\mu\text{m}^2$
- Calibration constant $C = 312.5$

Incident Light Meter Exposure Compute illuminance E_v at a point P given imaging parameters:

$$\begin{aligned} E_v &= C \frac{N^2}{tS} \\ &= 312.5 \frac{8 \cdot 8 \cdot 60}{100} = 12000\text{lx} \end{aligned}$$

Reflected Luminance Compute the reflected luminance with 18% reflective Lambertian plane:

$$\begin{aligned} L_v &= E_v \cdot \frac{\rho}{\pi} \\ &= 12000 \cdot \frac{0.18}{\pi} \simeq 687.549\text{nt} \end{aligned}$$

Entrance pupil distance Compute the distance a from the entrance pupil to the film-back given:

- Focal length $f = 24\text{mm}$
- Focus distance $o = 1\text{m}$

The lens equation in our case has the form

$$\frac{1}{f} = \frac{1}{a} + \frac{1}{o - a}$$

solving for a gives us a quadratic equation $a^2 - ao + fo = 0$ for which we choose the solution closest to the filmback:

$$a = \frac{o - \sqrt{o^2 - 4fo}}{2}$$

Substituting our data into this expression yields

$$a = \frac{1 - \sqrt{1 - 4 \cdot 0.024}}{2} \text{ m} \simeq 24.6\text{mm}$$

Solid Angle of the Aperture Calculate Ω_{obj} the solid angle of the aperture seen from point in object space:

$$\begin{aligned} \Omega_p^{obj} &\simeq \frac{\pi r^2}{(o - a)^2} \\ &= \frac{f^2}{4N^2(o - a)^2} \\ &\simeq 2.36497\text{sr} \end{aligned}$$

Luminous energy from Y value Given a pixel Y value we can calculate the luminous energy density in lx for this pixel by

$$\begin{aligned} Y_v &= \frac{Y \cdot K_{cd}}{k_i \cdot S \cdot \Delta t} \\ &= \frac{Y \cdot C}{4 \cdot S \cdot \Delta t} \left(\frac{f}{a} \right)^2 \quad [\text{lx}] \end{aligned}$$

For $Y = 0.18$ and the given input specifications we get:

$$\begin{aligned} Y_v &= \frac{Y \cdot C}{4 \cdot S \cdot \Delta t} \left(\frac{f}{a} \right)^2 \\ &= \frac{0.18 \cdot 312.5}{4 \cdot 100 \cdot 1/60} \left(\frac{0.024}{0.0246} \right)^2 \text{ lx} \\ &= 8.030934\text{lx} \end{aligned}$$

3.2 Emission constant

3.2.1 Area Light

Given following input parameters for an area light:

- luminous power $\Phi_v = 1000\text{lm}$
- area $|A| = 2 \times 2\text{m} = 4\text{m}^2$
- Lambertian angular distribution $D = \frac{1}{\pi}$
- emitter: black body radiator at $T = 6500\text{K}$

we want to compute the light constant k_e . From Section 2.3 we can have:

$$k_e = \frac{\Phi_v}{K_{cd} \cdot |A| \cdot \|D\| \cdot \langle \|T_{col}\|, \|col \cdot \hat{L}\|_{\vec{y}} \rangle}$$

Area Light Without Texturing Without a tint function this reduces to

$$k_e = \frac{\Phi_v}{K_{cd} \cdot |A| \cdot \|D\| \cdot \|\hat{L}\|_{\vec{y}}}$$

with $\|\hat{L}\|_{\vec{y}} = \|B_T\|_{\vec{y}}$ which can be precomputed with the closed-form expression in Chapter 4. This gives us

$$\begin{aligned} \|\hat{L}\|_{\vec{y}} &= \|B_{6500}\|_{\vec{y}} \simeq 2826.5 \\ k_e &= \frac{1000}{683 \cdot 4 \cdot 2826.5} \simeq 1.295 \cdot 10^{-4} \end{aligned}$$

Area Light With Texturing Using the same input parameters but adding a texture as a tint function, we have to calculate the following integrals:

$$\|T_{col}\| = \int T_{col}(x) dx$$

Under the assumption that the texture coordinate mapping onto the light has no area distortion, this integral reduces to average of the **RGB** values of the texture map scaled by the light area A :

$$\|T_{rgb}\| = A \bar{T}_{rgb}$$

where \bar{T}_{rgb} is the average of the pixel values in the texture, a value that can be precomputed and stored in the header of the texture.

The reduced luminous power vector $\|col \cdot \hat{L}\|_{\vec{y}}$ can also be precomputed for the black body radiator at the given temperature.

$$\|col \cdot \hat{L}\|_{\vec{y}} = \int col(\lambda) \cdot B_T(\lambda) \cdot \vec{y}(\lambda) d\lambda$$

where col are the basis functions of the space used to convert the texture's **RGB** data into its spectral representation. This gives us

$$\begin{aligned} k_e &= \frac{\Phi_v}{K_{cd} \cdot |A| \cdot \|D\| \cdot \langle \bar{T}_{rgb}, \|col \cdot \hat{L}\|_{\vec{y}} \rangle} \\ &= \frac{1000}{683 \cdot 4 \cdot \langle \bar{T}_{rgb}, \|col \cdot \hat{L}\|_{\vec{y}} \rangle} \end{aligned}$$

where $\langle \bar{T}, \varphi \rangle = \bar{T}_r |\varphi_r| + \bar{T}_g |\varphi_g| + \bar{T}_b |\varphi_b|$ in the simple case of a simplistic three basis functions lifting to spectral.

Other, more plausible ways of lifting **RGB** data to the spectral domain are possible, as explained in Appendix A.1.

For example, if using the algorithm proposed by Brian Smits in [Smits, 1999], the expression $\langle \bar{T}, \varphi \rangle$ this would be computed as follows: the various *col* functions will correspond to the seven basis functions of the Smits basis

$$w(\lambda), c(\lambda), m(\lambda), y(\lambda), r(\lambda), g(\lambda), b(\lambda)$$

yielding seven integrals $\varphi_w, \varphi_c, \varphi_m, \varphi_y, \varphi_r, \varphi_g, \varphi_b$ corresponding to $\varphi_w = \|w \cdot \hat{L}\|_{\bar{y}}$ and so on.

The algorithm produces a vector $\bar{T} \in \mathbb{R}^7$ in which at most three components are non-zero as follows: the first entry T_0 is the smallest component of \bar{T}_{rgb} , say that this was the green component. Then the basis vector from the secondaries is chosen (cyan, magenta and yellow: $c(\lambda), m(\lambda), y(\lambda)$) and its corresponding value (one of T_1, T_2, T_3) is set to the difference between the smallest value and the middle value. Lastly, the primary corresponding to the largest value is chosen (red, green, and blue: $r(\lambda), g(\lambda), b(\lambda)$) and its corresponding component (one of T_4, T_5, T_6) is set to the difference between the largest and middle values.

For example if $\bar{T}_{rgb} = (0.3, 0.1, 0.7)$ then T_0 is set to 0.1, then magenta is the complementary, so T_2 is set to $0.3 - 0.1 = 0.2$, then blue is the primary, so T_6 is set to $0.7 - 0.3 = 0.4$, yielding $\bar{T} = (0.1, 0, 0.2, 0, 0, 0, 0.4)$. An implementation in code of this algorithm is available in Appendix B.5.

3.3 Surface interaction

Compute the exitant luminance $L_{o,v}(\omega_o, \lambda)$ from a point P_s on a surface of normal N , given the incident radiance $L_{i,\lambda}(\omega_i, \lambda)$ and the object's BRDF $f(\omega_i, \omega_o, \lambda)$. Let us assume that the surface at P_s is made of Lambertian material of reflectance $\rho = 0.18$, i.e., $f(\omega_i, \omega_o, \lambda) = \frac{\rho}{\pi}$.

$$\begin{aligned} L_{o,v}(\omega_o) &= K_{cd} \int_{\lambda} \int_{\Omega} L_{i,\lambda}(\omega_i, \lambda) f(\omega_i, \omega_o, \lambda) d\omega^\perp \bar{y}(\lambda) d\lambda \\ &= K_{cd} \int_{\lambda} \int_0^\pi \int_0^{\frac{\pi}{2}} L_{i,\lambda}(\omega_i, \lambda) f(\omega_i, \omega_o, \lambda) \bar{y}(\lambda) \cos \theta \sin \theta d\theta d\varphi d\lambda \\ &= \int_0^\pi \int_0^{\frac{\pi}{2}} L_{i,v}(\omega_i) f(\omega_i, \omega_o) \cos \theta \sin \theta d\theta d\varphi \end{aligned}$$

Let's say that the light is a portion of a sphere of radius $r = 1\text{m}$, centered around our surface point P_s , extending in θ from $\frac{\pi}{6}$ to $\frac{\pi}{3}$ and in φ from 0 to $\frac{\pi}{2}$, and having Lambertian emission towards our surface of $L_{i,v} = 300\text{nt}$. In this configuration we obtain:

$$\begin{aligned} L_{o,v} &= \int_{\theta=\frac{\pi}{6}}^{\frac{\pi}{3}} \int_{\varphi=0}^{\frac{\pi}{2}} L_{i,v} \frac{\rho}{\pi} \cos \theta \sin \theta d\theta d\varphi \\ &= 300 \cdot \frac{0.18}{\pi} \int_{\theta=\frac{\pi}{6}}^{\frac{\pi}{3}} \int_{\varphi=0}^{\frac{\pi}{2}} \cos \theta \sin \theta d\theta d\varphi \\ &= 54 \frac{-\cos^2 \theta}{2} \Big|_{\frac{\pi}{6}}^{\frac{\pi}{3}} \\ &= 13.5\text{nt} \end{aligned}$$

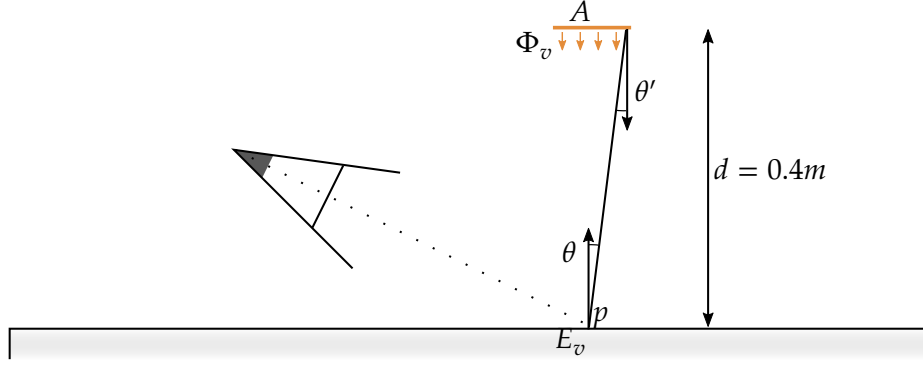


Figure 3.1: Integration over area light.

3.4 Light to sensor interaction

Given camera parameters $S = 100$, $N = 5.6$, $\Delta t = \frac{1}{60}$ and a small light source A oriented towards a Lambertian plane parallel to the light with distance $d = 0.4\text{m}$. If the luminance $Y(p)$ at the pixel corresponding to the center of the projection p equals the albedo ρ of the plane, what is the luminous power Φ_v of the light source?

According to Equation (2.8) the illuminance at the plane must be

$$E_v = \frac{C N^2}{\Delta t S} = 5880 \text{ lx}.$$

Say the light source has a cosine powered distribution $L_v^{\uparrow, \text{light}}(\omega) = \alpha \cos^n \theta'$, where θ' denotes the angle between emission direction ω and the light normal, then due to

$$M_v = \int_{\Omega} L_v^{\uparrow, \text{light}}(\omega) d\omega^\perp \stackrel{(4.8)}{=} \alpha \frac{2\pi}{n+2}$$

and $M_v = \Phi_v/|A|$ we have

$$L_v^{\uparrow, \text{light}}(\omega) = \frac{\Phi_v}{|A|} \frac{n+2}{2\pi} \cos^n \theta'. \quad (3.1)$$

The illuminance at p is

$$\begin{aligned} E_v &= \int_{\Omega} L_v^{\downarrow, \text{obj}}(\omega) d\omega^\perp = \int_A L_v^{\uparrow, \text{light}}(x \rightarrow p) \frac{\cos \theta \cos \theta'}{|x - p|^2} dx \\ &\stackrel{(3.1)}{=} \frac{\Phi_v}{|A|} \frac{n+2}{2\pi} \int_A \frac{\cos^{n+1} \theta \cos \theta'}{|x - p|^2} dx \approx \frac{\Phi_v}{|A|} \frac{n+2}{2\pi} \frac{|A|}{d^2} \stackrel{n \equiv 0}{=} \frac{\Phi_v}{\pi d^2} \end{aligned}$$

where the approximation holds if the light source is sufficiently small, hence the cosines are ≈ 1 and assuming a Lambertian emission ($n = 0$). Putting this together, it follows

$$\Phi_v = \pi 0.4^2 \text{m}^2 \cdot 5880 \text{ lx} = 2955.61 \text{ lm}.$$

Simple geometric setups like these can be reproduced in a render and are hence useful for validation purposes.

Part II

Reference

Chapter 4

Illuminants

4.1 Spectral Distribution Functions

4.1.1 Black body radiator

Black body spectral radiance as per Planck's law [Planck, 1914]:

$$B_T(\lambda) = \frac{2hc^2}{\lambda^5} \frac{1}{e^{\frac{hc}{\lambda kT}} - 1} \left[\frac{\text{W}}{\text{m}^2 \cdot \text{sr} \cdot \text{m}} \right] \quad (4.1)$$

where relevant constants and variables are:

k	Boltzmann constant	$1.3806488e - 23 \text{ J/K}$
h	Planck constant	$6.62606957e - 34 \text{ J} \cdot \text{s}$
c	speed of light in vacuum	$2.99792458e8 \text{ m/s}$
T	temperature in kelvins	[K]
λ	wavelength in meters	[m]
T_{kK}	temperature in kilokelvins	[kK]
$\lambda_{\mu m}$	wavelength in micrometers	[μm]

It is possible to get a formulation with every-day ranged constants and values in play by expressing the temperature in kilokelvins [kK] and the wavelength in micrometers [μm]:

$$B_T(\lambda) \approx \frac{119.104}{\lambda_{\mu m}^5} \frac{1}{e^{\frac{14.3878}{\lambda_{\mu m} T_{kK}}} - 1} \left[\frac{\text{W}}{\text{m}^2 \cdot \text{sr} \cdot \text{m}} \right] \quad (4.2)$$

Chromaticity White point for black body radiator. Black body's approximate chromaticity coordinates in CIE xy space can be computed following [Kang et al., 2002] as:

$$\begin{aligned} w &= 1/T_{kK} && \text{inverse of temperature in kiloKelvin} \\ x &= \begin{cases} -.2991239 w^3 - .234358 w^2 + .8776956 w + .17991 & T_{kK} \in [\frac{5}{3}, 4] \\ -3.0258469 w^3 + 2.1070379 w^2 + .2226347 w + .240390 & T_{kK} \in [4, 25] \end{cases} \\ y &= \begin{cases} -1.1063814 x^3 - 1.34811020 x^2 + 2.18555832 x - .20219683 & T_{kK} \in [\frac{5}{3}, \frac{20}{9}] \\ -.9549476 x^3 - 1.37418593 x^2 + 2.09137015 x - .16748867 & T_{kK} \in [\frac{20}{9}, 4] \\ 3.081758 x^3 - 5.8733867 x^2 + 3.75112997 x - .37001483 & T_{kK} \in [4, 25] \end{cases} \end{aligned} \quad (4.3)$$

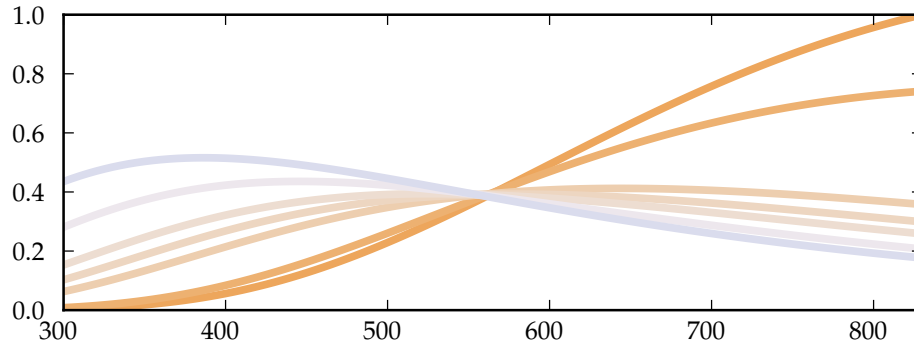


Figure 4.1: Spectral distributions of black body radiator at various temperatures

Plots of spectral distribution of black body radiator at temperatures of 2855.54, 3200, 4500, 5000, 5500, 6500, 7500 degrees Kelvin. In the rendition, the color of each curve is taken from the sRGB coordinates for the corresponding color, normalized so that the maximum sRGB linear value is 0.7

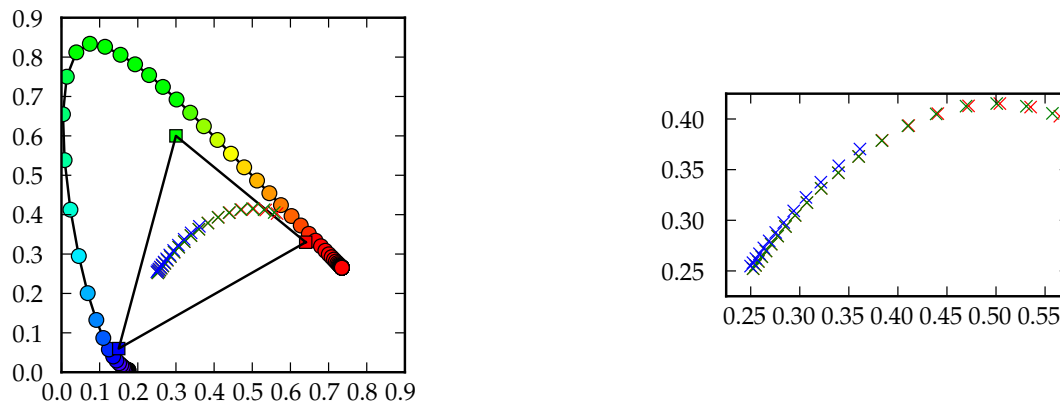


Figure 4.2: Comparison of CCTs for black body and Illuminant D

Red crosses show actual chromaticity for a black body emitter, green crosses show the result from the approximation in [Kang et al., 2002], blue crosses show the chromaticity of CIE Standard Illuminant D. The plot on the right is an enlargement of the central region of the plot on the left, the triangle in the left plot is the sRGB gamut

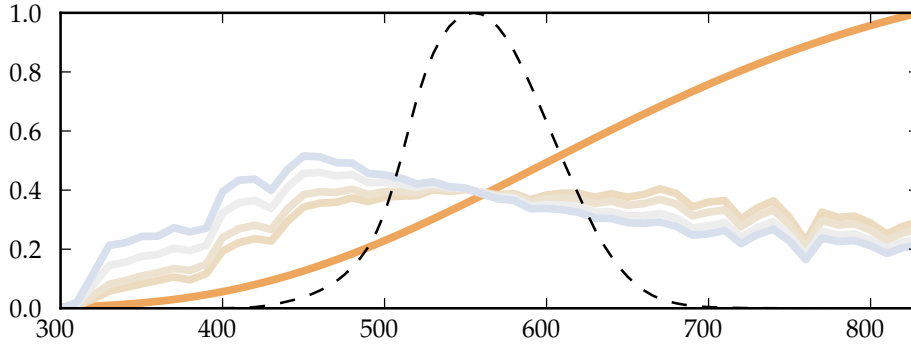


Figure 4.3: Spectral distributions of common Standard Illuminants

Plots of spectral distribution of Standard Illuminants A, D₅₀, D₆₅, normalized to equal luminance. In the rendition, the color of each curve is taken from the sRGB coordinates for the corresponding color, normalized so that the maximum sRGB linear value is 0.7. Data in line with [ISO/CIE 11664-2:2022] The CIE color matching function $\bar{y}(\lambda)$ is also plotted in black dashed line for reference

Luminance The luminance of a black body radiator $\|B_T\|_{\bar{y}} = \int B_T(\lambda) \bar{y}(\lambda) d\lambda$, this can be approximately computed as

$$\|B_T\|_{\bar{y}} \approx \frac{50471.2}{e^{\frac{14.3878}{0.0384919 + 0.541533 T_{kK}} - 1}} \begin{cases} \pm 0.375\% & T_{kK} \in [1.6, 2.5] \\ +0.23\% \pm 0.1\% & T_{kK} \in [2.5, 3.3] \\ \pm 0.155\% & T_{kK} \in [3.3, 8.5] \\ \pm 0.11\% & T_{kK} \in [9, 25] \end{cases} \left[\frac{\text{W}}{\text{m}^2 \cdot \text{sr}} \right] \quad (4.4)$$

4.1.2 CIE Standard Illuminants

A standard illuminant is a theoretical source of visible light with a profile (its spectral power distribution) which is published. Standard illuminants provide a basis for comparing images or colors recorded under different lighting. Standard Illuminants A, B, and C were introduced in 1931, with the intention of respectively representing average incandescent light, direct sunlight, and average daylight. Illuminants D represent phases of daylight, Illuminant E is the equal-energy illuminant, while Illuminants F represent fluorescent lamps of various composition. Over many years of work and many revision, data for illuminants A, D65 and D50 is available in [ISO/CIE 11664-2:2022].



This section is under construction

Update the plot to not include D55 and D75

Standard Illuminant A The standard illuminant A defined by the CIE is intended to represent typical, domestic, tungsten-filament lighting. Its relative spectral power distribution is that of a black body radiator at a temperature of approximately 2855.54K. Standard illuminant A should be used in all applications of colorimetry involving the use of incandescent lighting, unless there are specific reasons for using a different illuminant.

Using our previous expression for black body radiation we have

$$S_A(\lambda_{\mu m}) = B_{2855.54}(\lambda_{\mu m}) \approx \frac{119.104}{\lambda_{\mu m}^5} \frac{1}{e^{\frac{5.03855}{\lambda_{\mu m}}} - 1} \left[\frac{\text{W}}{\text{m}^2 \cdot \text{sr} \cdot \text{m}} \right] \quad (4.5)$$

where $\lambda_{\mu m}$ is the wavelength in micrometers.

The spectrum of this illuminant is published in [ISO/CIE 11664-2:2022].

Standard Illuminant D series The D series of illuminants were derived by Judd, Mac Adam and Wyszecki, from a large number of measurements of natural daylight. Although they are rather difficult sources to build accurately in real life, they are based on a simple PCA decomposition of the data gathered during the measurements, making them very convenient to work with numerically.

The spectral distribution $S_D(\lambda, T)$ is defined in terms of three tabulated spectral distributions $S_0(\lambda)$, $S_1(\lambda)$ and $S_2(\lambda)$ (data is tabulated and plotted in the appendix):

$$S_D(\lambda, T) = S_0(\lambda) + M_1(T)S_1(\lambda) + M_2(T)S_2(\lambda) \quad (4.6)$$

where the weighting functions $M_1(T)$ and $M_2(T)$ are defined in terms of the CIE chromaticity coordinates x_D, y_D as follows:

$$\begin{aligned} M &= 0.0241 + 0.2562x_D - 0.7341y_D \\ M_1 &= \frac{-1.3515 - 1.7703x_D + 5.9114y_D}{M} \\ M_2 &= \frac{0.03 - 31.4424x_D + 30.0717y_D}{M} \end{aligned}$$

Due to changes in constants that have happened since 1931, Standard Illuminant D_{65} corresponds to a temperature of 6504K and Standard Illuminant D_{50} to a temperature of 5003K. The spectra of these illuminants are published as tabulations in [ISO/CIE 11664-2:2022].

Chromaticity For D-series standard illuminants, CIE xy coordinates are:

$$\begin{aligned} w &= 1/T_{kK} \quad \text{inverse of temperature in kiloKelvin} \\ x &= \begin{cases} -4.6070w^3 + 2.9678w^2 + .09911w + .244063 & T_{kK} \in [4, 7] \\ -2.0064w^3 + 1.9018w^2 + .24748w + .237040 & T_{kK} \in [7, 25] \end{cases} \\ y &= -3x^2 + 2.87x - .275 \end{aligned} \quad (4.7)$$

Standard Illuminant E Standard Illuminant E is simply $S_E(\lambda) = 1$, an equal energy radiator

Standard Illuminant F series The F series of standard illuminants represent various types of fluorescent lighting. F_1 – F_6 “standard” fluorescent lamps consist of two semi-broadband emissions of antimony and manganese activations in calcium halophosphate phosphor, these are plotted in Figure 4.4. F_4 is of particular interest since it was used for calibrating the CIE Color Rendering Index (CRI) (the CRI formula was chosen such that

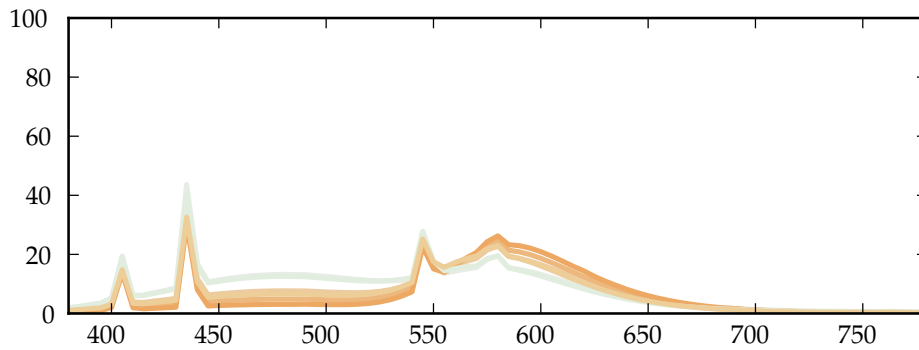


Figure 4.4: Spectral distributions of CIE Standard Fluorescent Illuminants

Plots of spectral distribution of Standard Illuminants F_1 to F_6 , standard spectra. In the rendition, the color of each curve is taken from the sRGB coordinates for the corresponding color, normalized so that the maximum sRGB linear value is 0.85.

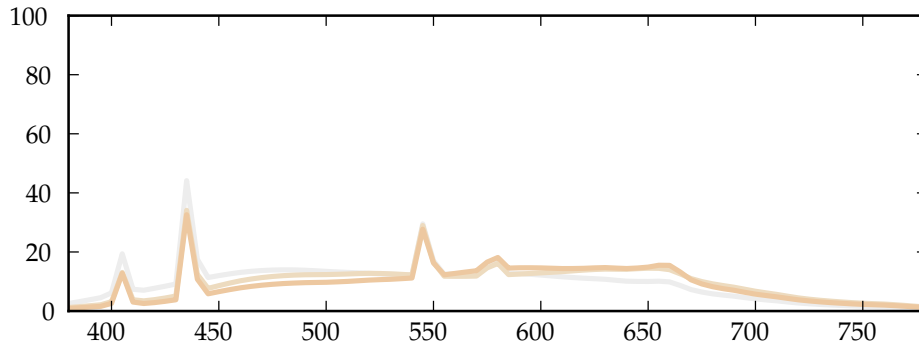


Figure 4.5: Spectral distributions of CIE Broadband Fluorescent Illuminants

Plots of spectral distribution of Standard Illuminants F_7 to F_9 , broadband spectra. In the rendition, the color of each curve is taken from the sRGB coordinates for the corresponding color, normalized so that the maximum sRGB linear value is 0.85.

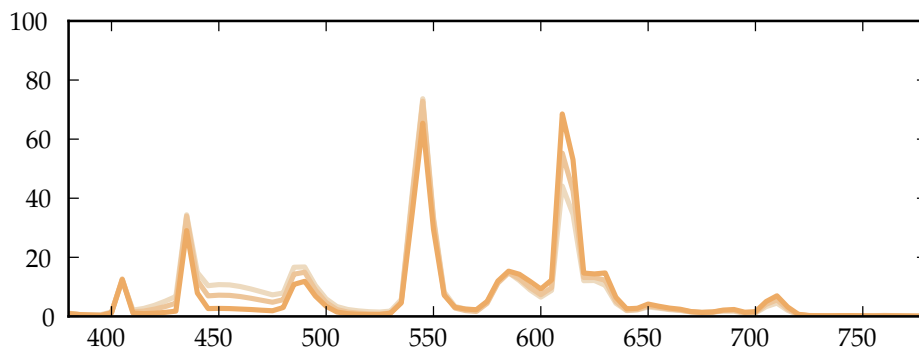


Figure 4.6: Spectral distributions of CIE Narrowband Fluorescent Illuminants

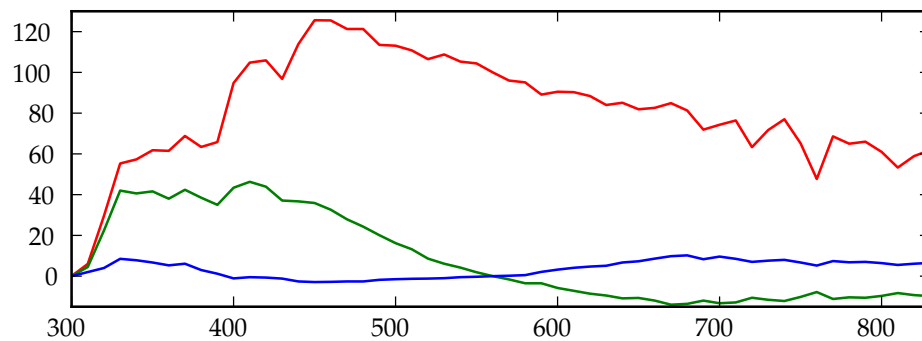
Plots of spectral distribution of Standard Illuminants F_{10} to F_{12} , narrowband spectra. In the rendition, the color of each curve is taken from the sRGB coordinates for the corresponding color, normalized so that the maximum sRGB linear value is 0.85.

F_4 would have a **CRI** of 51). F_7 – F_9 are “broadband” (full-spectrum light) fluorescent lamps with multiple phosphors, and higher **CRIs**, plotted in Figure 4.5. Finally, F_{10} – F_{12} are narrow triband illuminants consisting of three “narrowband” emissions (caused by ternary compositions of rare-earth phosphors) in the R,G,B regions of the visible spectrum, plotted in Figure 4.6. The phosphor weights can be tuned to achieve the desired **CCT**.

4.2 Standard Illuminants

4.2.1 Illuminant D

Data for CIE Standard Illuminant D, the three functions are $S_0(\lambda)$ in red, $S_1(\lambda)$ in green, $S_2(\lambda)$ in blue



λ	$S_0(\lambda)$	$S_1(\lambda)$	$S_2(\lambda)$	λ	$S_0(\lambda)$	$S_1(\lambda)$	$S_2(\lambda)$	λ	$S_0(\lambda)$	$S_1(\lambda)$	$S_2(\lambda)$
300	0.04	0.02	0.	480	121.30	24.30	-2.60	660	82.60	-12.	8.60
310	6.	4.50	2.	490	113.50	20.10	-1.80	670	84.90	-14.	9.80
320	29.60	22.40	4.	500	113.10	16.20	-1.50	680	81.30	-13.60	10.20
330	55.30	42.	8.50	510	110.80	13.20	-1.30	690	71.90	-12.	8.30
340	57.30	40.60	7.80	520	106.50	8.60	-1.20	700	74.30	-13.30	9.60
350	61.80	41.60	6.70	530	108.80	6.10	-1.	710	76.40	-12.90	8.50
360	61.50	38.	5.30	540	105.30	4.20	-0.50	720	63.30	-10.60	7.00
370	68.80	42.40	6.10	550	104.40	1.90	-0.30	730	71.70	-11.60	7.60
380	63.40	38.50	3.	560	100.	0.	0.	740	77.	-12.20	8.00
390	65.80	35.	1.20	570	96.	-1.60	0.20	750	65.20	-10.20	6.70
400	94.80	43.40	-1.10	580	95.10	-3.50	0.50	760	47.70	-7.80	5.20
410	104.80	46.30	-0.50	590	89.10	-3.50	2.10	770	68.60	-11.20	7.40
420	105.90	43.90	-0.70	600	90.50	-5.80	3.20	780	65.	-10.40	6.80
430	96.80	37.10	-1.20	610	90.30	-7.20	4.10	790	66.	-10.60	7.00
440	113.90	36.70	-2.60	620	88.40	-8.60	4.70	800	61.	-9.70	6.40
450	125.60	35.90	-2.90	630	84.00	-9.50	5.10	810	53.30	-8.30	5.50
460	125.50	32.60	-2.80	640	85.10	-10.90	6.70	820	58.90	-9.30	6.10
470	121.30	27.90	-2.60	650	81.90	-10.70	7.30	830	61.90	-9.80	6.50

4.3 Angular distributions

4.3.1 Powered cosine

The angular norm $\|D\|$ of $\langle \omega, \hat{n} \rangle^n$ is

$$\begin{aligned} \|D(\omega)\| &= \int_{\Omega^+} \langle \omega, \hat{n} \rangle \cos \theta \, d\omega = \int_{\varphi=0}^{2\pi} \int_{\theta=0}^{\pi/2} \cos^n \theta \cos \theta \sin \theta \, d\theta \, d\varphi \\ &= 2\pi \left. \frac{-\cos^{n+2} \theta}{n+2} \right|_0^{\pi/2} = \frac{2\pi}{n+2} \quad (4.8) \end{aligned}$$

4.3.2 IES profiles

The **Illuminating Engineering Society of North America (IES)** has a standard file format called LM-63 (available in three revisions LM-63-1986, LM-63-1991 and LM-63-1995) for photometric data describing luminaires. These files are often called **IES** profiles and are freely available from most manufacturers. For the purposes of this document, an **IES** profile is simply an (unnormalized) intensity distribution map $D(\omega) = D_{IES}(\theta, \varphi)$, intended to be a bilinear interpolation of the data in the corresponding tabulation from the file. As such it can simply be integrated numerically evaluating the angular norm integral

$$\|D(\omega)\| = \int_{\Omega^+} D_{IES}(\theta, \varphi) \cos \theta \, d\omega = \int_{\varphi=0}^{2\pi} \int_{\theta=0}^{\pi/2} D_{IES}(\theta, \varphi) \cos \theta \sin \theta \, d\theta \, d\varphi \quad (4.9)$$

implementation details are in Appendix B.

4.4 Tint functions

4.4.1 Texture maps



This section is under construction

Explain texture maps, their primaries, how to use custom primaries.
Explain differences between textured emitters and transmittance/reflectance data

4.4.2 Tabulated spectral data

Sometimes tabulated data is available for various gels or filters, Figure 4.7 includes plots of a subset of Rosco's *RoscoLux* series of gels.

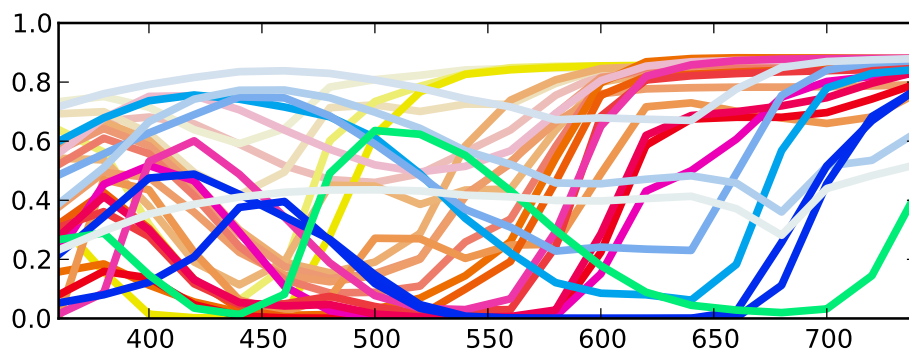


Figure 4.7: Spectral transmittance of RoscoLux gel series

Transmittance of the RoscoLux series of gels from Rosco. The coloration of the curve is the color of the gel as seen in front of a D65 illuminant

Chapter 5

Sensors

5.0.1 ISO Sensitivity

$$\frac{N^2}{t} = \frac{ES}{C} \quad (5.1)$$

Reference: http://en.wikipedia.org/wiki/Light_meter Reference: <http://en.wikipedia.org/wiki/F>

5.0.2 Counting photons

From the Planck relation we can compute the energy in a photon:

$$E = \frac{hc}{\lambda} \simeq \frac{1.98645}{\lambda_{\mu m}} \cdot 10^{-19} \text{ J} \in [2.5, 6] \cdot 10^{-19} \text{ J for visible light} \quad (5.2)$$

Reference: http://en.wikipedia.org/wiki/Planck_constant

5.0.3 Digital sensors

A digital sensor is made of electron wells, the well is able to absorb photons and keep a count, with a given efficiency (40-50% typical), and can count absorptions in the mid-10k's (40k to 80k typical). This means one well contains the equivalent of about $4e - 14J$ ($O(10^5)$ photons of $4e - 19J$ each).

Reference: <http://www.clarkvision.com/articles/digital.sensor.performance.summary/>

Example: An isotropic source radiating 1W at 555nm (which is a monochromatic source of 683lm) emits $2.793e18$ photons per second. At 1m distance from a Canon 7D sensor ($22.3 \times 14.9\text{mm}$, $5184 \times 3456\text{pxl}$, well size $4.3 \times 4.3\mu\text{m}$), the well area is $18.5\mu\text{m}^2$, whereas the total area the source is radiating onto is $4\pi\text{m}^2$ which is $1.475e - 12$ of the total area, meaning the pixel would receive $1.893e6$ photons per second or about 31550 photons at ET 1/60s, if the camera had infinitely wide aperture, and the camera lens absorbed no light and had no focusing effect.

Adding a lens

Let's now say that the same source is imaged onto a single pixel through a camera lens of focal length $f = 24\text{mm}$, set at aperture $f/8$ and exposure time $t = 1/60\text{s}$.

The **aperture** area is $2.25\pi\text{mm}^2$ (the diameter of the aperture is $24/8 = 3\text{mm}$), so that the aperture is $0.625e - 6$ of the total area, meaning the pixel would receive $1.746e12$

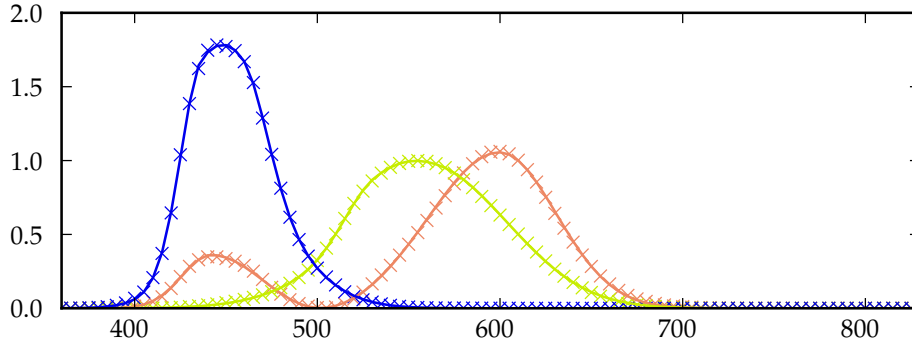


Figure 5.1: Comparison of color matching functions from Wyman vs. CIE data

Data from CIE 1931 is plotted with crosses, the functions from [Wyman et al., 2013] are plotted with solid lines. The three functions are $\bar{x}(\lambda)$ in red, $\bar{y}(\lambda)$ in green, $\bar{z}(\lambda)$ in blue

photons per second or about $2.909e10$ photons at exposure time $1/60s$ (assuming no lens absorption).

5.1 Color matching functions

Chris Wyman 2013 proposes a simple and fairly accurate analytical fitting for the color matching functions (CIE 1931/1964, 2 deg/10 deg observers). For the 2 degree observer these are:

$$\left. \begin{aligned} x_1(\lambda) &= (\lambda - 442) \cdot (0.0624 \diamond 0.0374) \\ x_2(\lambda) &= (\lambda - 599.8) \cdot (0.0264 \diamond 0.0323) \\ x_3(\lambda) &= (\lambda - 501.1) \cdot (0.049 \diamond 0.0382) \end{aligned} \right\} \quad \bar{x}(\lambda) = \begin{aligned} &0.362 G(x_1(\lambda)) \\ &+ 1.056 G(x_2(\lambda)) \\ &- 0.065 G(x_3(\lambda)) \end{aligned} \quad (5.3)$$

$$\left. \begin{aligned} y_1(\lambda) &= (\lambda - 568.8) \cdot (0.0213 \diamond 0.0247) \\ y_2(\lambda) &= (\lambda - 530.9) \cdot (0.0613 \diamond 0.0322) \end{aligned} \right\} \quad \bar{y}(\lambda) = 0.821 G(y_1(\lambda)) + 0.286 G(y_2(\lambda)) \quad (5.4)$$

$$\left. \begin{aligned} z_1(\lambda) &= (\lambda - 437) \cdot (0.0845 \diamond 0.0278) \\ z_2(\lambda) &= (\lambda - 459) \cdot (0.0385 \diamond 0.0725) \end{aligned} \right\} \quad \bar{z}(\lambda) = 1.217 G(z_1(\lambda)) + 0.681 G(z_2(\lambda)) \quad (5.5)$$

In the expressions above the function $G(x)$ is a Gaussian

$$G(x) = e^{-\frac{x^2}{2}} \quad (5.6)$$

and the \diamond operator behaves as follows

$$a \cdot (b \diamond c) = \begin{cases} ab & a < 0 \\ ac & a \geq 0 \end{cases} \quad (5.7)$$

Table 5.1 contains the data for the color matching functions $\bar{x}(\lambda)$, $\bar{y}(\lambda)$, $\bar{z}(\lambda)$ as published in **smithgould1931**.

5.2 Camera sensitivity data

This section contains spectral sensitivity data and plots for a few interesting cameras.

λ	$\bar{x}(\lambda)$	$\bar{y}(\lambda)$	$\bar{z}(\lambda)$	λ	$\bar{x}(\lambda)$	$\bar{y}(\lambda)$	$\bar{z}(\lambda)$
360	0.0001299	0.000003917	0.0006061	600	1.0622	0.631	0.0008
365	0.0002321	0.000006965	0.001086	605	1.0456	0.5668	0.0006
370	0.0004149	0.00001239	0.001946	610	1.0026	0.503	0.00034
375	0.0007416	0.00002202	0.003486	615	0.9384	0.4412	0.00024
380	0.001368	0.000039	0.00645	620	0.85445	0.381	0.00019
385	0.002236	0.000064	0.01055	625	0.7514	0.321	0.0001
390	0.004243	0.00012	0.02005	630	0.6424	0.265	0.00005
395	0.00765	0.000217	0.03621	635	0.5419	0.217	0.00003
400	0.01431	0.000396	0.06785	640	0.4479	0.175	0.00002
405	0.02319	0.00064	0.1102	645	0.3608	0.1382	0.00001
410	0.04351	0.00121	0.2074	650	0.2835	0.107	0.
415	0.07763	0.00218	0.3713	655	0.2187	0.0816	0.
420	0.13438	0.004	0.6456	660	0.1649	0.061	0.
425	0.21477	0.0073	1.03905	665	0.1212	0.04458	0.
430	0.2839	0.0116	1.3856	670	0.0874	0.032	0.
435	0.3285	0.01684	1.62296	675	0.0636	0.0232	0.
440	0.34828	0.023	1.74706	680	0.04677	0.017	0.
445	0.34806	0.0298	1.7826	685	0.0329	0.01192	0.
450	0.3362	0.038	1.77211	690	0.0227	0.00821	0.
455	0.3187	0.048	1.7441	695	0.01584	0.005723	0.
460	0.2908	0.06	1.6692	700	0.01135916	0.004102	0.
465	0.2511	0.0739	1.5281	705	0.008110916	0.002929	0.
470	0.19536	0.09098	1.28764	710	0.005790346	0.002091	0.
475	0.1421	0.1126	1.0419	715	0.004109457	0.001484	0.
480	0.09564	0.13902	0.81295	720	0.002899327	0.001047	0.
485	0.05795	0.1693	0.6162	725	0.00204919	0.00074	0.
490	0.03201	0.20802	0.46518	730	0.001439971	0.00052	0.
495	0.0147	0.2586	0.3533	735	0.0009999493	0.0003611	0.
500	0.0049	0.323	0.272	740	0.0006900786	0.0002492	0.
505	0.0024	0.4073	0.2123	745	0.0004760213	0.0001719	0.
510	0.0093	0.503	0.1582	750	0.0003323011	0.00012	0.
515	0.0291	0.6082	0.1117	755	0.0002348261	0.0000848	0.
520	0.06327	0.71	0.07825	760	0.0001661505	0.00006	0.
525	0.1096	0.7932	0.05725	765	0.000117413	0.0000424	0.
530	0.1655	0.862	0.04216	770	0.00008307527	0.00003	0.
535	0.22575	0.91485	0.02984	775	0.00005870652	0.0000212	0.
540	0.2904	0.954	0.0203	780	0.00004150994	0.000015	0.
545	0.3597	0.9803	0.0134	785	0.00002935326	0.0000106	0.
550	0.43345	0.99495	0.00875	790	0.00002067383	0.0000074657	0.
555	0.5120501	1.	0.00575	795	0.00001455977	0.0000052578	0.
560	0.5945	0.995	0.0039	800	0.00001025398	0.0000037029	0.
565	0.6784	0.9786	0.00275	805	0.000007221456	0.0000026078	0.
570	0.7621	0.952	0.0021	810	0.000005085868	0.0000018366	0.
575	0.8425	0.9154	0.0018	815	0.000003581652	0.0000012934	0.
580	0.9163	0.87	0.00165	820	0.000002522525	0.00000091093	0.
585	0.9786	0.8163	0.0014	825	0.000001776509	0.00000064153	0.
590	1.0263	0.757	0.0011	830	0.000001251141	0.00000045181	0.
595	1.0567	0.6949	0.001				

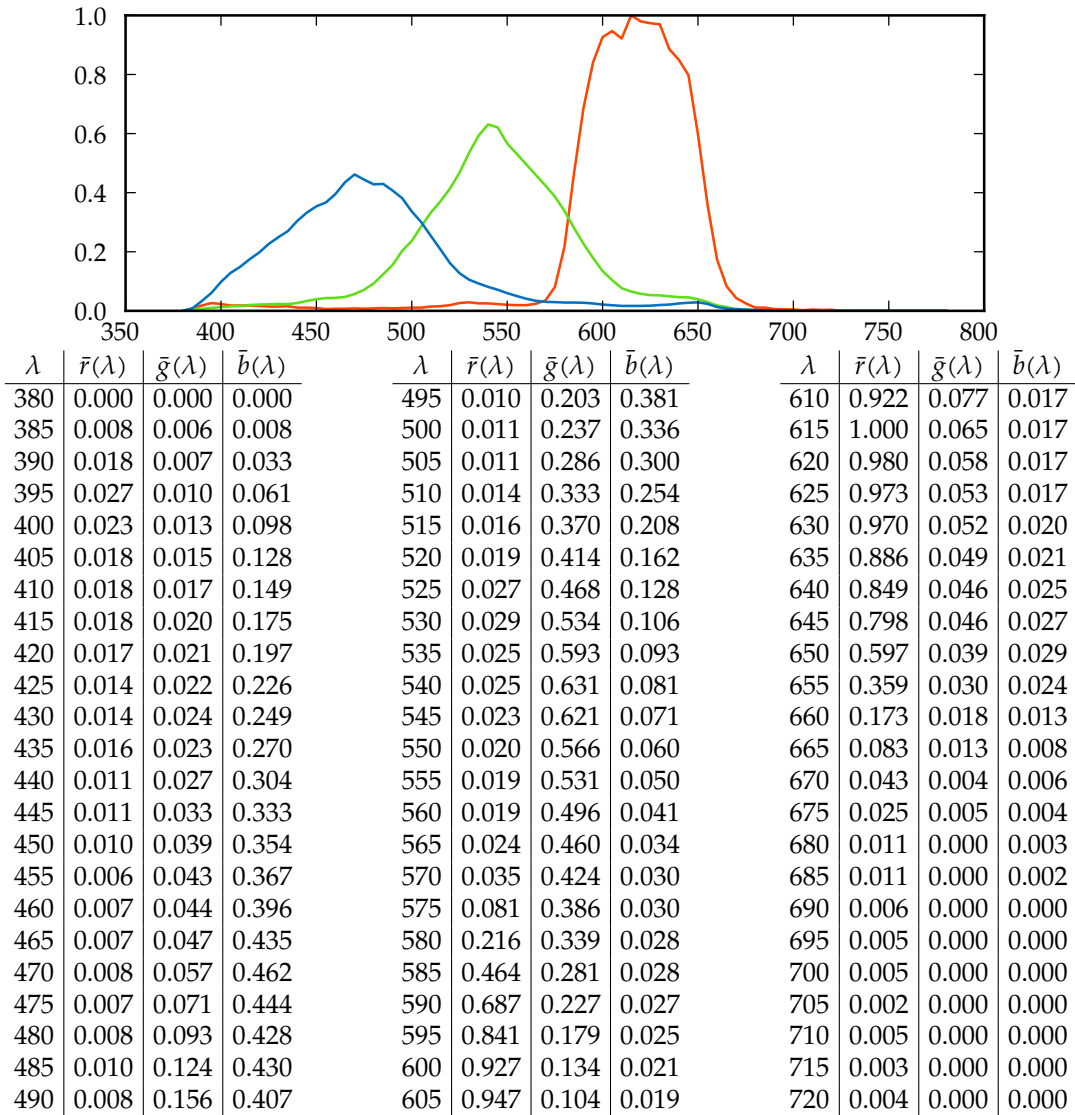
Table 5.1: Data for the CIE Color matching functions $\bar{x}(\lambda)$, $\bar{y}(\lambda)$, $\bar{z}(\lambda)$

5.2.1 Red Mystery X

Camera **RGB** data is obtained through the curves in Section 5.2.1 and is converted into **SRGB** linear with the following matrix

$$C_{Rec709} = M_{MysteryX} C_{CamRGB} = \begin{bmatrix} 1.369 & 0.0137 & -0.3068 \\ -0.18 & 1.326 & -0.1541 \\ 0.01454 & -0.5008 & 1.331 \end{bmatrix} C_{CamRGB}$$

The data is from Alain Sarlat's submission *Using a spectral source to characterize a digital camera and build an ACES input device transform*, submitted to the Color Imaging Conference of 2012. A copy of the manuscript is available at http://colorpipe.mikrosimage.eu/wp-content/uploads/2012/03/CIC_Sarlat_draft.pdf



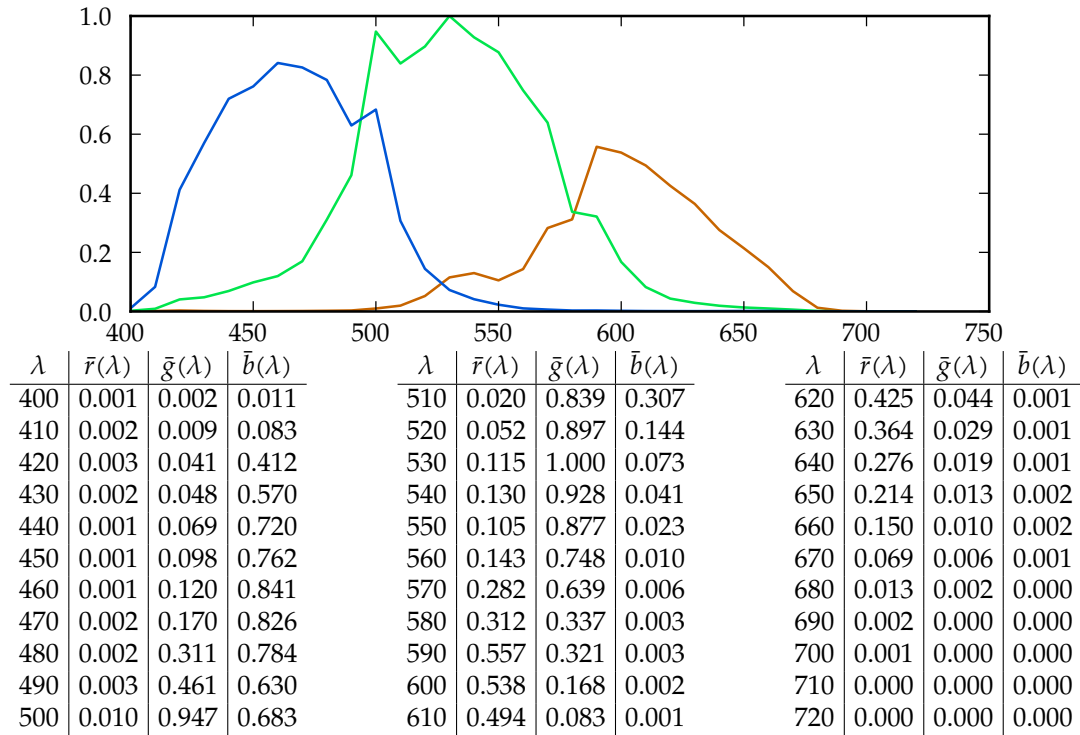
Spectral sensitivity data for Red Mystery X sensor, the three functions are $\bar{r}(\lambda)$ in red, $\bar{g}(\lambda)$ in green, $\bar{b}(\lambda)$ in blue, the color of each curve is taken from the **SRGB** coordinates for the corresponding curve, normalized so that the maximum **SRGB** linear value is $Y = 0.55$

5.2.2 Canon 1D Mark III

Camera **RGB** data is obtained through the curves in Section 5.2.2 and is converted into **SRGB** linear with the following matrix

$$C_{Rec709} = M_{Canon1DMkIII} C_{CamRGB} = \begin{bmatrix} 1.847 & -0.8233 & 0.06127 \\ -0.1107 & 1.446 & -0.35 \\ 0.03539 & -0.3862 & 1.185 \end{bmatrix} C_{CamRGB}$$

The data is from Jun Jiang et al.'s submission *What is the space of spectral sensitivity functions for digital color cameras?*, submitted to the IEEE Workshop on the Applications of Computer Vision (WACV) of 2013. A copy of the manuscript and database of measurements is available at <http://www.cis.rit.edu/jwgu/research/camspec/>



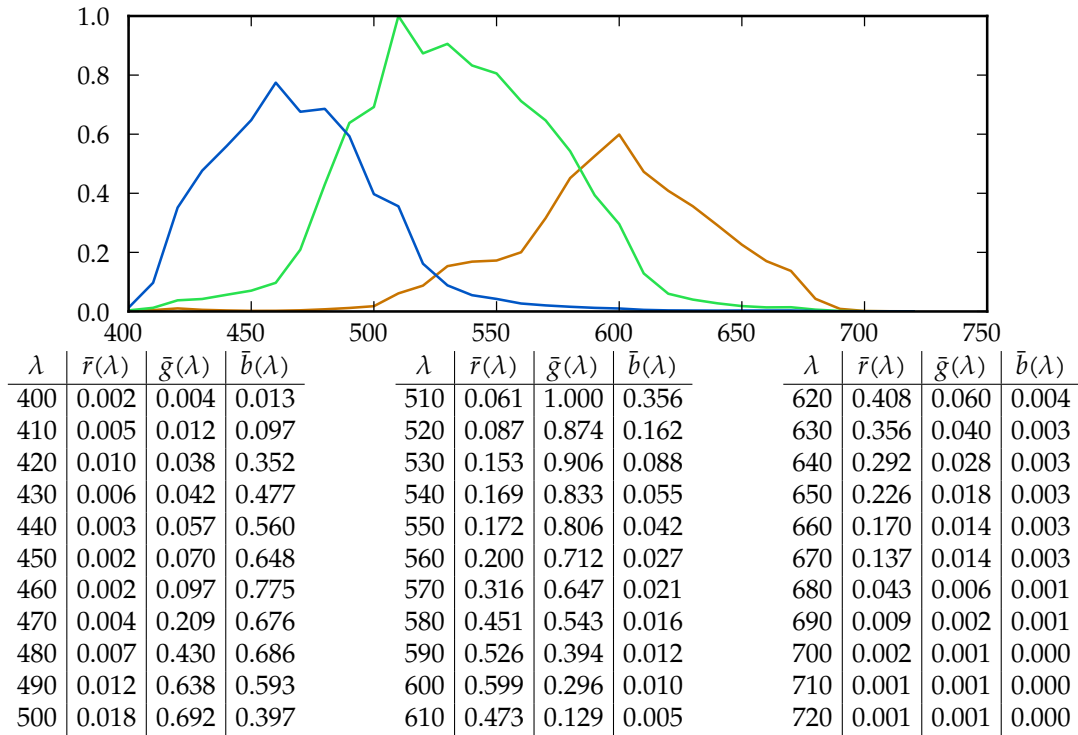
Spectral sensitivity data for Canon 1D Mark III, the three functions are $\bar{r}(\lambda)$ in red, $\bar{g}(\lambda)$ in green, $\bar{b}(\lambda)$ in blue, the color of each curve is taken from the **SRGB** coordinates for the corresponding curve, normalized so that the maximum **SRGB** linear value is $Y = 0.55$

5.2.3 Canon 5D Mark II

Camera **RGB** data is obtained through the curves in Section 5.2.3 and is converted into **SRGB** linear with the following matrix

$$C_{Rec709} = M_{Canon5DMkII} C_{CamRGB} = \begin{bmatrix} 2.043 & -1.065 & 0.107 \\ -0.1959 & 1.581 & -0.3999 \\ 0.05331 & -0.4666 & 1.248 \end{bmatrix} C_{CamRGB}$$

The data is from Jun Jiang et al.'s submission *What is the space of spectral sensitivity functions for digital color cameras?*, submitted to the IEEE Workshop on the Applications of Computer Vision (WACV) of 2013. A copy of the manuscript and database of measurements is available at <http://www.cis.rit.edu/jwgu/research/camspec/>



Spectral sensitivity data for Canon 5D Mark II, the three functions are $\bar{r}(\lambda)$ in red, $\bar{g}(\lambda)$ in green, $\bar{b}(\lambda)$ in blue, the color of each curve is taken from the **SRGB** coordinates for the corresponding curve, normalized so that the maximum **SRGB** linear value is $Y = 0.55$

Part III

Appendices

Appendix A

Handling color

A.1 Spectral basis representation

Several contemporary renderers are based on spectral light transport: they represent color values as functions of wavelength internally, instead of relying purely on tristimulus values. This allows effects such as dispersion at dielectric boundaries to be reproduced with much higher fidelity.

Since input data is often provided to the renderer in some **RGB** space, a spectral lifting procedure is required. Such a procedure takes tristimulus color values as an input and produces a spectrum that corresponds to the same color.

The conversion from a spectrum $S(\lambda)$ to tristimulus values (X, Y, Z) amounts to a projection onto a basis $(\bar{x}, \bar{y}, \bar{z})(\lambda)$:

$$\begin{pmatrix} X \\ Y \\ Z \end{pmatrix} = \int_{\Lambda} S(\lambda) \begin{pmatrix} \bar{x}(\lambda) \\ \bar{y}(\lambda) \\ \bar{z}(\lambda) \end{pmatrix} d\lambda \quad (\text{A.1})$$

While this operation is unique in the sense that there exists exactly one value (X, Y, Z) for any given spectrum $S(\lambda)$ and any particular basis $(\bar{x}, \bar{y}, \bar{z})$, the inverse operation is not. This phenomenon is called *metamerism*: spectra that are metameric to each other correspond to the same tristimulus color value with respect to the given basis.

As a simple example, consider the family of box spectra

$$S_i(\lambda) = \begin{cases} i/200, & \lambda \in [(500 - 100/i)\text{nm}, (500 + 100/i)\text{nm}], \\ 0, & \text{otherwise} \end{cases}$$

for $i \geq 1$ and the sensitivity function

$$\bar{x}(\lambda) = 1.$$

There are infinitely many such S_i , but for each of them,

$$\int_{380\text{nm}}^{780\text{nm}} S_i(\lambda) \bar{x}(\lambda) d\lambda = \int_{(500-100/i)\text{nm}}^{(500+100/i)\text{nm}} S(\lambda) d\lambda = \frac{i}{200} \cdot \frac{200}{i} = 1,$$

and so these spectra are metamers with respect to \bar{x} .

This ambiguity is the main problem that needs to be solved in spectral lifting procedures: out of the infinitely many spectra that, in general, correspond to any given tristimulus value, one needs to be selected.

One possible selection criterion is spectrum smoothness, because naturally occurring reflectance spectra are generally smooth functions of wavelength [Maloney, 1986]. The widely used technique by Smits (1999) therefore attempts to find spectra that maximize a specific smoothness criterion in an expensive precomputation. The precomputation is run for seven colors: the sRGB primaries Red(λ), Green(λ), and Blue(λ), their complements Cyan(λ), Magenta(λ), and Yellow(λ), and White(λ). Smits uses a run-time interpolation scheme that, for any given input color, attempts to use as much as possible of the smoothest available spectrum by first mixing in the white spectrum, then one of the complement color spectra, and only then a primary spectrum. This can be conceptualized as an application of something inspired by the Gram-Schmidt process, where an orthonormal basis is constructed by a sequence of reductions, each lowering the dimension of the residual.

As an example, consider the input color $c_0 = (0.9, 0.4, 0.1)_{\text{sRGB}}$:

$$\begin{aligned} \min(c_{0,r}, c_{0,g}, c_{0,b}) &= 0.1 \\ c_1 &= c_0 - 0.1 \cdot (1, 1, 1)_{\text{sRGB}} = (0.7, 0.3, 0)_{\text{sRGB}} \\ \min(c_{1,r}, c_{1,g}) &= 0.3 \\ c_2 &= c_1 - 0.3 \cdot (1, 1, 0)_{\text{sRGB}} = (0.4, 0.0, 0)_{\text{sRGB}} \end{aligned}$$

The result of this scheme is the interpolated spectrum

$$S(\lambda) = 0.1 \cdot \text{White}(\lambda) + 0.3 \cdot \text{Yellow}(\lambda) + 0.4 \cdot \text{Red}(\lambda), \quad (\text{A.2})$$

which corresponds to the input color since Equation (A.1) is linear.

This technique is bound to the sRGB color space, and the sparse sampling with only seven precomputed spectra can lead to poor results if a wider-gamut color space is used, instead [Meng et al., 2015]: saturated primary colors correspond to narrow band spectra, which in turn produce mixtures of narrow band spectra in Smits' lifting procedure. This can limit the maximum attainable reflectance if per-wavelength energy conservation is required [Schrödinger, 1920], and can be detrimental in rendering systems based on random or quasi-random Monte Carlo integration.

Meng et al. (2015) generalize the method using a much denser sampling of the xy chromaticity space, decoupling the spectral lifting method from the input color space.

Other authors have argued that a simple smoothness criterion can be problematic in scenes with dominant indirect illumination: General smoothness simply ensures that the spectrum will be reasonably well-behaved under reflection as even narrow band incident lighting is reflected by a wide band reflectance spectrum. However, in the presence of multiple reflections, intricate color shifts may occur in natural materials. Otsu et al. (2017) therefore attempt to extract, for any given input color, a metameric spectrum a principle component analysis on measured spectral reflectance data.

This approach might benefit from domain-specific measured data sets: For example, there might be a set of measured spectra for leaves that is used when an artist wants to recreate the appearance of leaves.

Appendix B

Reference implementation

B.1 Pipeline integration



This section is under construction

Review this section

As a virtual movie making pipeline is comprised of many parts, from content creation, to scene assembly and asset management, there is a need to be certain that all interpretations of values match across the various components.

Components that will likely need adaptation or revision are:

- Host applications / **Digital Content Creation (DCC)** tools (such as Maya, Motion Builder, Katana, Houdini)
- Scene translation bridges and scene representation formats, such as **Universal Scene Description (USD)**
- Light management systems
- Shader libraries
- Renderers

this is a fairly direct consequence of common custom so far. Until this point, it has been fairly common to use physical units in physics simulation systems, but not for lighting descriptions. Much like cameras have their focal length specified in millimeters in the user interface, similar adaptations will be needed for various other quantities, such as filmback, light sensitivity and so on. Similarly, as the renderers will be adapted to receive data referred to physical units, the bridges would need to make sure they are capable of transporting and translating such data appropriately, and various shading libraries might need various levels of adaptation for correctness. These changes are discussed in detail in the rest of this document: while Section 2.1 focuses on the theoretical background for these revisions, Appendix B has code reference for the specifics of a working implementation.

Scene representation Scene representations will now need bindings from scene units to **SI** units, so the renderer is aware of the physical dimensions of the entities involved.

For example, in **RenderMan Interface Bytestream (RIB)** this might look like this:

		RIB	source
Option "units"	"float length" [0.01]	# scene unit is 1 cm	
"float time"	[0.04166] # 24 fps		

where `units:length` is the size of 1 scene unit in meters, and `units:time` is the size of 1 time unit in seconds.

Although light transport simulations are fundamentally spectral, at present the majority of the commercially available image synthesis systems have been based on tristimulus **RGB** transport. In recent times, especially as facilitated by the increasing availability of the OpenColorIO library, these systems have evolved to implement an ability to receive data in a number of different color spaces, transforming it all into a common color space used for computation, and then being able to produce images in a target color space specified by the user. Some of these systems are also capable of transforming spectral data into tristimulus values. In the spectral approach, all light transport computations happen in the spectral domain and the transformation into the imaging color space happens at the end of the pipeline. This requires a facility to lift **RGB** input data to the renderer to some spectral representation to handle inputs that are **RGB** to start with, such as common texture maps.

There are various reasons why one might choose an approach versus the other, and image synthesis systems that have had a long history are most often tristimulus-based. Further, as the computational and storage requirements of a tristimulus approach tend to be somewhat lighter, this is convenient on less powerful machines or systems that are otherwise constrained in compute resources, or maybe need a very high frame rate and can sacrifice some accuracy to gain performance. On the other hand, a number of light phenomena such as dispersion or an accurate accounting of metameric effects are expensive to simulate accurately in a tristimulus-based system, while they simply happen as a part of the system in a spectral system.

B.2 Tristimulus rendering

All the following assumes the **RGB** working space is sRGB linear scene referred, which will be indicated as sRGB_ℓ . When gamma corrected values are used, their color space will be subscripted with a γ such as sRGB_γ . As sRGB and Rec709 use the same primaries, sRGB_ℓ is effectively the same as Rec709_ℓ , whereas sRGB_γ and Rec709_γ differ due to the different definition of their gamma correction formulation.

B.2.1 Area lights

Tint vector The tint vector is the average value of the texture map, computed in sRGB_ℓ space. Assuming the file actually contains data sRGB_ℓ space, this can be obtained either with a **RenderMan Shading Language (RSL)** call like

	Shading Language	source
<pre>color tint = texture(filename, 0.5, 0.5, // access at center "blur", 1.0, // filter the entire texture into the result "filter", "box"); // use box filtering (compute average)</pre>		

or the average value can be computed with code similar to the following, in which the incremental average formulation from [Knuth, 1997] is used

C++ source

```
// assume type float3 supports standard vector-like arithmetic operators
float3* image = ...;
float3 tint = float3(0.f, 0.f, 0.f);

for (int i = 0; i < pixelcount; ++i)
{
    tint += (image[i] - tint) / float(i+1);
}
```

Reduced luminance vector Introduce sensitivity primaries here

Compute $\|col \cdot \hat{L}\|_{\tilde{y}}$: we know that col is our CameraRGB space $col = (\bar{r}(\lambda), \bar{g}(\lambda), \bar{b}(\lambda))$, so the integrals can be precomputed for the supported cases with code like this (for example in the case of $\hat{L}(\lambda)$ being Illuminant D50):

Python source

```
# load spectral sensitivity of the camera
# this is effectively col
camera = Camera.Camera("Red_Mysterium_X")
# get CIE 1931 Color Matching Functions
cmf = CIE.CMF_1931
# get Illuminant D50 data: Illuminant D at 5003 K
# this is  $\hat{L}$ 
illuminant = SPD.IlluminantD.at(cmf.lnms, 5003)
# reduced luminance vector  $\|col \cdot \hat{L}\|_{\tilde{y}}$ 
redlum_camRGB = [0,0,0]

# tp_integral() is the triple product integral
#  $\int \bar{r}(\lambda) \bar{ill}(\lambda) \bar{y}(\lambda) d\lambda$ 
redlum_camRGB[0] = tp_integral(camera.rbar, illuminant, cmf.ybar)
redlum_camRGB[1] = tp_integral(camera.gbar, illuminant, cmf.ybar)
redlum_camRGB[2] = tp_integral(camera.bbar, illuminant, cmf.ybar)

# now transform into sRGBt primaries, M is CameraRGB to sRGBt
M = [[ 1.369, 0.0137, -0.3068],
      [-0.18, 1.326, -0.1541],
      [0.01454, -0.5008, 1.331]]
redlum_sRGB = M * redlum_camRGB
```

Angular norm From Section 4.3 we see that the angular norm $\|D\|$ of $\langle \omega, \hat{n} \rangle^n$ is $2\pi/(n+2)$, which is easily implemented as

C++ source

```
float cospower = /* from light parameters */
float angularnorm = (2.f * M_PI) / (2.f + cospower);
```

Ies profiles can be integrated using 2-dimensional Newton-Cotes quadrature of degree 1 (also called *trapezium rule*) because the error introduced in the sampling of the luminaire dominates the error in the sampling of the $\cos \theta \sin \theta$ factor in the integral. What’s called “vertical angle” in the **Ies** profile specification corresponds to angle θ and what’s called “horizontal angle” corresponds to φ , this means the rows in the “candela values” data in the file are constant- φ measurements of the described luminaire.

Emission constant The emission constant k_e is computed as

C++ source

```

const float K_{cd} = 683;

float Phi_v = /* luminous power from light parameters */;
float A      = /* area of the light from geometry */;

float angularnorm = /* computed as above */;
float3 tint       = /* computed as above */;
float3 redlum_sRGB = /* computed as above */;

float k_e = Phi_v / (K_{cd} * A * angularnorm * dot(tint, redlum_sRGB));

```

Reduced radiance To compute radiance we need to first compute the reduced radiance $\|col \cdot \hat{L}\|$: we know that col is our $cameraRGB_l$ space $col = (\bar{r}(\lambda), \bar{g}(\lambda), \bar{b}(\lambda))$, so the integrals can be precomputed for the supported cases with code like this (for example in the case of $\hat{L}(\lambda)$ being Illuminant D50):

Python source

```

# load spectral sensitivity of the camera
camera = Camera.Camera("Red_Mysterium_X")
# get CIE 1931 Color Matching functions
cmf = CIE.CMF_1931
# get Illuminant D50 data, Illuminant D at 5003 K
illuminant = SPD.IlluminantD.at(cmf.lnms, 5003)
# reduced radiance vector, r, g, b components
redrad_camRGB = [0,0,0]

# p_integral() is the product integral
redrad_camRGB[0] = p_integral(camera.rbar, illuminant)
redrad_camRGB[1] = p_integral(camera.gbar, illuminant)
redrad_camRGB[2] = p_integral(camera.bbar, illuminant)

# now transform into sRGB primaries, M is CameraRGB to sRGB
M = [[ 1.369,  0.0137, -0.3068],
      [-0.18,  1.326, -0.1541],
      [0.01454, -0.5008,  1.331]]
redrad_sRGB = M * redrad_camRGB

```

Radiance from the source At this point the radiance from this source is simply

Shading Language source

```

float k_e = /* computed as above */;
color redrad_sRGB = /* computed as above */;

color radiance =
    k_e *
    texture(filename, s, t) *
    redrad_sRGB *
    pow(normalize(L).normalize(N), cospower);

```

B.2.2 Image Based Lighting sources



This section is under construction

Add code defining what is in radiance

Irradiance coloration vector Compute the average of the **IBL** map times $\cos \theta$ in $sRGB_l$. Be careful with long sums, mipmapping can't be used. Use Knuth-style incremental averaging (probably in double for accuracy).

Tint vector Compute $\|T \cdot col\|_{\tilde{y}}$

B.2.3 Sun lights



This section is under construction

Add code defining what is in radiance

Angular norm The norm of D_{ω_c} need to be computed, write down a few common cases

Tint vector Compute the average of the tint texture map in **sRGB**. Be careful with long sums, either use mipmapping or Knuth-style incremental averaging (probably in double for accuracy).

Reduced illuminance vector Compute $\|col \cdot \hat{L}\|_{\tilde{y}}$: we know that col is **CIE XYZ** space, so the integrals can be precomputed for the supported cases, and stored somewhere. This needs some attention to detail

B.2.4 Materials

Materials in **RGB** renderers operate as if there were only three wavelengths in the world, that is picking $sRGB_l$ data from the textures, converting it to the working color space and proceeding to multiply component by component such values with the incoming radiance to produce outgoing radiance.

B.2.5 Imaging

This section outlines how to apply the imaging parameters to the resulting value c_i containing the **RGB** radiance flowing towards the image plane. White balance is achieved dividing out the whitepoint color in $cameraRGB_l$ coordinates. This is implemented as a matrix multiply for convenience, which does in one go the whole operation of going from working space, to camera space, multiplying by the inverse of the white point, and transforming back. Such matrix is built in the helper method `buildWhitebalanceTransform()` outlined below.

The binding in a *RenderMan* system can be implemented by means of a pixel-sample imager shader, bound with the call `RiPixelSampleImager()`

A minimal version of such a shader follows, built on the convention that the incoming `ci` contains radiance, as above. The code of the shader has been separated into a few code sections for clarity.

```

class physLightImaging(
    // camera focal length, in mm
    float focalLength = 24;
    // focus distance, in scene units
    float focusDistance = 100;
    // aperture f-number
    float apertureNumber = 8;
    // exposure time, in seconds.
    // -1 picks it up from the RIB
    float exposureTime = -1;
    // film speed, ISO/ASA
    float filmSpeed = 100;
    // white point, in Kelvin
    float whitepoint_T = 6500;
)
{
    constant matrix c_whitebalance;
    constant float c_imagingRatio;

    // return the color of a blackbody of temperature T
    // in cameraRGB_l space
    color blackBody2CameraRGBl(float T) { /* ... */ }

    // return the size of one meter in scene units
    float getOneMeter() { /* ... */ }

    // get the exposure time from a shader parameter or from the RIB
    float getExposureTime() { /* ... */ }

    // get the aperture distance
    float getApertureDistance(float f; float o) { /* ... */ }

    // build a tranformation to apply whitebalance in cameraRGB_l space
    matrix buildWhitebalanceTransform() { /* ... */ }

    // rebalance the color for a white point at the given temperature
    color apply_whitebalance(color C)
    {
        return (color) transform(c_whitebalance, (point) C);
    }

    public void construct() { /* ... */ }

    public void imager(output varying color Ci, Oi)
    {
        // apply whitebalance
        Ci = apply_whitebalance(Ci);
        // apply exposure parameters
        Ci *= c_imagingRatio;
    }
}

```

The `construct()` method initializes the white balance transform and the imaging

ratio. These are then used in the `imager()` method to convert incoming radiance into appropriately scaled irradiance at the **filmback**.

Shading Language source

```
public void construct()
{
    c_whitebalance = buildWhitebalanceTransform();

    float oneMeter = getOneMeter();
    float exposureTime = getExposureTime();
    float f = focalLength / 1000;
    float o = focusDistance / oneMeter;
    float a = getApertureDistance(f, o);
    float r = f / (2 * apertureNumber);
    float apertureRatio = PI * r*r / (a*a);

    // the imaging constant, Equation (2.6)
    float k_i = 4 * 683 / 312.5;

    // scale as per Equation (2.15)
    // note the missing division by  $K_{cd}$  as here  $C_i$  is already in
    // radiometric units
    c_imagingRatio = c_exposureTime * k_i * filmSpeed * c_apertureRatio;
}
```

The helper method `getOneMeter()` returns the number of scene units in a meter using the **RIB** option `units:length`

Shading Language source

```
// get the size of one meter in scene units
float getOneMeter()
{
    float lengthscale = .01;
    option("units:length", lengthscale);
    return 1 / lengthscale;
}
```

The helper method `getApertureDistance()` computes the distance of the aperture from the filmback, in the notation of Section 2.1

Shading Language source

```
// get the aperture distance
// f - the focal length
// o - the focus distance, from the filmback
float getApertureDistance(float f; float o)
{
    o /= 2;
    return o - sqrt(o*o - 2 * f * o);
}
```

The helper method `getExposureTime()` computes the exposure time using either the **RIB** option `units:time` or the shader parameter `exposureTime` in case it's not the sentinel value -1

Shading Language source

```
// get the exposure time from a shader parameter or from the RIB
float getExposureTime()
{
    float result = exposureTime;
    if (result == -1)
    {
```



```

    float timescale = 1/24;
    option("units:time", timescale);
    float shutter[2] = {0,0};
    option("Ri:Shutter", shutter);
    result = (shutter[1] - shutter[0]) * timescale;
}

return result;
}

```

White balance is achieved transforming into cameraRGB_ℓ , divide component by component by color of illuminant (also in cameraRGB_ℓ) and transforming back into sRGB_ℓ .

Shading Language source

```

matrix buildWhitebalanceTransform()
{
    // this is M_MysteriumX from Section B.2, transposed because
    // RenderMan is row-vectors
    uniform matrix cam2sRGB = {
        1.369,  -0.18,   0.01454,  0,
        0.0137,  1.326,  -0.5008,  0,
        -0.3068, -0.1541, 1.331,   0,
        0,       0,     0,        1};

    uniform matrix sRGB2cam = 1 / cam2sRGB;

    // white point, in cameraRGB
    uniform color whitepoint = 1 / blackBody2CameraRGB_l(whitepoint_T);
    uniform matrix wpm = {
        whitepoint[0], 0, 0, 0,
        0, whitepoint[1], 0, 0,
        0, 0, whitepoint[2], 0,
        0, 0, 0, 1};

    c_whitebalance = cam2sRGB * wpm * sRGB2cam;
}

```

The `blackBody2CameraRGB_l` method returns the color coordinates of a black body radiator in cameraRGB_ℓ space and is here in python:

Python source

```

# return the color of a blackbody of temperature T
# in cameraRGB_l
def blackBody2CameraRGB_l(T):
    camera = Camera.Camera("Red_Mysterium_X")

    illuminant = SPD.BlackBody.at(camera.lnms, 6500)
    illuminantE = SPD.IlluminantE.at(camera.lnms)
    illXYZ = ColorSpace.XYZ_lv(camera.lnms, illuminant)
    illEXYZ = ColorSpace.XYZ_lv(camera.lnms, illuminantE)

    illuminant /= illXYZ[1]
    illuminant *= illEXYZ[1]

    bbCameraRGB = ColorSpace.RGB_lv(camera.lnms, illuminant, camera)
    bbCameraRGB /= ColorSpace.RGB_lv(camera.lnms, illuminantE, camera)

    return bbCameraRGB

```

B.3 Spectral setting

The typical assumption in the tristimulus setting is that transformations between the various color spaces has no adverse effects, and that it is appropriate to use the **CIE** $\bar{x}(\lambda), \bar{y}(\lambda), \bar{z}(\lambda)$ color matching curves to map from spectral to tristimulus **XYZ** space.

We introduce the use of cameraRGB color space, the color space determined by spectral response curves coming from a physical camera, together with a matrix to map this space into **CIE XYZ** (or sRGB_ℓ). Examples of such data are given in the appendix, Section 5.2.

B.3.1 Lights

This section is under construction

Integrals to store:

- $\|D\|$ angular norm
- $\|T_\star\|$ store tint with texture
- precomputed integrals for common illuminants

Angular norm angular distributions should be normalized to integrate to 1.

Texture norms

$$|T_\star| = \int_A T_\star(x) dx$$

where A is the area of the light. The integral is actually an average of the pixel values scaled with the light area. we can precompute the average of the per channel pixel values and store them in the header of the file.

Reduced quantities Precompute

$$|\varphi_\star| = \int_\lambda \star(\lambda) E(\lambda) \bar{y}(\lambda) d\lambda$$

$$|\varphi| = \int_\lambda E(\lambda) \bar{y}(\lambda) d\lambda$$

for the most common radiators. (black body, illuminant D_{65} , ..)

B.4 Color space conversion code

Color spaces

Quick summary of useful color space conversions

xyY to XYZ If $Y = 0$ the result is (0,0,0), otherwise

$$X = Y \frac{x}{y}$$

$$Y = Y$$

$$Z = Y \frac{1 - x - y}{y}$$

Python source

```
# Computes XYZ coordinates from the given xy coordinates
# and Y value, assumes xy to be not imaginary
def XYZ(xy, Y):
    x, y = xy
    X = Y * x / y
    Z = Y * (1 - x - y) / y
    return (X, Y, Z)
```

XYZ to xy

$$x = \frac{X}{X + Y + Z}$$

$$y = \frac{Y}{X + Y + Z}$$

Python source

```
# Computes xy coordinates from the given XYZ coordinates
def xy(XYZ):
    X, Y, Z = XYZ
    x = X / (X+Y+Z)
    y = Y / (X+Y+Z)
    return (x,y)
```

XYZ to sRGB/Rec. 709 primaries, linear

$$C_{Rec709} = M_{Rec709} C_{XYZ} = \begin{bmatrix} 3.2404542 & -1.5371385 & -0.4985314 \\ -0.9692660 & 1.8760108 & 0.0415560 \\ 0.0556434 & -0.2040259 & 1.0572252 \end{bmatrix} C_{XYZ}$$

Python source

```
# Computes XYZ coordinates from the given set of
# color matching functions
# l - list of wavelengths
# v - list of values
# xyzcmf an object containing
# .lnms - list of wavelengths
# .xbar - values for  $\bar{x}(\lambda)$ 
# .ybar - values for  $\bar{y}(\lambda)$ 
# .zbar - values for  $\bar{z}(\lambda)$ 
def XYZ_lv(l, v, xyzcmf = CIE.CMF_1931):
    X = _integrate(l, v, xyzcmf.lnms, xyzcmf.xbar)
    Y = _integrate(l, v, xyzcmf.lnms, xyzcmf.ybar)
    Z = _integrate(l, v, xyzcmf.lnms, xyzcmf.zbar)

    return numpy.array([X, Y, Z])
```

B.5 Texture maps

B.5.1 RGB to spectrum conversions

It's common practice to use **RGB** texture maps to encode various kind of spatially varying spectral distributions. In order to use them in a spectral pipeline, a way is needed to try and reconstruct a plausible spectrum from the data in these files. Chapter 2 introduced the idea of discussing spatially varying spectra in terms of n -dimensional vectors in a color basis called generically $col(\lambda)$ for which a simple example was given for a naive reconstruction from **RGB** as

$$M(p, \lambda) = \langle M_{rgb}(p), rgb(\lambda) \rangle$$

Although appealing in its simplicity, this way of reconstructing a spectral distribution from a texture would turn out to be only appropriate to model emissive objects, for example some kind of **RGB** monitor, but would be a fairly poor approach to represent richer, more natural reflectance or transmittance spectra. In absence of sidecar information regarding what kind or class of spectral distribution should be used to perform a reconstruction from a given texture, a more believable way to rebuild spectral distributions from **RGB** triples is the algorithm proposed by Brian Smits in [Smits, 1999]: given 7 spectra for white, cyan, magenta, yellow, red, green, blue:

$$smits(\lambda) = (w(\lambda), c(\lambda), m(\lambda), y(\lambda), r(\lambda), g(\lambda), b(\lambda)) : \mathbb{R}^+ \rightarrow \mathbb{R}^7$$

a simple procedure is described to build a vector

$$M_{smits} = (M_w, M_c, M_m, M_y, M_r, M_g, M_b) \in \mathbb{R}^7$$

in which at most three coordinates are non-zero. Then the resulting spectrum would be

$$M(p, \lambda) = \langle M_{smits}(p), smits(\lambda) \rangle$$

Spectra recovered this way have some desirable guarantees in terms of smoothness, and the algorithm lends itself to a very efficient implementation. The data presented here is based on a 10 bin spectral representation from 380nm to 720nm. The bins are all equal size, the function `bin()` return the bin index from a given wavelength

C++ source

```
const uint32_t c_numBins = 10;
const uint32_t c_numSpectra = 7;
const float c_minWavelength = 380.f;
const float c_maxWavelength = 720.f;

uint32_t bin(float wavelength)
{
    using std::min;
    using std::max;

    float binWidth = (c_maxWavelength - c_minWavelength) / c_numBins;

    uint32_t bin = static_cast<uint32_t>(
        (wavelength - c_minWavelength) / binWidth);

    return min(max(bin, 0u), c_numBins - 1);
}
```

Follows the table of Smits' original data

```

C++ source
const float c_table[c_numBins * c_numSpectra] =
{
// bin    white    cyan    magenta    yellow    red    green    blue
/* 0 */    1.0000f, 0.9710f, 1.0000f, 0.0001f, 0.1000f, 0.0000f, 1.0000f,
/* 1 */    1.0000f, 0.9426f, 1.0000f, 0.0000f, 0.0515f, 0.0000f, 1.0000f,
/* 2 */    0.9999f, 1.0007f, 0.9685f, 0.1088f, 0.0000f, 0.0273f, 0.8916f,
/* 3 */    0.9993f, 1.0007f, 0.2229f, 0.6651f, 0.0000f, 0.7937f, 0.3323f,
/* 4 */    0.9992f, 1.0007f, 0.0000f, 1.0000f, 0.0000f, 1.0000f, 0.0000f,
/* 5 */    0.9998f, 1.0007f, 0.0458f, 1.0000f, 0.0000f, 0.9418f, 0.0000f,
/* 6 */    1.0000f, 0.1564f, 0.8369f, 0.9996f, 0.8325f, 0.1719f, 0.0003f,
/* 7 */    1.0000f, 0.0000f, 1.0000f, 0.9586f, 1.0149f, 0.0000f, 0.0369f,
/* 8 */    1.0000f, 0.0000f, 1.0000f, 0.9685f, 1.0149f, 0.0000f, 0.0483f,
/* 9 */    1.0000f, 0.0000f, 0.9959f, 0.9840f, 1.0149f, 0.0025f, 0.0496f
};

```

and a helper function evalBin() which contains the core of Smits's algorithm

```

C++ source
float evalBin(float r, float g, float b, uint32_t bin)
{
    const float* const row = c_table + bin * c_numSpectra;

    if (r <= g && r <= b) // red is smallest
        return r * row[0] + ((g <= b) ? // white
            ((g - r) * row[1] + // cyan
            (b - g) * row[6]) : // blue
            ((b - r) * row[1] + // cyan
            (g - b) * row[5])); // green

    if (g <= r && g <= b) // green is smallest
        return g * row[0] + ((r <= b) ? // white
            ((r - g) * row[2] + // magenta
            (b - r) * row[6]) : // blue
            ((b - g) * row[2] + // magenta
            (r - b) * row[4])); // red

    // blue is smallest
    return b * row[0] + ((r <= g) ? // white
        ((r - b) * row[3] + // yellow
        (g - r) * row[5]) : // green
        ((g - b) * row[3] + // yellow
        (r - g) * row[4])); // red
}

```

The last remaining function is evalSpectrum() which relies on the seven basis functions being piecewise constant

```

C++ source
float evalSpectrum(float3 rgb, float wavelength)
{
    return evalBin(rgb[0], rgb[1], rgb[2], bin(wavelength));
}

```

Appendix C

Radiance

An extract from [Nicodemus, 1963], introducing the formal definition of radiance. The excerpt has been retypeset, the symbols designating the various quantities brought in line with current practice, SI units substituted and references adapted to the typographic style of this document.

American Journal of Physics, Vol. 31, pg. 368–377, 1963

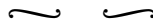


FRED E. NICODEMUS

Sylvania Electronic Systems

West, Electronic Defense Laboratories, Mountain View, California

(Received 22 October 1963)



ABSTRACT

Wide generality for optical radiometry can be achieved by treating the basic radiometric quantities as field quantities. The treatment is that of classical ray optics, with emphasis on the geometrical relations involved. It is shown that radiance, defined as

$$L_e \equiv \frac{\partial^2 \Phi_e}{\partial \omega \cos \theta \partial A} \quad \left[\frac{\text{W}}{\text{m}^2 \cdot \text{sr}} \right],$$

the radiant flux or power per unit solid-angle-in-the-direction-of-a-ray per unit projected-area-perpendicular-to-the-ray, has the same value at any point along this ray within an isotropic medium, in the absence of losses by absorption, scattering, or reflection. More generally, the quantity L/n^2 (where n is the index of refraction of the medium) in the direction of a ray is shown to be invariant along that ray, even across a smooth boundary between different lossless media. The usefulness of this invariant property of radiance is illustrated by examples of practical applications.

C.1 Introduction

Why does a photographic exposure meter give the same reading over a wide range of distances from a uniformly illuminated blank wall with a rough, weathered surface? Of course the indication changes when it is held so close to the wall that its shadow, or that of the supporting arm and hand, reduces the illumination, or when it is held so far away that radiation is also received from the surrounding background beyond the edges of the wall. But between these extremes, the indication will remain constant. Nor

is it possible with an external lens, however large or “fast,” to focus more radiant power from the wall onto the exposure meter to obtain a higher reading.

Why does a spectroscopist obtain maximum energy with the following procedure? Focus an image of the source onto the entrance slit of the spectroscope. Arrange the source and focusing optics so that the image is just large enough to fill the slit completely (if the source is not uniform, the slit must be filled by the brightest uniform region of the image), and so that the rays which cross to form the image diverge widely enough after passing through the slit that they completely fill the collimating optics of the spectroscope. Once this condition has been achieved, it is useless to attempt to focus more radiant power through the instrument from the same source.

If it is given that the earth’s surface radiates a total (in all directions) of w W/m², how can we quickly estimate the irradiance E_e , in W/m² due to this source alone without atmospheric attenuation, at a horizontal receiving surface carried on an earth satellite vehicle? For simplicity, assume that the earth is a perfectly diffuse radiator.

These situations all involve extended sources of radiation. It has been my experience that most people find it peculiarly difficult to master the fundamental concepts and relations of radiometry (or photometry) as they apply to extended sources. And I have come to believe that the key to this difficulty lies in the interrelated concepts of an elementary beam of radiation and its radiance (or luminance).

A brief definition of radiance is given in the abstract and is discussed in more detail directly. It is helpful to note here that radiance is analogous to the familiar property of visual brightness, or more exactly to the photometric quantity luminance. Also for convenience, Table 1.1¹ lists the radiometric quantities, symbols, and units used in this paper.

Sometimes radiance is defined as applying only to sources of radiation (see [Kelton et al., 1963]², [E. E. Bell, 1959]³ and [Jenkins and White, 1950]). Frequently it is applied also to images of a source, and it is shown that, in the absence of attenuation, the radiance (or luminance) of an image is equal to that of the source in the direction of any ray reaching it from the source (see [Jenkins and White, 1950]).

The usefulness of defining radiance more broadly as a field quantity which can be evaluated at any point along a ray is also pointed out, particularly with reference to diffuse sources such as a volume of emitting gas (see [Kelton et al., 1963]). It is established that radiance has the same value everywhere and in all directions, within an isotropic region in thermal equilibrium (see [Planck, 1957], p. 183–196 and [Richtmyer and Kennard, 1947]). However, I have not found anywhere a completely general treatment of invariant property of radiance, defined as a field quantity, although such a treatment can greatly simplify the understanding of many radiometric situations, as well as the computation or estimation of the amount of radiant power or flux incident on a receiver or detector, or passing through some aperture of interest, in a wide variety of circumstances. None of the material presented here is new, rather it is implicit in many publications, but it is not explicitly in any that I am aware of.

¹[Table I in the original—*Ed.*]

²[Cited in the original as “Report of WGIRB (Working Group on Infrared Backgrounds)—Infrared Target and Background Radiometric Measurements—Concepts, Units, and Techniques”, Report 2389-64-T, NAVEXOS P-2406 (IRIA, Institute of Science and Technology, University of Michigan, Ann Arbor, Michigan, January 1962), pp. 3-4 Contract No. Nonr-1224(12) —*Ed.*]

³Essentially the same material also appears as “Report of the Working Group on Infrared Backgrounds; Part II: Concepts and Units for the Presentation of Infrared Background information,” Report No. 2389-3-5 (Engineering Research Institute, University of Michigan, Ann Arbor, Michigan, November 1956), Contract No. Nonr-1224 (12)

For generality, we define radiance as a field quantity which can be evaluated at any point on any surface through which radiant power or flux is passing. This includes, but is not restricted to, the surfaces of a source, a receiver, or any intermediate optical element such as a mirror, lens, or stop (aperture limiting a beam of radiation). On this basis, radiance is defined as the radiant flux or power per unit solid-angle-in-the-direction-of-a-ray per unit projected-area-perpendicular-to-the-ray. More precisely, in a given direction from a point on a surface through which radiant energy is passing,

$$L_e \equiv \frac{\partial^2 \Phi_e}{\partial \omega \cos \theta \partial A} \left[\frac{\text{W}}{\text{m}^2 \cdot \text{sr}} \right], \quad (\text{C.1})$$

where L_e = the radiance at that point in the given direction, Φ_e = the radiant flux or power flowing through the surface (within the solid angle ω and the area A) [W], ω = the solid angle filled by the rays along which the radiation is propagated (including, of course, the ray extending in the given direction through the given point of the surface) [sr], A = the area of the surface (including, of course, the given point) [m²], and θ = the angle between the given direction and the normal to the surface at the given point [rad]. We return to this definition later as the basic radiometric quantities are presented in a logical sequence leading up to the proof of the invariance property. It is shown that the value of L in the direction of any ray has the same value at all points along that ray within an isotropic medium, in the absence of losses by absorption, scattering, or reflection. More generally, the quantity L/n^2 (where n is the index of refraction of the medium) in the direction of a ray is shown to be invariant along that ray, even across a smooth non-reflecting boundary between different lossless media. The treatment of real situations, where absorption, scattering, and reflection can not be neglected, is also discussed.

C.2 Analysis

We define a radiation field as a region in which radiant power is propagated, at a velocity characteristic of the region or medium and independent of direction, along straight non-interfering rays which may pass in any direction through any point within the region. The radiant power or flux may vary with position and direction, but only in a continuous manner, so that a finite amount of power can flow only through a finite area and a finite solid angle. Thus, here and in actuality, there is no such thing as a point source, with all of the power traveling along rays which intersect at a single mathematical point; nor is there such a thing as a perfectly collimated beam with all of the power traveling along rays which are perfectly parallel⁴.

In order to analyze this situation, let us first consider only the distribution of power flow as a function of direction. We define an elementary pencil of rays through a point Q as including all of the rays which pass from Q through an element of area dA at a distance D from Q which is very large in relation to the linear dimensions of dA (see Figure C.1). The solid angle subtended at Q by dA is given by

$$d\omega = \frac{\cos \theta dA}{D^2} \quad [\text{sr}],$$

⁴ The assumptions involved here are discussed with greater rigor by Planck. It can be shown that his analysis does not conflict with the results presented here, although there are apparent differences due to the very different terminology and symbols used. See [Planck, 1957], pp. 173–177

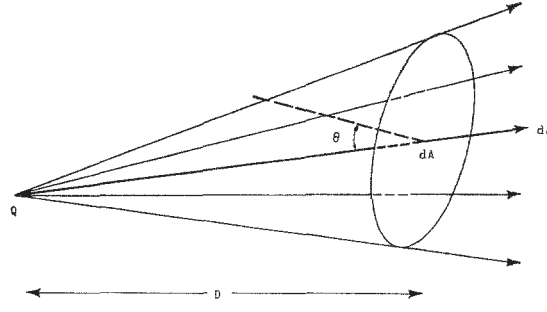


Figure C.1: An elementary pencil of radiation

where θ is the angle between the normal to dA and the pencil of rays, i.e., $\cos \theta dA$, is the projected area of dA normal to this pencil. If we next consider Q not as a mathematical point, but as having dimensions which, however, are very small compared to the dimensions of dA (and, hence, extremely small compared to D), the power which flows along the rays in this pencil from Q to dA can be expressed as

$$d\Phi_e = I_e d\omega = I_e \frac{\cos \theta dA}{D^2} \quad [\text{W}],$$

where

$$I_e \equiv \frac{\partial \Phi_e}{\partial \omega} \quad \left[\frac{\text{W}}{\text{sr}} \right] \quad (\text{C.2})$$

is defined as the *radiant intensity* (see Table 1.1) of Q as a “point” source of radiation (e.g., a virtual source, such as the image of an illuminated pin hole) *in the direction of the pencil* (the direction of dA from Q). Note that I_e may vary with direction and is a constant only for an isotropic source. In general, the power received from a distant “point” source is given by

$$\Phi_e = \int I_e d\omega \quad [\text{W}], \quad (\text{C.3})$$

where the integration is carried out over the entire solid angle subtended at the source by the receiver.

For completeness, we also look briefly at the purely spatial variation, although this quantity is more easily understood and is not so often a source of difficulty or misunderstanding. If we consider an element of surface dA , situated anywhere in a radiation field, the total amount of radiant power passing through it (either into it from a hemisphere, or out of it into a hemisphere) can be expressed as

$$d\Phi_e = E_e dA \quad \text{or} \quad d\Phi_e = M_e dA \quad [\text{W}],$$

where

$$E_e \equiv \frac{\partial \Phi_e}{\partial A} \quad \left[\frac{\text{W}}{\text{m}^2} \right] \quad (\text{C.4})$$

is the *irradiance* (see Table 1.1), the surface density of radiant power flowing into the surface at a point from a complete hemisphere (or, sometimes, from a stated solid angle which is less than a hemisphere), and where

$$M_e \equiv \frac{\partial \Phi_e}{\partial A} \quad \left[\frac{\text{W}}{\text{m}^2} \right] \quad (\text{C.5})$$

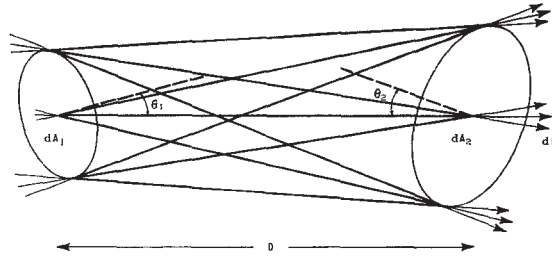


Figure C.2: An elementary beam of radiation between two surface elements dA_1 and dA_2

is the *radiant exitance*⁵ (see Table 1.1), the surface density of radiant power flowing out of the surface at a point into a complete hemisphere. Both of these quantities may vary from point to point over an extended surface, so that the total radiant power flowing into the surface of a receiver is given by

$$\Phi_e = \int E_e dA \quad [\text{W}], \quad (\text{C.6})$$

and that flowing out of the surface of a source is given by

$$\Phi_e = \int M_e dA \quad [\text{W}], \quad (\text{C.7})$$

where the integration is carried out over the entire surface of interest in each case.

We now consider the simultaneous distribution of radiant flux in both space and direction by examining an elementary beam of radiation. The elementary beam of radiation between two elements of area dA_1 and dA_2 , situated anywhere in a radiation field where they are separated by a distance D which is very large compared to the linear dimensions of either element of area, is defined as including all of the rays which pass from dA_1 to dA_2 (or from dA_2 to dA_1 , since either may be the source and the other the receiver). By inspection of Figure C.2, it can be seen that the cross section of the beam at either end is determined by the projected area of the element at that end, i.e., by $\cos \theta_1 dA_1$ and $\cos \theta_2 dA_2$, respectively. Also, the solid angle subtended at the opposite end by each element is equal to this projected area divided by D^2 in each case, giving

$$d\omega_1 = \frac{\cos \theta_1 dA_1}{D^2} \quad [\text{sr}]$$

and

$$d\omega_2 = \frac{\cos \theta_2 dA_2}{D^2} \quad [\text{sr}]. \quad (\text{C.8})$$

If we compute the projected-area-solid-angle-product (which has also been referred to as the “throughput”⁶) at each end we have

$$\begin{aligned} dG_1 &= \cos \theta_1 dA_1 d\omega_2 = \cos \theta_1 dA_1 \frac{\cos \theta_2 dA_2}{D^2} \\ dG_2 &= \cos \theta_2 dA_2 d\omega_1 = \cos \theta_2 dA_2 \frac{\cos \theta_1 dA_1}{D^2} \end{aligned}$$

⁵[*radiant emittance* in the original—Ed.]

⁶ The term “throughput” appears in the instruction manual issued by Block Associates, Inc., for an interferometer spectrometer. It is not known who originated the term or the precise way in which he would define it, but it appears to agree with the way in which it is used here

But

$$dG_1 = dG_2 = dG \quad \left[\text{m}^2 \cdot \text{sr} \right]. \quad (\text{C.9})$$

Next, let us recall the definition of *radiance*, the power per unit projected area per unit solid angle at a point and in a particular direction, as

$$L_e \equiv \frac{\partial^2 \Phi_e}{\partial \omega \cos \theta \partial A} \quad \left[\frac{\text{W}}{\text{m}^2 \cdot \text{sr}} \right].$$

If the radiance at dA_1 is L_{e1} and that at dA_2 is L_{e2} , the power flowing through each surface element is given, respectively, by

$$\begin{aligned} d\Phi_{e1} &= L_{e1} \cos \theta_1 dA_1 d\omega_2 = L_{e1} dG \\ d\Phi_{e2} &= L_{e2} \cos \theta_2 dA_2 d\omega_1 = L_{e2} dG. \end{aligned} \quad (\text{C.10})$$

But the same power is flowing through both of the surface elements that define the beam, since all rays through one also pass through the other and energy is conserved (we have postulated no loss), so

$$d\Phi_{e1} = d\Phi_{e2} \quad \text{and} \quad L_{e1} = L_{e2} = L_e. \quad (\text{C.11})$$

Since the choice of dA_1 and dA_2 is quite arbitrary, and they can define a beam between any widely separated points along a particular ray, it follows that *the value of L_e in the direction of a ray must be invariant along that ray within an isotropic medium*. The value of L_e at any point will vary with direction, and the value of L_e for rays from a particular direction (parallel rays) will vary with position on any surface which they intersect. Hence, in general, the flux passing through a given surface and within a given solid angle is given by

$$\Phi_e = \int \int L_e \cos \theta dA d\omega \quad [\text{W}], \quad (\text{C.12})$$

where the integration is carried out over the entire surface (with respect to the projected area perpendicular to any given direction) and over all directions included within the given solid angle.

In order to generalize still further, we examine the situation where a beam of radiation passes through a smooth surface separating two media with different refractive indices (see Figure C.3). The power incident on any surface element dA through any element of solid angle $d\omega$ in the first medium and that from the same beam emerging from the same surface element into a solid angle $d\omega'$ in the second medium must be the same, if there are no losses by reflection, absorption, or scattering (we are still concerned purely with ray geometry and defer questions of Fresnel reflection losses, etc., until later). This power is given by

$$d\Phi_e = L_e \cos \theta dA d\omega = L'_e \cos \theta' dA d\omega' \quad [\text{W}]. \quad (\text{C.13})$$

By Snell's law of refraction, we write

$$n \sin \theta = n' \sin \theta' \quad (\text{C.14})$$

$$\therefore n \cos \theta d\theta = n' \cos \theta' d\theta'. \quad (\text{C.15})$$

Also,

$$d\omega = \sin \theta d\theta d\varphi \quad \text{and} \quad d\omega' = \sin \theta' d\theta' d\varphi \quad (\text{C.16})$$

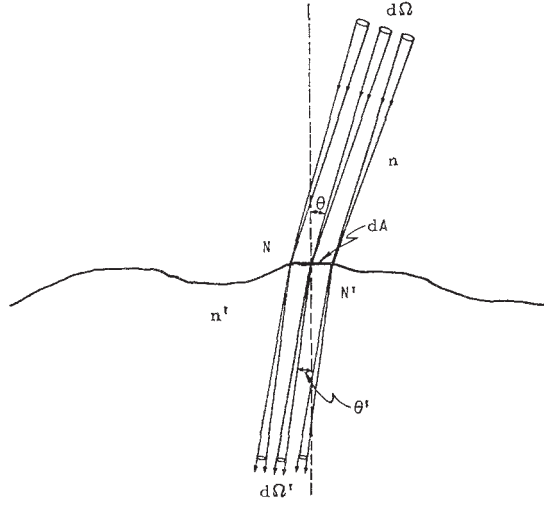


Figure C.3: Refraction at a smooth boundary between media of different refractive indices (n and n')

(the azimuth angle φ of a ray is not changed by refraction). Hence,

$$\frac{L_e dA \cos \theta d\omega}{L'_e dA \cos \theta' d\omega'} = \frac{L_e \cos \theta \sin \theta d\theta d\varphi}{L'_e \cos \theta' \sin \theta' d\theta' d\varphi} \frac{L_e n'^2}{L'_e n^2} = 1$$

$$\therefore \frac{L_e}{n^2} = \frac{L'_e}{n'^2} \quad (\text{C.17})$$

Thus, the quantity L/n^2 in the direction of a ray is invariant along that ray, even as it passes through a smooth boundary surface between media of different refractive indices, if there are no losses by reflection, absorption, or scattering (see [Martin, 1960]⁷). It is also apparent from Equation (C.17) that the value of L_e in the direction of a ray will be the same at any point along such a ray which lies in a medium with the same index, regardless of passage through other media, such as refractive lenses, at intermediate points. Total reflection from a smooth surface merely changes the direction of a beam and does not alter L_e . This can be verified in detail by an analysis similar to that just given for refraction at a smooth boundary.

A “smooth” surface, as the term is used here, is defined to include any surface where it is possible everywhere to construct a tangent plane, i.e., where every surface element can be treated as common to the surface and to a plane tangent to the surface at that point.

It should be recognized, of course, that all real situations involve some losses by absorption, scattering, or reflection, although it is frequently possible to keep the losses to negligible amounts by careful design. Also, in real situations we are concerned with sources and receivers, not hypothetical elements of surface.

In the foregoing analysis, we have attempted to achieve as much generality as possible by considering radiation fields and surface elements placed in those fields with as few restrictions as possible. In this way, the results of the analysis can be extended widely to describe the radiometric quantities at the surfaces of almost any receiver of radiation in terms of those quantities at any source, or at any intermediate location where it may

⁷Martin’s proof is given only for the luminance L_v of an image [Martin, 1960], pp. 266–268, but with only slight modification it, too, is easily generalized to apply to any point along a ray.

be convenient to specify or measure them. This has been done purely in terms of ray geometry, neglecting losses by absorption, scattering, and reflection. Such losses, where they are not negligible, can be accounted for by multiplying the radiometric quantities, determined from ray geometry only, by the appropriate factors. For example, if the radiance along a particular ray at a source is L_{es} , and the radiant transmittance (see Table 1.1) along its path (taking into account the source spectrum and the spectral transmittance (see Table 1.1) of the intervening medium) from source to receiver is τ , and source and receiver both lie in the same medium (same index of refraction), then the radiance at the receiver in the direction of this same ray is given by $L_{er} = \tau L_{es}$. If, in addition, this same ray has also been imperfectly reflected by a mirror at some point along its path to the receiver, the radiance at the receiver becomes $L_{er} = \rho \tau L_{es}$, where ρ is the radiant reflectance (see Table 1.1) of the mirror.

A situation of even more importance, perhaps, is the effect of reflection loss on the radiance along a ray which is refracted at a boundary between two media of different refractive indices. Fresnel's equations require that there be some reflectance at any simple boundary between two such media. Here, if the radiance along the incident ray is L_e , and if the radiant reflectance for the particular angle of incidence is ρ , the radiance along the refracted ray in the second medium will be given by

$$L'_e = L_e \frac{n'^2}{n^2} (1 - \rho) \quad \left[\frac{\text{W}}{\text{m}^2 \cdot \text{sr}} \right]. \quad (\text{C.18})$$

Note, however, that it may be possible to reduce ρ to a negligible value, at least for a limited range of wavelengths and angles of incidence, by the use of so-called antireflection coatings, thus approaching the condition described by Equation (C.17).

C.3 Practical applications

[omitted—*Ed.*]

C.4 Discussion of introductory examples

In the Introduction we described three situations involving extended sources. It should be clear from Equation (C.13) that the exposure meter must give the same response, regardless of distance or orientation, as long as all of the radiation entering it has the same value of radiance. If the wall is perfectly diffuse, all of the rays from it will have the same radiance. An external lens cannot change either the area or angle through which the meter accepts radiation, whether it comes directly from the wall or after it passes through the lens, and the value of radiance also cannot be changed (except by attenuation, which is assumed negligible). In the same way, once the full receiving area (entrance slit) and solid angle (subtended at the slit by the collimating optics) of the spectrometer are filled with rays of the maximum available radiance, there remains no way to increase any of these quantities with additional lenses. In the last example, we must first determine the radiance L_e of the earth's surface. From Equation (C.1) and Equation (C.5) we can write for a uniform plane diffuse radiator for which both L_e and M_e are constants:

$$\Phi_e = \int M_e dA = \int \int L_e \cos \theta dA d\omega \quad [\text{W}],$$

$$\therefore M_e = L_e \int \cos \theta d\omega \quad \left[\frac{W}{m^2} \right], \quad (C.19)$$

If we choose spherical coordinates with the z axis perpendicular to the radiating surface,

$$d\omega = \sin \theta d\theta d\varphi \quad [\text{sr}]$$

and

$$M_e = L_e \int_{\varphi=0}^{2\pi} \int_{\theta=0}^{\frac{\pi}{2}} \cos \theta \sin \theta d\theta d\varphi = L_e \varphi \left|_0^{2\pi} \frac{\sin^2 \theta}{2} \right|_{\theta=0}^{\frac{\pi}{2}} = \pi L_e \quad \left[\frac{W}{m^2} \right]. \quad (C.20)$$

Similarly, from Equation (C.1) and Equation (C.4), the irradiance at a plane surface due to uniform radiation of radiance L_e , arriving within a cone of half-angle θ , is given by

$$E_e = L_e \int \cos \theta d\omega = \pi L_e \sin^2 \theta \quad \left[\frac{W}{m^2} \right]. \quad (C.21)$$

This gives the desired result for an earth of uniform radiance $L_e = M_e / \pi$ which subtends a cone of half-angle θ at the receiver ($E_e = M_e \sin^2 \theta$).

C.5 Summary

It has been established that in any radiation field radiance is invariant along a ray, in the direction of the ray, within an isotropic medium, and that the quantity L_e / n^2 is invariant along a ray, in the direction of the ray, across smooth boundaries between media with different refractive indices, so that L_e has the same value at all points along the ray lying in media of the same index, regardless of passage through other media at intermediate points. Practical applications of the usefulness of this invariant property have been presented. They show that it facilitates the evaluation of the radiant power flowing through any surface where it is possible to determine the cross section of a beam (the projected area of its intersection with the surface) and the solid angle from which rays are flowing through each point of that surface, if the value of radiance is known at any point along each of the rays. In practical optical systems, such surfaces are usually found at the stops (aperture stop and field stop) and their images (e.g., the entrance and exit pupils and windows), and at the surfaces of sources and receivers, and their images.

Evaluation of radiant power becomes a simple matter for a beam passing through a well-defined plane surface (θ is not a function of position) of area A and within a well-defined solid angle ω that is the same at all points of the surface (no vignetting) whenever it is possible to assume a uniform value of radiance L_e throughout the beam. The general expression in Equation (C.12) can then be simplified as follows:

$$\Phi_e = \int \int L_e \cos \theta dA d\omega = L_e A \int \int \cos \theta d\omega = L_e A \Omega^\perp \quad [W]. \quad (C.22)$$

The expression $\Omega^\perp = \int \int \cos \theta d\omega$ has been called the “weighted solid angle” or “projected solid angle” (see [Jones, 1960]). The area-solid-angle-product, “optical invariant” (see [Jones, 1962a]⁸), “throughput”⁶ or “étendue” (see [Connes, 1958]⁹) can be given for the unvignetted beam through a plane surface or aperture of area A as

$$G = A \Omega^\perp = A \int \int \cos \theta d\omega \quad [m^2 \cdot \text{sr}]. \quad (C.23)$$

⁸Although not flagged out, the concept of invariance of the $A\Omega$ product is also used by R. Clark Jones in two other papers: [Jones, 1953]; [Jones, 1962b]

⁹I am indebted to Dr. R. Clark Jones for calling my attention to this reference

Furthermore, in most cases the solid angle is a circular cone of half-vertex-angle θ , with its axis perpendicular to the plane. Then, using spherical coordinates with the z axis perpendicular to the plane, the integration can be carried out thus:

$$G = A \int_{\varphi=0}^{2\pi} \int_{\theta=0}^{\theta} \cos \theta \sin \theta \, d\theta \, d\varphi = \pi A \sin^2 \theta \quad [\text{m}^2 \cdot \text{sr}]. \quad (\text{C.24})$$

and

$$\Phi_e = L_e G = \pi L_e A \sin^2 \theta \quad (\text{C.25})$$

C.6 Acknowledgement

In this report, the author has made extensive use of the ideas of others, gained from many stimulating and helpful discussions and from published books and papers, over an extended period. To attempt to list and acknowledge all of these sources would be impossible, and it has not been attempted except in the few instances where specific reference has been made to published items. However, the development of this treatment of the subject would have been impossible without such help and encouragement.

C.7 Bibliography

- | | |
|---------------------------|---|
| [Bell, 1959] | E. E. Bell. “Radiometric Quantities, Symbols, and Units”. In: <i>Proceedings of the IRE</i> 47.9 (Sept. 1959), pp. 1432–1434. ISSN: 0096-8390. DOI: 10 . 1109 / JRPROC . 1959 . 287031 (cit. on p. 70). |
| [Connes, 1958] | P. Connes. “L’étalon de Fabry-Perot sphérique”. In: <i>J. Phys. Radium</i> 19.3 (Mar. 1958), pp. 262–269 (cit. on p. 77). |
| [Jenkins and White, 1950] | F. A. Jenkins and H. E. White. <i>Fundamentals of Optics</i> . Second. New York: McGraw-Hill, 1950, pp. 104–108 (cit. on p. 70). |
| [Jones, 1953] | R. Clark Jones. “On Reversibility and Irreversibility in Optics”. In: <i>J. Opt. Soc. Am.</i> 43.2 (Feb. 1953), pp. 138–143. DOI: 10.1364/JOSA.43.000138 . URL: http://www.opticsinfobase.org/abstract.cfm?URI=josa-43-2-138 (cit. on p. 77). |
| [Jones, 1960] | R. Clark Jones. “Proposal of the Detectivity D^{**} for Detectors Limited by Radiation Noise”. In: <i>J. Opt. Soc. Am.</i> 50.11 (Nov. 1960), pp. 1058–1059. DOI: 10.1364/JOSA.50.001058 . URL: http://www.opticsinfobase.org/abstract.cfm?URI=josa-50-11-1058 (cit. on p. 77). |
| [Jones, 1962a] | R. Clark Jones. “Immersed Radiation Detectors”. In: <i>Appl. Opt.</i> 1.5 (Sept. 1962), pp. 607–613. DOI: 10.1364/AO.1.000607 . URL: http://ao.osa.org/abstract.cfm?URI=ao-1-5-607 (cit. on p. 77). |

- [Jones, 1962b] R. Clark Jones. “Ultimate Performance of Polarizers for Visible Light”. In: *J. Opt. Soc. Am.* 52.7 (July 1962), pp. 747–750. DOI: [10 . 1364 / JOSA . 52 . 000747](https://doi.org/10.1364/JOSA.52.000747). URL: <http://www.opticsinfobase.org/abstract.cfm?URI=josa-52-7-747> (cit. on p. 77).
- [Kelton et al., 1963] Gilbert Kelton et al. “Infrared target and background radiometric measurements—Concepts units and techniques”. In: *Infrared Physics* 3.3 (1963), pp. 139–169 (cit. on p. 70).
- [Martin, 1960] L. C. Martin. *Technical optics*. Second. Vol. 2. Technical Optics. London: Sir Isaac Pitman & Sons, 1960 (cit. on p. 75).
- [Nicodemus, 1963] F. E. Nicodemus. “Radiance”. In: *American Journal of Physics* 31 (1963), pp. 368–377. DOI: [10 . 1119 / 1 . 1969512](https://doi.org/10.1119/1.1969512) (cit. on p. 69).
- [Planck, 1957] M. Planck. *Theory of heat*. Vol. 5. Introduction to Theoretical Physics. Macmillan, 1957. Chap. 2. Translation by E. L. Brose, originally published in 1914 (cit. on pp. 70, 71).
- [Richtmyer and Kennard, 1947] F. K. Richtmyer and E. H. Kennard. *Introduction to Modern Physics*. Fourth. New York: McGraw-Hill, 1947, p. 145 (cit. on p. 70).

Appendix D

Notation and symbols

- \square a placeholder to indicate the location of some symbol
- $[\square]$ square brackets indicate the contained symbol is a unit, brackets will be empty of *pure numbers*
- \square^\uparrow an arrow pointing up \uparrow is used to indicate exitant quantities, that is leaving the object or location
- \square^\downarrow an arrow pointing down \downarrow is used to indicate incident quantities, that is arriving at the object or location
- $\delta\square$ a small, differential amount of \square
- Ω a solid angle
- ω a direction, usually within the solid angle Ω
- S a light source, or the region where its light originates
- R a light receiver, or the region where it receives light
- t [s] a time period
- k_i imaging constant: scale factor between luminous exposure and pixel values
- p^{img} location on the filmback or image plane
- $W_{pos}(p^{img})$ local response of the filmback
- $W_{col}(\lambda)$ spectral response of the filmback
- $W(p^{img}, \lambda)$ film response function
- λ [m] wavelength
- ν [Hz] frequency
- C incident-light meter calibration constant $312.5 = 100^{25/8}$ for this document
- f focal length
- N aperture number
- o focus distance
- Δt exposure time
- S film speed
- T_{cp} **CCT** of a white point
- N aperture number
- N_p [] number of photons
- Q_p [J] energy of one photon
- Q_e [J] radiant energy
- h Planck's constant (see [**BIPM SI.2019**])
- K_{cd} luminous efficacy of monochromatic radiation (see [**BIPM SI.2019**])
- J unit: joule, measures amounts of energy
- W unit: watt, measures power, being energy per unit of time $[W] = [J/s]$
- Hz unit: watt, measures power, being energy per unit of time $[Hz] = [1/s]$

rad unit: radian, measures angles
sr unit: steradian, measures solid angles

Vector-valued functions and integrals



This section is under construction

Explain the meaning of this expression

$$\begin{pmatrix} X \\ Y \\ Z \end{pmatrix} = \int_{\Lambda} S(\lambda) \begin{pmatrix} \bar{x}(\lambda) \\ \bar{y}(\lambda) \\ \bar{z}(\lambda) \end{pmatrix} d\lambda$$

Scalar product Given two vectors $x, y \in \mathbb{R}^n$ we will indicate their components using a subscript index, for example for $n = 2$ we would have $x = (x_1, x_2)$. We will write their *scalar product* using angle bracket notation $\langle \cdot, \cdot \rangle$:

$$\langle x, y \rangle = \sum_{i=1}^n x_i y_i = xy^t,$$

where the second equality signifies row-vector notation (vectors are thought of as matrices of one row). Sometimes it's useful to inject an $n \times n$ matrix M "in the middle" of a scalar product, defined as follows $\langle x, y \rangle_M := \langle Mx, My \rangle$.

An often useful construct is the following relation: given three vectors $x, y, z \in \mathbb{R}^n$

$$\langle x, y \rangle \langle y, z \rangle = (xy^t) (yz^t) = x(y \otimes y)z^t = \langle x, z \rangle_y$$

where the symbol \otimes indicates the *outer product* defined as $x \otimes y := x^t y$. Here is an example in \mathbb{R}^3 :

$$x \otimes y = \begin{bmatrix} x_1 y_1 & x_1 y_2 & x_1 y_3 \\ x_2 y_1 & x_2 y_2 & x_2 y_3 \\ x_3 y_1 & x_3 y_2 & x_3 y_3 \end{bmatrix}.$$

Scalar product of functions Given two functions $f, g : X \rightarrow \mathbb{R}$ we define their scalar product $\langle f, g \rangle$ as

$$\langle f, g \rangle := \int_X f(x)g(x) dx, \quad \langle f, g \rangle_{\mu} := \int_X f(x)g(x)\mu(x) dx.$$

Norm of a function Given a function $f(x) : X \rightarrow \mathbb{R}$ we will often speak about the integral norm over its domain X , sometimes after weighting with a second positive valued function $\mu(x) : X \rightarrow \mathbb{R}^+$, this will be notated as follows

$$\|f\| := \int_X |f(x)| dx, \quad \|f\|_{\mu} := \int_X |f(x)|\mu(x) dx$$

it is sometimes useful to consider the p -norm of a function f :

$$\|f\|^p := \int_X |f(x)|^p dx, \quad \|f\|_{\mu}^p := \int_X |f(x)|^p \mu(x) dx.$$

In the case of a function $g(x) : X \rightarrow \mathbb{R}^n$ valued in \mathbb{R}^n we apply the relations above to each component separately, for example, in the case of $n = 2$ we would have $g(x) = (g_1(x), g_2(x))$, where $g_1, g_2 : X \rightarrow \mathbb{R}$

$$\|g\|_{\mu} := (\|g_1\|_{\mu}^2 + \|g_2\|_{\mu}^2)^{1/2} \in \mathbb{R}.$$

Appendix E

Index and glossary

aperture An opening through which light can pass. In an optical system such as a camera lens this is also called *entrance pupil* or *diaphragm* and is normally mounted inside the barrel of the lens to admit light through it. When the aperture is well approximated by a circle, it is normally measured in one of two ways: either the diameter is specified directly, usually in [mm], or when discussing camera lenses, the ratio of the aperture's diameter to the focal length is given, and is called the *aperture number*. 8, 46, see also **aperture number**

aperture number In a camera system, the aperture is usually given as a ratio to the focal length, and marked such as $f/2.8$: on a 50mm camera lens, this would mean the diameter of the lens's aperture is $50/2.8 \approx 17.8\text{mm}$. Like other series used in photography, the numbers found on most lenses are taken from this standard series: $f/1.4, f/2, f/2.8, f/4, f/5.6, f/8, f/11, f/16, f/22, f/32$, each in an approximate ratio of $\sqrt{2}$ to the next one, corresponding to a doubling/halving of admitted light from the previous one. The aperture number is also called *f-number* and indicated with the symbol N , where $N = 8$ indicates an $f/8$ aperture., see also **aperture, f-number & T-stop**

ASA American Standards Association. see also **ANSI**

black body 9

brightness The strength of the visual perception caused by the luminance emitted or reflected by an object. It is a subjective property of the object being observed and it is used in this document in its loose, plain spoken-English sense. Other terms are used to designate specific properties. 5, 12

camera lens An assembly of optical lenses meant for use in conjunction with a camera body to make images of objects by focusing the light arriving from the scene onto the camera's filmback. The various optical lenses in a camera lens are called *elements* and are held in a *barrel* or approximately cylindrical shape. Around the barrel are normally *rings* which the photographer can operate to achieve focus, to choose the aperture number and, in zoom lenses, to control the focal length. Some high quality lenses also include a shutter, suitably placed inbetween the elements in the barrel and very near to the aperture. In some cases the shutter can serve double duty and precisely open just to the desired aperture size., see also **aperture number**

candela TODO. 15

CCD An integrated device containing an array of linked capacitors, these can be charged upon receiving photons and their charge later read out to recover what is effectively

- a photon count. Used in this document to indicate a specific class of photosensors used in contemporary digital cameras. [12](#), [21](#), *see also* [CMOS](#)
- cct** The temperature of a black body having chromaticity closest to the chromaticity of interest, as measured on a modified 1976 [CIE](#) Uniform Chromaticity Scale [UCS](#) diagram, where u' and $2/3v'$ are the coordinates of the Planckian locus and of the other stimulus. [17](#), [24](#), [43](#), [77](#)
- cgs** The traditional system of units in use in Europe for physics and related fields, proposed in 1873 by Maxwell and Thomson among many others. It was supplanted by the [MKS](#) system in the 1940s which then turned into the [SI](#) system in the 1960s. *see also* [SI](#) & [MKS](#)
- CIE** Commission Internationale de l'Éclairage (International Commission on Illumination) is the international standards body that regulates over quantities related to illumination. [7](#), [15](#), [19](#), [20](#), [24](#), [40](#), [41](#), [59](#), [63](#)
- CMOS** Currently one of the main technologies used in integrated circuit construction, this is used in this document to indicate a specific class of photosensors used in contemporary digital cameras. [12](#), [21](#), *see also* [CCD](#)
- color** The visual perception based on the distribution of photon wavelengths arriving at an observer's eye. Care should be taken to keep in mind that color is a property of light, as opposed to materials. All materials do is reflect, transmit or absorb light thereby *altering* its color. [8](#)
- CRI** Color Rendering Index. [41](#), [43](#)
- DCC** Digital Content Creation. [55](#)
- diffuse** A material model (or component thereof) where light bounces off a material so that equal luminance is received by all observers in the front half-space of the surface (in the case of *diffuse reflection*) or the back half-space (in the case of *diffuse transmission*). *see also* [material model](#)
- emission** TODO. [9](#)
- entrance pupil**, *see* [aperture](#)
- exitant** In radiometry and photometry, and adjective used to characterize the direction of flow as leaving the object. [8](#), [10](#)
- exposure** A measure of the area density of incident energy. [11](#), [12](#), [17–19](#)
- exposure meter** A device used to read out the illuminance at a location. The value is often available both in lx as well as *foot-candle*, being one lm per *square foot*. Being a photographer's tool, an exposure meter normally also has provisions to quickly solve the exposure equation for the current lighting conditions: a dial might be use to choose the film speed. *see also* [illuminance](#)
- exposure time** The amount of time for which a camera shutter is kept open in order to admit light onto the filmback, this quantity is measured in seconds and uses the symbol t . On photographic cameras, the value is called *shutter speed* and is indicated in fractions of a second, standard timings being taken from the series 1, $1/2$, $1/4$, $1/8$, $1/15$, $1/30$, $1/60$, $1/125$, $1/250$, $1/500$, $1/1000$, $1/2000$. In motion pictures the convention is to speak of *shutter angle*: in a motion picture film camera the shutter is made of two half circle "blades" each covering 180 degrees and set up to complete one revolution per frame. During setup these can be set to leave an opening between 0 and the full 180 degrees during which light is admitted onto the film stock. The remaining time, called *blanking*, is used to advance the film to the position of the following frame. The exposure time resulting from this approach on a given angle α in degrees is then $\alpha/360/24s$ when the camera is running at 24 [FPS](#). [22](#), *see also*

shutter

exposure value A number used to combine the shutter speed and aperture number into an exposure setting. Symbols used are EV , Ev and E_v , although when used to indicate an exposure setting it would be most correct to include the film speed associate with the value, such as EV_{100} for ISO 100 stock. For an exposure time of t and aperture number N , the relation is $EV_{100} = \log_2 \frac{N^2}{t}$. *see also* shutter speed & aperture number

f-number , *see also* aperture number & T-stop

film response function A function capturing the response of film to a given wavelength and at a given location on the film back. 19, *see also* filmback

film speed A measure for the sensitivity of photosensitive film stock. The **ISO** scale is commonly used, with values in powers of two such as 100, 200, 400, 800, 1600, 3200, each corresponding to a one stop increment. The standard had previously been proposed by **ASA** (now called **ANSI**) and is often found on film stock as **ISO/ASA**. Also common was the German system standardized by **DIN**, which instead used a scaled logarithmic scale where a film speed of **ISO** 100 was equivalent to DIN 21°. The sensitivity marking on film stock would often include both values, such as “**ISO/ASA** 100/21°”. For some higher end film stock, intermediate sensitivity rating were also available, usually along this series 100/21°, 125/22°, 160/23°, 200/24° and so on. 19, 21, 22, *see also* stop

filmback The area in a camera body onto which an image is to be formed. In modern cameras the filmback contains a photosensitive digital sensor, whereas in non-digital models, the filmback would be covered by photosensitive film. 18, 19, 61, *see also* sensor

footage In cinema photography, a segment of motion picture material. The name derives from the days of physical film: at 24 frames per second, being the standard frame rate for 35mm physical film, one second of film is exactly 1.5ft. Today the term is used to indicate motion picture content, be that on physical media or stored in digital files. 5

human observer An observer with a light sensitivity equal to the *standard human*, being some kind of a mythical creature. The **CIE** has spent considerable effort to characterize the response to light of the visual system in humans, producing several tabulations each suitable for different uses. It is very important to remember that human subjects exhibit a very wide range in how they perceive light, even when the observations are restricted to only consider subjects not affected by color blindness. Combined with the difficulty of making objective measurements on a wide range of subjects, the width of this variation is one of the reasons why color science is such a complex subject. 5

IBL Image based lighting. 26, 28–30, 59

IEC International Electrotechnical Commission. 7

IES Illuminating Engineering Society of North America. 44, 57

illuminance 15, 18, *see also* brightness

illuminant A source of light, meant to focus on the part of a light-emitting object that specifically emits the light, as opposed to other elements of it. All together these constitute a *light fixture*. 5, *see also* virtual scene

image 18

imaging equation 17

incident In radiometry and photometry, and adjective used to characterize the direction of flow as arriving at an object. 8, 10

irradiance 12, 18, *see also* **brightness**

iso International Organization for Standardization. 7

LED Light emitting diode. 5

luminance 15

luminous efficacy The ratio of light emitted by a source to its absorbed power. More precisely, the ratio of luminous power to radiant power for the source, a quantity measured in lm/W. 5

luminous flux 15

material model TODO. 5, *see also* **shader**

mks The traditional name for the International System of Units, after meter/kilogram/second. *see also* **SI** & **CGS**

photometry The science of measurement of the strength of visible light, through which are defined units that capture its perceived brightness to the human eye. In photometry, light has *luminous power* measured in lm. 5, 15, 17, *see also* **radiometry**

pipeline The set of processes and software tools used for the production of digital images, especially in digital movie-making. The word is used to draw attention to the large number of connections that must be put in place to connect the various major tools in a production workflow, where many kinds of files flow together and get combined to produce the result images. 6

pixel filter TODO. 21

radiance The fundamental elemental quantity for light transport, radiance is the subject of Appendix C. 6, 10, 17–19, 21

radiant intensity 10

radiant power The power Φ_e emitted by a source as electromagnetic waves, also known as *radiant flux* and measured in $W = J/s$. Sometimes there is discussion of *spectral radiant power*, which is the radiant power per unit frequency or wavelength. In most cases the radiant power is the integral of spectral radiant power over all wavelengths, but for the purposes of this document it is occasionally a useful thought exercise to restrict the integration domain to just the visible wavelengths instead. 12, 17, *see also* **spectral**

radiometry The science of measurement of the strength of electromagnetic radiation, measuring its total energy, or in some cases the energy corresponding to a part of its spectrum. In radiometry, visible light has *radiant power*, measured in W. 5, 8, 15, *see also* **photometry**

radiosity 9

reflection TODO. 9

rendering The process of generating an image from a virtual model, or virtual scene by means of a computer program. This is also called *image synthesis*. A scene file will normally contain information about the shapes of the objects to be rendered, their appearance, also called *shading*, as well as descriptions of the camera or cameras and lighting configuration to use. 7, *see also* **shader**, **material model** & **virtual scene**

RGB RGB color space of generic primaries. 20, 24–27, 34, 49–51, 53, 56, 59, 65

RIB RenderMan Interface Bytestream. 55, 61

RSL RenderMan Shading Language. 56

- scene** In filmmaking and theater, a scene is a sequence of actions that compose a small narrative unit (in cinema a scene is composed by several *shots*). The word takes of an additional meaning in virtual cinematography, where a *scene* is also a set of objects intended to be rendered. These virtual scenes are kept in files edited with Digital Content Creation software. In rendering, the scene will comprise all the objects to be rendered for one frame, including their material models, the lights and the cameras. 5, 17
- sensor** In a digital camera, the device installed at the filmback onto which the image is formed. Photons hitting the sensor displace electrons or otherwise build an electric field proportional to the photon count. An **ADC** then provides a digital readout of the magnitude of this field. 5, *see also* **filmback**
- shader** A program meant to compute the visual appearance of an object. This is usually achieved implementing one or more material models in software which is then fed to a renderer along with geometric descriptions of the object to be represented. Shaders often read data from files called *textures* to provide surface detail such as patterns or surface decorations, and also often use procedural approaches to synthesize other surface details such as rust marks, stains or scuffs. In many cases shaders are written in domain specific languages, such as **RSL** or **CUDA** that facilitate certain aspects of the implementation or control of specific hardware.
- shot** In filmmaking, a shot is a series of frames that runs for an uninterrupted period of time, typically a few seconds to a few minutes. Shots are then composed to form scenes through the editing process, using cuts and other kinds of transitions. *see also* **scene**
- shutter** A component in a camera design to open for a brief period of time, called the *exposure time*, to permit light to arrive at the filmback. Most often the shutter is mounted on the camera body between the camera lens and the filmback, but in large format photography leaf shutters are available as independent parts of the kit, and are sometimes installed “sandwiched” in the middle of a so-called two-part lens, so it sits as close as possible to the aperture., *see also* **aperture**, **camera lens**, **exposure time & filmback**
- shutter speed** *see* **exposure time**
- SI** The *International System of Units* (Système International d’Unités) is a coherent system of units of measurement (based on the **meter-kilogram-second (mks)** system) built around seven base units: *kelvin* [K] (temperature), *second* [s] (time), *meter* [m] (length), *kilogram* [kg] (mass), *candela* [cd] (luminous intensity), *mole* [mol] (amount of substance) and *ampere* [A] (electric current). 6, 7, 15, 16, 55, 67
- SPD** Spectral Power Distribution. *see* **spectral distribution**
- spectral** An adjective to indicate the value in question (usually a radiometric quantity) is to be intended as per unit wavelength. For example, *spectral radiant power* $\Phi_\lambda = \partial\Phi_e/\partial\lambda$ is the partial derivative of radiant power with respect to the wavelength. This is measured in W/m or sometimes W/nm. It is also common (but not used in this document), to use the partial derivative with respect to frequency, for which a ν subscript is used, as in Φ_ν . 6, 17–19
- spectral distribution** A function (*distribution*) relating the spectral density of a quantity to a given wavelength. For example, the spectral power distribution **SPD** is the derivative of radiant power with respect to wavelength. Distributions are a key concept in the field of probability, where continuous distributions are called *densities*. 15, *see* **spectral**
- sRGB** sRGB color space. 19, 20, 49–51, 59

standard air Standard air is defined in **cie:018.2019** as *dry air at 15° [°C] and 101325 [Pa], containing 0.045% by volume of carbon dioxide*. [16](#)

stop In photography, stops are changes to the exposure settings that double or halve the amount of light admitted during one exposure. They are so called because they correspond to the action of going to the next detent position on the shutter timing gear on the camera or on the aperture ring on the lens barrel, which respectively doubles the exposure time or the aperture area. For consistency, film stock is usually rated also in stops, resulting in the base ratings as described in [film speed](#). Stops tend to be subdivided in thirds, which correspond to an increment of 1 unit on the [DIN](#) sensitivitiy scale., *see also* [film speed](#), [exposure time & aperture](#)

T-stop A *transmission stop* is a way to mark aperture numbers on a camera lens where the physical size of the aperture is calibrated at manufacturing time to compensate for the light lost through the various elements of the lens, so to admit as much light as it would be admitted if these elements had 100% transmittance. Camera lenses intended for cinema use are normally calibrated with T-stops, because this enables producing footage of identical brightness independent of which one camera lens is used from the cinematographer's lens kit selected for the show., *see also* [f-number](#), [aperture number & camera lens](#)

transmission TODO. [9](#)

tristimulus values A triple of values meant to represent a color. [17](#)

usd Universal Scene Description. [55](#)

virtual We use the word *virtual* to indicate a digital counterpart to some real-world process, object or set of objects. [5](#)

virtual scene *see* [scene](#)

wattage *see* [radiant power](#)

wavelength TODO. [7](#)

xyz CIE XYZ color space. [19](#), [20](#), [24](#), [59](#), [63](#)

Appendix F

References

Documents published by standards organizations and motion pictures are in their own sections

- [Dutr   et al., 2003] Philip Dutr  , Philippe Bekaert, and Kavita Bala. *Advanced Global Illumination*. Natick, MA: A. K. Peters, 2003. ISBN: 9781568811772 (cit. on p. 19).
- [Fairman et al., 1997] Hugh S. Fairman, Michael H. Brill, and Henry Hemmendinger. “How the CIE 1931 color-matching functions were derived from Wright-Guild data”. In: *Color Research & Application* 22.1 (1997), pp. 11–23. doi: [https://doi.org/10.1002/\(SICI\)1520-6378\(199702\)22:1<11::AID-COL4>3.0.CO;2-7](https://doi.org/10.1002/(SICI)1520-6378(199702)22:1<11::AID-COL4>3.0.CO;2-7) (cit. on p. 22).
- [Jakob et al., 2022] Wenzel Jakob et al. *Mitsuba 3 renderer*. Version 3.0.1. <https://mitsuba-renderer.org>. 2022 (cit. on p. 22).
- [Kang et al., 2002] B. Kang et al. “Design of Advanced Color Temperature Control System for HDTV Applications”. In: *Journal of the Korean Physical Society* 41.6 (Dec. 2002), pp. 865–871 (cit. on pp. 40, 41).
- [Knuth, 1997] Donald E. Knuth. *Seminumerical Algorithms*. Third. Vol. 2. The Art of Computer Programming. Boston, MA, USA: Addison-Wesley Longman Publishing Co., Inc., 1997. ISBN: 0-201-89684-2 (cit. on p. 58).
- [Kolb et al., 1995] Craig Kolb, Don Mitchell, and Pat Hanrahan. “A Realistic Camera Model for Computer Graphics”. In: *Proceedings of the 22nd Annual Conference on Computer Graphics and Interactive Techniques*. SIGGRAPH ’95. New York, NY, USA: Association for Computing Machinery, 1995, pp. 317–324. ISBN: 0897917014. doi: [10.1145/218380.218463](https://doi.org/10.1145/218380.218463). URL: <https://doi.org/10.1145/218380.218463> (cit. on p. 19).
- [Maloney, 1986] Laurence T. Maloney. “Evaluation of linear models of surface spectral reflectance with small numbers of parameters”. In: *Journal of the Optical Society of America* 3.10 (1986), pp. 1673–1683 (cit. on p. 56).

- [Meng et al., 2015] Johannes Meng et al. “Physically Meaningful Rendering using Tristimulus Colours”. In: *Computer Graphics Forum (Proceedings of Eurographics Symposium on Rendering)*. Vol. 34. June 2015, pp. 31–40 (cit. on p. 56).
- [Meyer-Arendt, 1968] Jurgen R. Meyer-Arendt. “Radiometry and Photometry: Units and Conversion Factors”. In: *Appl. Opt.* 7.10 (Oct. 1968), pp. 2081–2084. doi: 10.1364/AO.7.002081. URL: <http://ao.osa.org/abstract.cfm?URI=ao-7-10-2081> (cit. on pp. 17, 18).
- [Nicodemus, 1963] F. E. Nicodemus. “Radiance”. In: *American Journal of Physics* 31 (1963), pp. 368–377. doi: 10.1119/1.1969512 (cit. on pp. 8, 12).
- [Nicodemus et al., 1977] F. E. Nicodemus et al. “Radiometry”. In: ed. by Lawrence B. Wolff, Steven A. Shafer, and Glenn Healey. USA: Jones and Bartlett Publishers, Inc., 1977. Chap. Geometrical Considerations and Nomenclature for Reflectance, pp. 94–145. ISBN: 0-86720-294-7 (cit. on p. 9).
- [Otsu et al., 2017] Hisanari Otsu, Masafumi Yamamoto, and Toshiya Hachisuka. “Reproducing Spectral Reflectances from Tristimulus Colors”. In: *Computer Graphics Forum* 36.5 (2017), pp. 1–11 (cit. on p. 56).
- [Pharr et al., 2023] Matt Pharr, Wenzel Jakob, and Greg Humphreys. *Physically Based Rendering: From Theory To Implementation*. Fourth ed. San Francisco, CA, USA: The MIT Press, Mar. 2023. ISBN: 9780262048026 (cit. on pp. 19, 22, 23).
- [Planck, 1914] Max Planck. *Theory of heat radiation*. Trans. by Morton Masius. P. Blakiston’s Son & Co., 1914 (cit. on p. 40).
- [Schrödinger, 1920] E. Schrödinger. “Theorie der Pigmente von größter Leuchtkraft”. In: *Annalen der Physik* 367.15 (1920), pp. 603–622 (cit. on p. 56).
- [Smith and Guild, 1931] T. Smith and J. Guild. “The CIE colorimetric standards and their use”. In: *Transactions of the Optical Society* 33.3 (1931), p. 73 (cit. on pp. 18, 22).
- [Smits, 1999] Brian E. Smits. “An RGB-to-Spectrum Conversion for Reflectances”. In: *J. Graphics, GPU, & Game Tools* 4.4 (1999), pp. 11–22. doi: 10.1080/10867651.1999.10487511 (cit. on pp. 37, 56, 67).
- [Ward, 1994] Gregory J. Ward. “The RADIANCE Lighting Simulation and Rendering System”. In: *Proceedings of the 21st Annual Conference on Computer Graphics and Interactive Techniques. SIGGRAPH ’94*. New York, NY, USA: ACM, 1994, pp. 459–472. doi: 10.1145/192161.192286 (cit. on p. 22).

- [Wyman et al., 2013] Chris Wyman, Peter-Pike Sloan, and Peter Shirley. “Simple Analytic Approximations to the CIE XYZ Color Matching Functions”. In: *Journal of Computer Graphics Techniques (JCGT)* 2.2 (July 2013), pp. 1–11. ISSN: 2331-7418. URL: <http://jcgt.org/published/0002/02/01/> (cit. on p. 49).

Appendix G

Standards and technical reports

This section lists standards and technical reports

- [BIPM SI.2019] BIPM. *The International System of Units (SI)*. Standard. Paris, FR: International Committee for Weights and Measures, Dec. 2022. URL: <https://www.bipm.org/en/publications/si-brochure>.
- [CIE 015.2018] CIE. *Colorimetry*. Technical Report. Vienna, AT: Commission Internationale de l'Éclairage, Oct. 2018. DOI: 10.25039/TR.015.2018. URL: <https://cie.co.at/publications/colorimetry-4th-edition>.
- [CIE S 017.2020] CIE. *ILV: International Lighting Vocabulary*. Standard. Vienna, AT: Commission Internationale de l'Éclairage, Dec. 2020. DOI: 10.25039/S017.2020. URL: <https://cie.co.at/publications/ilv-international-lighting-vocabulary-2nd-edition-0>.
- [IEC 60050-845:2020] IEC. *IEV: International Electrotechnical Vocabulary – Part 845: Lighting*. Standard. Geneva, CH: International Electrotechnical Commission, Dec. 2020. URL: <https://webstore.iec.ch/publication/26592>.
- [ISO 80000-7:2020] ISO. *Quantities and units – Part 7: Light and radiation*. Standard. Geneva, CH: International Organization for Standardization, Aug. 2019. URL: <https://www.iso.org/obp/ui/%5C#iso:std:iso:80000:-7:ed-2:v1:en>.
- [ISO 9288:2022] ISO. *Thermal insulation — Heat transfer by radiation — Vocabulary*. Standard. Geneva, CH: International Organization for Standardization, Aug. 2022. URL: <https://www.iso.org/standard/82088.html>.
- [ISO/CIE 11664-2:2022] CIE. *Colorimetry — Part 2: CIE standard illuminants*. Standard. Geneva, CH: Commission Internationale de l'Éclairage / International Organization for Standardization, Aug. 2022. DOI: 10.25039/DS1664-2.2022. URL: <https://www.iso.org/standard/77215.html>.

Appendix H

Motion pictures

This section lists motion pictures

[, 2014]

Interstellar. Christopher Nolan (dir). Emma Thomas, Christopher Nolan, and Lynda Obst (prod). Paramount Pictures and Warner Bros. Pictures. 2014.